

1974

Tin-119 And Iodine-129 Moessbauer Studies Of Bonding In Organometallic Compounds

Kevin David Butler

Follow this and additional works at: <https://ir.lib.uwo.ca/digitizedtheses>

Recommended Citation

Butler, Kevin David, "Tin-119 And Iodine-129 Moessbauer Studies Of Bonding In Organometallic Compounds" (1974). *Digitized Theses*. 783.

<https://ir.lib.uwo.ca/digitizedtheses/783>

This Dissertation is brought to you for free and open access by the Digitized Special Collections at Scholarship@Western. It has been accepted for inclusion in Digitized Theses by an authorized administrator of Scholarship@Western. For more information, please contact tadam@uwo.ca, wlsadmin@uwo.ca.

119-TIN AND 129-IODINE MÖSSBAUER STUDIES
OF BONDING IN ORGANOMETALLIC COMPOUNDS

by

Kevin David Butler

Department of Chemistry

Submitted in partial fulfillment
of the requirements for the degree of
Doctor of Philosophy

Faculty of Graduate Studies
The University of Western Ontario
London, Ontario

July, 1974

© Kevin David Butler, 1974

to Gwen

ABSTRACT

¹¹⁹-tin Mössbauer centre shift (CS) and quadrupole splitting (QS) parameters have been measured for fifty compounds containing tin and a transition metal (including Mn, Fe, Co and Ni). The QS values for these and other previously reported compounds are rationalised in terms of an additivity model, which utilises ligand partial quadrupole splitting parameters. Pqs values are derived for a number of organometallic transition metal complex ligands, and these are used, with previously derived pqs values for other ligands, to calculate QS and η parameters for a large number of four co-ordinate tin compounds. Agreement between such predicted QS values and measured QS values is within $\pm 0.4 \text{ mm s}^{-1}$, over a range of $\sim \pm 3 \text{ mm s}^{-1}$, for over 90% of these compounds. However, agreement between calculated and observed η values is generally poor.

The CS parameters are used to determine the order of tin s character in tin-ligand bonds for a number of ligands, and this "s-character series" is in good agreement with previously published ¹H nmr, ⁵⁹Co nqr and structural data for organotin compounds. The CS parameters are also shown to reflect the valency of a tin atom, rather than its formal oxidation state, as was previously assumed.

Ratios of e^2qQ values of isoelectronic, isostructural complexes of different elements are used to rationalise bonding in

analogous pairs of Sb/Sn and Mn/Fe compounds, and to calculate nuclear quadrupole parameters for ^{119}Sn .

The 129-iodine Mössbauer spectra for a series of $\text{trans}-[^{129}\text{I}(\text{L}(\text{PtQ}_2)]\text{PF}_6$ and $\text{trans}-[^{129}\text{I}(\text{X}(\text{PtQ}_2)]$ complexes were recorded (L = neutral ligand; X = anionic ligand); and the resulting $e^2qQ(5/2)$ and $e^2qQ(7/2)$ parameters used to place the ligands L and X into their order of *trans*-influence. The Williams-Bancroft method of multiline Mössbauer spectral analysis was tested for these compounds, and statistically analysed. It was shown to yield very accurate parameters, with straightforward calculations and no approximations.

ACKNOWLEDGEMENTS

I would like to express my sincere appreciation to Dr. G. M. Bancroft under whose direction and encouragement this work was completed.

In addition I would like to thank Drs. H. C. Clark, T. G. Appleton and J. E. H. Ward who suggested some of the areas for investigation, and assisted in evaluation of results. I am also indebted to the faculty members, post-doctoral fellows, graduate students, technical staff and visitors at Western for much appreciated and informative discussions.

Thanks are also due to Drs. T. Wonnacott and A. Heinicke of the Department of Mathematics, U.W.O., for suggesting and discussing the statistical approach for estimating errors.

I gratefully acknowledge the financial support of the University of Western Ontario and the National Research Council of Canada.

Finally I am very grateful to my wife, Gwen, for her patience and understanding during the course of this work.

CHAPTER 1

Introduction and Experimental Techniques

A. Mössbauer Spectra and Derived Parameters

The phenomenon of recoil-free nuclear resonance with gamma radiation was first discovered by Rudolph Mössbauer¹, and has become widely applied to chemical problems since it was shown² that ^{57}Fe exhibited the effect, and that hyperfine interactions occur in chemical compounds. The majority of Mössbauer research so far has been carried out using ^{119}Sn and ^{57}Fe , since spectra are most easily obtained for these isotopes. However, over forty other isotopes have been shown to exhibit the effect³, and chemically useful information has been obtained for compounds of Ge, Sb, Te, I, Xe, Kr, Ni, Ru, W, Ir, Au, Np and a number of the rare earths. In theory, the effect is present for all excited-ground state γ -ray transitions, although its magnitude can be so low as to preclude detection with current techniques.

The unique feature of Mössbauer spectroscopy is the production of highly monochromatic radiation, so that it can be used to resolve minute energy differences, such as variations in the interaction of a nucleus with its electronic environment for

CHAPTER 3 - THE ADDITIVITY MODEL FOR QUADRUPOLE SPLITTINGS, AND ITS APPLICATION TO FOUR CO-ORDINATE TIN SYSTEMS	35
A. Determination of Partial Quadrupole Splittings	35
B. Application of the Additivity Model to Four Co-ordinate Tin	42
C. Consideration of Structural Distortions	63
D. References	69
 CHAPTER 4 - CENTRE SHIFTS FOR COMPOUNDS CONTAINING A TIN-TRANSITION METAL BOND	72
A. Introduction	72
B. The s-character Series and nmr Coupling Constants	73
C. Molecular Geometry in Four Co-ordinate Tin Compounds	82
D. 59-Cobalt e^2qQ Values	87
E. The Oxidation State and Valency of Tin	90
F. References	95
 CHAPTER 5 - RATIOS OF QUADRUPOLE SPLITTINGS	99
A. Introduction	99
B. Theory	100
C. 119-Tin and 121-Antimony Quadrupole Splittings	101
D. Quadrupole Splittings in $[cpM(CO)_2L]$ Complexes (M = Fe, Mn, Re)	110
E. References	118

CHAPTER 6 - THE EFFECT OF trans LIGANDS ON 129-IODINE

MÖSSBAUER PARAMETERS IN SQUARE-PLANAR

PLATINUM(II) COMPLEXES 122

A. Introduction - The "trans-Influence"	122
B. Results (Structures and Mössbauer Spectra)	124
C. Discussion (trans-Influence Series, Correlations)	130
D. Conclusion	139
E. Experimental	139
F. References	144

* * * *

APPENDIX 1 - ANALYTICAL DETERMINATION OF THE HYPERFINE

MÖSSBAUER PARAMETERS FROM 129-IODINE SPECTRA 146

A. The EFG - Nuclear Quadrupole Interaction	146
B. The Determination of Energy Levels	149
C. Solution of the Polynomials	151
D. Sample Calculation	152
E. References	155

APPENDIX 2 - ESTIMATION OF THE ERRORS IN DERIVED

¹²⁹I MÖSSBAUER PARAMETERS 161

VITA xvi

PUBLICATIONS xvii

LIST OF TABLES

Table	Description	Page
1.1	Components of the Electric Field Gradient Tensor.	7
2.1	¹¹⁹ -Sn Mössbauer Parameters Observed for some Tin-Transition Metal Bonded Complexes at -78K.	14
2.2	Mössbauer Parameters Derived from Magnetic Spectra at 4.2K.	25
2.3	Analytical Data for New Tin-Transition Metal Complexes.	30
3.1	Components of the efg Tensor for Four Co-ordinate "tetrahedral" Sn Compounds.	36
3.2	Ligand pqs Values for Four Co-ordinate Tin.	38
3.3	Ligand pqs Values for Four Co-ordinate Tin.	40
3.4	¹¹⁹ -Tin Quadrupole Splittings (Observed and Predicted from Partial Quadrupole Splittings) for Four Co-ordinate Tin Compounds.	44
3.5	¹¹⁹ -Tin Quadrupole Splitting Data for some Organotin Halide Complexes.	58

Table	Description	Page
3.6	Measured Values of the Asymmetry Parameter, η , for Tin-Transition Metal Compounds.	60
3.7	Calculated Absolute pqs Values (method 1).	65
3.8	Calculated Absolute pqs Values (method 2).	67
3.9	Calculated and Observed QS Values for some Four Co-ordinate Tin Compounds; Using Crystallographically Measured Bond Angles.	67
4.1	^{119}Sn Mössbauer Centre Shift Data for some Four Co-ordinate Tin Complexes.	74
4.2	^1H nmr and ^{119}Sn Mössbauer Data for some Me_3SnL Compounds.	77
4.3 a-d	Bond Angle Data for some Tetrahedral Organo-tin Compounds.	83
4.4	CS Values for some Tin-Transition Metal Complexes.	91
5.1	^{119}Sn and ^{121}Sb Nuclear and Bonding Parameters.	107
5.2	^{57}Fe Mössbauer Parameters for the Derivatives $[\text{cpFe}(\text{CO})_2\text{L}]^+\text{X}^-$.	111
5.3	Predicted Quadrupole Parameters for Isoelectronic $\text{cpM}(\text{CO})_2\text{L}$ ($\text{M} = \text{Mn}, \text{Fe}$) Derivatives.	116

Table	Description	Page
6.1	^{129}I Mössbauer Parameters for <i>trans</i> - $[\text{}^{129}\text{IPtQ}_2]$ and <i>trans</i> - $[\text{}^{129}\text{IPtQ}_2]\text{PF}_6$.	128
6.2	Physical Data for the Complexes <i>trans</i> - $[\text{ILPtQ}_2]\text{PF}_6$ and <i>trans</i> - $[\text{IPtQ}_2]$.	142
A2.1	Derived Errors in η and e^2qQ , with Confidence Limits, for some <i>trans</i> - $[\text{}^{129}\text{IQ}_2\text{PtL}]$ Complexes.	165

LIST OF FIGURES

Figure	Description	Page
1.1	Typical ^{119}Sn Mössbauer Spectrum	5
1.2	Nuclear Energy Level Diagram for ^{119}Sn ; showing Quadrupole and Magnetic Splitting.	5
2.1	^{119}Sn Mössbauer Spectra of (a) $\text{trans}-(\text{Cl}_2\text{Sn})_2\text{Fe}(\text{p-MeO.C}_6\text{H}_4.\text{NC})_2$ and (b) $\text{MeCl}_2\text{SnMn}(\text{CO})_5$ at -78K .	22
2.2	^{119}Sn Mössbauer Spectrum of $\text{Ph}_3\text{SnMn}(\text{CO})_5$ at -78K ; showing one peak and two peak fits to the data.	23
2.3	^{119}Sn Mössbauer Spectra of $\text{MeCl}_2\text{SnMn}(\text{CO})_5$ and $\text{Me}_2\text{ClSnMn}(\text{CO})_5$ at 4.2K in a magnetic field of 42 kG .	26
3.1	Calculated vs Observed ^{119}Sn Quadrupole Splittings for Four Co-ordinate Tin Compounds.	53
3.2	Variation of Calculated η Values with pqs of the Ligands for $\text{Me}_2\text{ClSnMn}(\text{CO})_5$.	61
3.3	Variation of Calculated QS Values with pqs of the Ligands for $\text{Me}_2\text{ClSnMn}(\text{CO})_5$.	62

Figure	Description	Page
4.1	Plot of $ ^2J(^{119}\text{Sn}-\text{C}^1\text{H}_3) $ against ^{119}Sn Centre Shift for $\text{Me}_n\text{SnM}_{4-n}$ Compounds.	81
4.2	Plot of ^{119}Sn Mössbauer Centre Shift versus $(^{59}\text{Co})e^2qQ$ (from nqr) for some $\text{X}_n\text{Sn}[\text{Co}(\text{CO})_4]_{4-n}$ Compounds.	88
5.1	Plot of ^{121}Sb versus ^{119}Sn $ e^2qQ $ Values for Isostructural, Isoelectronic Analogues.	103
6.1	^{129}I Mössbauer Spectrum of $\text{trans}-[^{129}\text{IQ}_2\text{PtP}(\text{OMe})_3]\text{PF}_6$ at 4.2K.	127
6.2	Plots of ^{129}I $e^2qQ(7/2)$ Values for $\text{trans}-[^{129}\text{IQ}_2\text{PtL}]$ against $ ^2J(^{195}\text{Pt}-\text{C}^1\text{H}_3) $ for $\text{trans}-[\text{MeQ}_2\text{PtL}]$ and $\nu(\text{Pt}-\text{Cl})$ for $\text{trans}-[\text{Cl}(\text{PEt}_3)_2\text{PtL}]$.	137
A1.1	Nuclear Energy Level Diagram for the ^{129}I Atom in $\text{trans}-[^{129}\text{IQ}_2\text{PtP}(\text{OMe})_3]\text{PF}_6$.	153

ABBREVIATIONS

Me	- methyl	Et	- ethyl
Bu	- n-butyl	t-Bu	- t-butyl
Neo	- neophyl (PhCMe ₂ CH ₂)	Ph	- phenyl
cp	- h ⁵ -cyclopentadienyl		
Me-cp	- h ⁵ -methylcyclopentadienyl		
depe	- 1,2-bis(diethylphosphino)ethane		
dppe	- 1,2-bis(diphenylphosphino)ethane		
py	- pyridine		
THF	- tetrahydrofuran		
DMSO	- dimethylsulphoxide		
NBD	- norbornadiene		
COD	- cyclo-octa-1,5-diene		
CS	- centre shift		
QS	- quadrupole splitting		
efg, EFG	- electric field gradient		
pfg	- partial field gradient		
pqs	- partial quadrupole splitting		
pcs	- partial centre shift		
eV	- electron volt		
nmr	- nuclear magnetic resonance		
nqr	- nuclear quadrupole resonance		
ESCA	- X-ray photoelectron spectroscopy		

The author of this thesis has granted The University of Western Ontario a non-exclusive license to reproduce and distribute copies of this thesis to users of Western Libraries. Copyright remains with the author.

Electronic theses and dissertations available in The University of Western Ontario's institutional repository (Scholarship@Western) are solely for the purpose of private study and research. They may not be copied or reproduced, except as permitted by copyright laws, without written authority of the copyright owner. Any commercial use or publication is strictly prohibited.

The original copyright license attesting to these terms and signed by the author of this thesis may be found in the original print version of the thesis, held by Western Libraries.

The thesis approval page signed by the examining committee may also be found in the original print version of the thesis held in Western Libraries.

Please contact Western Libraries for further information:

E-mail: libadmin@uwo.ca

Telephone: (519) 661-2111 Ext. 84796

Web site: <http://www.lib.uwo.ca/>

CHAPTER 1

Introduction and Experimental Techniques

A. Mössbauer Spectra and Derived Parameters

The phenomenon of recoil-free nuclear resonance with gamma radiation was first discovered by Rudolph Mössbauer¹, and has become widely applied to chemical problems since it was shown² that ^{57}Fe exhibited the effect, and that hyperfine interactions occur in chemical compounds. The majority of Mössbauer research so far has been carried out using ^{119}Sn and ^{57}Fe , since spectra are most easily obtained for these isotopes. However, over forty other isotopes have been shown to exhibit the effect³, and chemically useful information has been obtained for compounds of Ge, Sb, Te, I, Xe, Kr, Ni, Ru, W, Ir, Au, Np and a number of the rare earths. In theory, the effect is present for all excited-ground state γ -ray transitions, although its magnitude can be so low as to preclude detection with current techniques.

The unique feature of Mössbauer spectroscopy is the production of highly monochromatic radiation, so that it can be used to resolve minute energy differences, such as variations in the interaction of a nucleus with its electronic environment for

different compounds of the same element. To observe resonance, a range of gamma photon energies is scanned by employing the Doppler effect. The energy of the γ -ray emitted by a radioactive source as it collapses from an excited nuclear state to a lower state (always the ground state) is modulated by imparting a continuous range of velocities (v) to the source. The change in energy of the γ -ray (ΔE) relative to that emitted by the stationary source (E_γ) is given by

$$\Delta E = \frac{v}{c} E_\gamma$$

(where c is the velocity of light). The ΔE at which a particular compound absorbs is known as its Centre Shift (CS) relative to the source; and it arises predominantly because of a difference in the interaction between the charge distribution of the nucleus and those electrons which have a finite probability of being found in the region of the nucleus for source and absorber. A small shift, due to thermal motion of the Mössbauer atom, and known as the second order Doppler shift (SOD), can sometimes comprise part of the CS; but generally it is very small and can be neglected. For ^{119}Sn the CS, relative to a constant source, increases as the electron density for s electrons - the only ones which penetrate the nucleus - increases at the nucleus. Thus the CS is most sensitive to direct changes in s electron density, but will also change, to a lesser extent, on addition or removal of p or d electrons by deshielding.

Any nuclear state with a spin quantum number (I) $> \frac{1}{2}$ has a non-spherical charge distribution, giving rise to a quadrupole

term (among other multipoles). The magnitude of the charge deformation is described as the nuclear quadrupole moment (Q), whose sign depends on whether the nucleus is oblate (negative) or prolate (positive) with respect to the spin axis.

In many chemical compounds the electronic charge distribution is not spherically symmetric. The electric field gradient (efg), due to this non-symmetric electron environment, is the gradient of the electric field at the nucleus (E) which, in turn, is the negative gradient of the potential (V). Thus

$$\begin{aligned} \text{efg} &= \nabla E = -\nabla^2 V \\ &= - \begin{bmatrix} V_{xx} & V_{xy} & V_{xz} \\ V_{yx} & V_{yy} & V_{yz} \\ V_{zx} & V_{zy} & V_{zz} \end{bmatrix} \quad \dots (1.1) \end{aligned}$$

where $V_{xx} = \frac{\partial^2 V}{\partial x^2}$, $V_{xy} = \frac{\partial^2 V}{\partial x \partial y}$, etc.

Under a suitable transformation to axes X , Y and Z (called the "principal efg axes"), this tensor may be diagonalized, and the Laplace equation ($V_{xx} + V_{yy} + V_{zz} = 0$) requires that the tensor be traceless. Consequently, only two independent parameters are needed to specify the efg completely, and the two which are usually chosen are V_{zz} , and an asymmetry parameter, η , defined as $\eta = (V_{yy} - V_{xx})/V_{zz}$. Using the convention $|V_{xx}| \leq |V_{yy}| \leq |V_{zz}|$ ensures that $0 < \eta < 1$. By convention the axis system of the Mössbauer atom is defined so that V_{zz} is equal to eq, the maximum value of the efg (where $e \equiv$ electronic charge). The interaction

between eq and Q is called the quadrupole coupling, manifested in a Mössbauer spectrum as the Quadrupole Splitting (QS), which is equal to $\frac{1}{2}e^2qQ$ for ^{119}Sn . In general, the Hamiltonian describing the interaction is

$$\mathcal{H} = \frac{e^2qQ}{4I(2I-1)} (3I_z^2 - I(I+1) + \eta(I_x^2 + I_y^2)/2) \quad \dots(1.2)$$

where $I \equiv$ nuclear spin

and $I_{x,y,z} \equiv$ component spin operators.

When $I = 3/2$ (eg. for ^{119}Sn and ^{57}Fe) application of the Hamiltonian gives

$$QS = \frac{1}{2}e^2qQ(1 + \eta^2/3)^{1/2} \quad \dots(1.3)$$

A typical Mössbauer spectrum for ^{119}Sn is shown in figure 1.1. Since the selection rule $\Delta m_I = 0, \pm 1$ applies, two transitions occur. The corresponding energy level scheme in figure 1.2 corresponds to a positive QS, as the higher spin level lies at higher energy. The degeneracy of the $\pm 3/2$ and $\pm 1/2$ excited levels is lifted in the presence of a strong magnetic field, as shown in figure 1.2, and this is the most common method of determining the sign of the QS. However, exploitation of this phenomenon increases the complexity of the experiment considerably, and relatively few signs have been determined.

B. The Additivity Model

A semi-quantitative model, in which the QS of a compound is considered to be the sum of independent contributions from ligands about the Mössbauer atom, has facilitated the interpretation

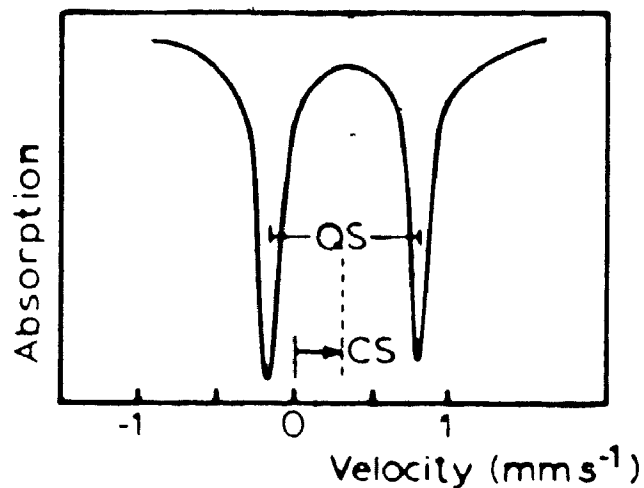


Figure 1.1: Typical ^{119}Sn Mossbauer Spectrum, with non-zero CS and QS (no applied magnetic field).

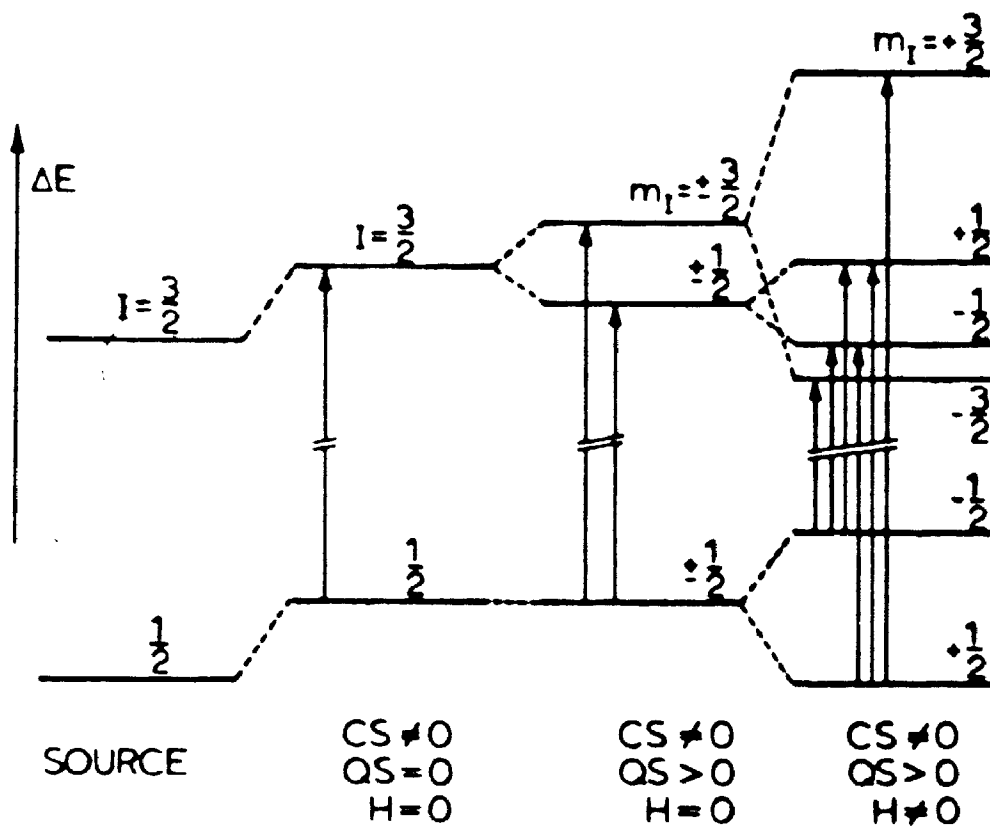


Figure 1.2: Nuclear Energy Level Diagram for ^{119}Sn ; showing quadrupole and magnetic (H) splitting.

of quadrupole splittings for a number of systems - such as Fe(II) low spin⁴, Fe(-II)⁵, and Sn(IV)⁶ - where the QS is determined purely by the nature and distribution of the metal-ligand bonds, and not by unequal occupation of sets of degenerate orbitals. Thus it should be useful in rationalizing QS values for compounds of other Mössbauer and nuclear quadrupole resonance nuclei where all valence shells are filled, half-filled or empty (eg. Ir(III), Ru(II), W(O), Co(III), Mn(I), Fe(III) high spin).

The simplest formulation of the additivity model is the point-charge approximation, where the contributions of the ligands about the Mössbauer atom to the efg, which are independent of each other, are similar to that of an array of point charges (Z_i) about the central atom (cf. the crystal field model for transition metal complexes). The elements of the efg tensor are given, in geometric form, in table 1.1; where r , θ and ϕ are the normal polar co-ordinate parameters. The term Z_i/r_i^3 will be approximately constant from compound to compound for any given ligand, and may be replaced by the constant $[L]$, which will represent the contribution of the ligand L to the efg, and is known as the "partial field gradient" of L .

The application of the additivity model to real chemical systems requires that a number of approximations be made, the most drastic of which are

- (a) that the QS can be regarded as a sum of the independent contributions from each ligand bound to the Mössbauer atom, and contributions from

table 1,1

The electric field gradient (EPG) tensor

$$\text{EPG} = \begin{bmatrix} V_{xx} & V_{xy} & V_{xz} \\ V_{yx} & V_{yy} & V_{yz} \\ V_{zx} & V_{zy} & V_{zz} \end{bmatrix}$$

$$V_{xx} = e \sum_i \frac{Z_i}{r_i^3} (3 \sin^2 \theta_i \cos^2 \phi_i - 1)$$

$$V_{yy} = e \sum_i \frac{Z_i}{r_i^3} (3 \sin^2 \theta_i \sin^2 \phi_i - 1)$$

$$V_{zz} = e \sum_i \frac{Z_i}{r_i^3} (3 \cos^2 \theta_i - 1)$$

$$V_{xy} = V_{yx} = e \sum_i \frac{Z_i}{r_i^3} (3 \sin^2 \theta_i \sin \theta_i \cos \phi_i)$$

$$V_{xz} = V_{zx} = e \sum_i \frac{Z_i}{r_i^3} (3 \sin \theta_i \cos \theta_i \cos \phi_i)$$

$$V_{yz} = V_{zy} = e \sum_i \frac{Z_i}{r_i^3} (3 \sin \theta_i \cos \theta_i \sin \phi_i)$$

It should be noted that the units of pfg ($=Z_i/r_i^3$) are those of q (rather than eq), consistent with the literature⁹.

other species (such as counter ions) are negligible;

(b) that the partial field gradient for a particular ligand L is constant from compound to compound, for a particular isotope with a given electronic state and co-ordination number;

(c) that all bond angles are ideal (e.g. that they are 90° in octahedral and 109.47° in tetrahedral complexes);

and (d) that principal efg axes will often correspond to high order molecular axes.

In the original formulation of this model for 119-tin by Parish and Platt⁶, the same pfg values were assigned to the same ligand in different stereochemical situations. However, it has been subsequently shown⁷ that much better agreement between theoretical and experimental results is obtained when different pfg values are assigned to a particular ligand when the co-ordination number of the Mössbauer atom is different. Exact mathematical relationships between the pfg values for a ligand in some different stereochemical situations have been derived.

Experimentally, pfg values are more easily determined and used as *partial quadrupole splittings* (pqs), where the two parameters have the relationship

$$\begin{aligned} (L) &= \frac{1}{2}e^2|Q|(L) \\ &\equiv \text{pqs of ligand L} \end{aligned}$$

The components of the efg, and thus the QS, have been calculated

for a number of stoichiometric configurations^{8,9}. In this study appropriate expressions and pqs values are derived for four coordinate tin, and applied to a large number of such compounds, including a number which contain a tin to transition metal bond.

The additivity model has also been formulated in terms of molecular orbital models for Fe(II) low spin⁴ and Sn(IV)⁷. The conclusions drawn from the MO treatments parallel those of the point charge formulation. This is to be expected, since additive electric field gradients are, in fact, manifestations of underlying special symmetry features, which have been elegantly elucidated by Clark¹⁰.

C. 129-Iodine Mössbauer Spectra

When the spin state of a nucleus is $>3/2$, more complex Mössbauer spectra are observed, and the analysis of the data to yield CS and QS values is not quite so straightforward. However, further useful parameters - such as the sign of the QS, n, and orbital populations - can often be calculated.

Iodine has at least two isotopic forms with high nuclear spin states, and Mössbauer spectra of iodine compounds may be obtained by utilizing either the 57.6 keV (7/2 \rightarrow 5/2) transition of ¹²⁷I, or the 27.7 keV (5/2 \rightarrow 7/2) transition of ¹²⁹I. Unfortunately both isotopes present problems. In the case of 100% naturally occurring ¹²⁷I, the resolution of the spectra is generally poor while, although ¹²⁹I spectra are generally well resolved, the necessity of synthesizing all absorbers from

radioactive ^{129}I presents considerable experimental inconvenience. For both isotopes the spins of the ground and excited states allow both η and the sign of e^2qQ to be determined from polycrystalline samples without the application of special techniques - unlike the case for ^{119}Sn and ^{57}Fe . The values of e^2qQ and η are complementary to those obtained from ^{127}I nuclear quadrupole resonance (nqr) spectra, but the extra parameters (i.e. the centre shift, and the sign of e^2qQ) available from Mössbauer spectra generally enable a more meaningful analysis of the data to be made.

The Mössbauer e^2qQ and η parameters are generally interpreted using the theory developed originally by Townes and Dailey¹¹ for analysing nqr spectra. This theory postulates that the principal contribution to the efg arises from an aspherical distribution of the valence electrons. Generally the 5d orbitals are little occupied, so that if 5d contributions to the efg are neglected, then

$$q = K_p (-N_{p_z} + \frac{1}{2}(N_{p_y} + N_{p_x})) \quad \dots(1.4)$$

where K_p is a constant. The latter term is often abbreviated as

$$U_p = -N_{p_z} + \frac{1}{2}(N_{p_y} + N_{p_x}) \quad \dots(1.5)$$

so that U_p is the p electron imbalance. The asymmetry parameter is given by

$$\eta = -3/2(N_{p_x} - N_{p_y})/U_p \quad \dots(1.6)$$

Using equation 1.4, the principal value of the molecular efg ($eq_{mol.}$) has been related to that for the atomic efg ($eq_{at.}$) by

$$eq_{mol.} = -eq_{at.} U_p \quad \dots(1.7)$$

The ground state e^2qQ for atomic 127-iodine has been accurately measured¹² as +2293 MHz. For convenience, e^2qQ values from 129-iodine Mössbauer spectra are generally converted to the 127-iodine scale, using the factor $^{127}Q/^{129}Q$, for comparison with 127-iodine nqr results. Hence, from equation 1.7, we may write

$$(e^2q \ ^{127}Q)_{mol} = -2293 U_p \quad (\text{MHz}) \quad \dots(1.8)$$

The centre shifts, δ , of iodine compounds depend directly on the 5s electron population, and indirectly (because of shielding) on the 5p population. If h_s and h_p are the magnitudes of the "holes" in the s and p shells, relative to the closed shells in I^- , then the centre shift with respect to an arbitrary source is given by

$$\delta = K[-h_s + \gamma(h_p + h_s)(2 - h_s)] + S \quad \dots(1.9)$$

where S is the shift of the source from I^- , and the constant K depends on $\delta R/R$. From the spectra of molecular iodine, the alkali iodides, and several oxyiodo-anions, the constants in equation 1.9 have been evaluated¹³, so that, relative to the commonly used $^{66}Zn, ^{129}Te$ source,

$$\delta_{ZnTe} = -9.2h_s + 1.5h_p - 0.54 \quad (\text{mm} \cdot \text{s}^{-1}) \quad \dots(1.10)$$

By definition

$$h_p = 6 - (N_{p_x} + N_{p_y} + N_{p_z}) \quad \dots(1.11)$$

Hence, if we wish to determine the parameters U_p , N_{p_x} , N_{p_y} , N_{p_z} , h_s and h_p from equations 1,5,6,8,10 and 11, we must make some assumptions to reduce the number of variables. If the iodine atom has a single bond or two co-linear bonds, then $n = 0$ and $N_{p_x} = N_{p_y}$. Another widely used assumption is that the bonding is purely p in character, so that $h_s = 0$. This assumption may be tested since, h_p and $|U_p|$ should be equal for pure p bonding.

In this study, ^{129}I Mössbauer spectroscopy has been applied in a series of square planar platinum (II) complexes of the types *trans*- $[\text{}^{129}\text{I}_2\text{PtX}]$ and *trans*- $[\text{}^{129}\text{I}_2\text{PtL}]\text{PF}_6$ ($Q = \text{Me}_2\text{PhP}$; $X = \text{I}$, CF_3 , Me ; $L = \text{P}(\text{OMe})_3$, $\text{P}(\text{OMe})_2\text{Ph}$, PPh_3 , AsPh_3 , EtNC , $p\text{-MeO.C}_6\text{H}_4.\text{NC}$), to investigate the effect of *trans* ligands on the ^{129}I Mössbauer parameters (see Chapter 6).

The analysis of iodine Mössbauer spectra is still somewhat of a problem. Most recent workers have used numerical iterative methods to extract the ^{129}I Mössbauer parameters. However the very large χ^2 values reported recently¹⁵ point out some of the problems associated with this method. For example, $Q(5/2)/Q(7/2)$ - which is not yet accurately established - has to be assumed, and peak intensities have to be constrained to their expected values for random samples with no Goldanskii-Karyagin effects. As part of this investigation, the analytical method of

Williams and Bancroft¹⁶ for multiline Mössbauer spectral analysis was tested, and the method and conclusions are described in appendix 1. This method yielded accurate parameters with no approximations and straightforward calculations.

In addition, the errors which occur in e^2qQ and η values as a result of errors in line positions have been statistically estimated (in appendix 2), using a method widely employed in Econometrics¹⁷. This method enables checks of the internal and external consistency of the Williams-Bancroft method of analysis of the data to be made.

D. Mössbauer Experimental Technique and Spectral Data Processing

(i) 119-Tin Spectra

With the exception of the three magnetic spectra - which were run at PCMU, Harwell, U.K., and are described in chapter 2 - all ¹¹⁹Sn Mössbauer spectra reported in this thesis were run in the way most commonly used⁹ by chemical Mössbauer researchers. A sample compound, in the form of a polycrystalline solid, was sealed in a perspex holder and cooled to -77K by attachment to a copper rod which dipped into a large dewar filled with liquid nitrogen. The sample assembly was insulated from ambient temperatures by a cover of thick polystyrene foam. The sample was then subject to radiation from a 5 mCi radioactive source of Ba ^{119m}SnO₃, in the form of a solid embedded in a perspex disc, supplied by New England Nuclear Corporation.

The source was driven through a velocity range of approx-

imately $\pm 4.5 \text{ mm s}^{-1}$ using a vibrator assembly and drive unit (Austin Science Associates, Texas, U.S.A.), which scanned the velocity range linearly. The form of the vibrational motion was a symmetric "saw-tooth", so that mirror image spectra were produced, corresponding to positive and negative velocity scans of the same range of values.

The 23.9 keV gamma ray for $^{115m}\text{Sn} \rightarrow ^{115}\text{Sn}$ was selectively detected, using a proportional counter with a detection tube of CO_2 -quenched krypton at 1 atmosphere. A 512 channel analyser (Nuclear Data Corp., Chicago, U.S.A.) was used to store the counts from the detector, the channels being synchronised with the velocity scan, so that each channel corresponded to a constant velocity increment. The instrument was calibrated using four of the six lines of the ^{57}Fe Mössbauer spectrum of 99.99% natural iron foil, whose line positions are accurately known³.

The source radiation for Mössbauer experiments is highly monochromatic. The ratio of the linewidth of the gamma beam to the energy of the radiation itself is generally $\sim 10^{-12}$, so that the monochromaticity of this radiation is unequalled in any other branch of spectroscopy³. Because the radiation does not have to be collimated using slits,

peaks encountered in Mössbauer spectra have very well defined Lorentzian profiles. Consequently the digital data produced in the Mössbauer experiments were fitted to the sum of appropriate numbers of Lorentzian line shapes (generally 1 or 2) using non-linear multiple regression methods. This was achieved with a

FORTRAN IV computer program written by Dr. A. J. Stone, University of Cambridge, U.K., which is an updated version of that described in reference 18. The constraint facility of this program enabled the detection of small, visually unresolved splittings.

Approximately 300,000 - 1,000,000 counts/channel were accumulated for all spectra. χ^2 values were in the range 450 - 550, linewidths for individual lines were 0.9 - 1.2 mm s⁻¹, and reproducibility of the parameters was within 0.02 mm s⁻¹.

(ii) 129-Iodine Spectra

129-Iodine Mössbauer spectra were recorded over 248 channels at PCMU, Harwell, U.K., on polycrystalline samples, using a ⁶⁶Zn¹²⁹Te source, with both source and absorbers at 4.2K. The resulting spectra were fitted as the sum of 9 component Lorentzian lines, by the regression method just described for tin spectra. The very small ninth peak is due to adsorbed or residual Na¹²⁹I. Consequently, the peak due to this impurity was fixed at its reported¹² value (-0.46 mm s⁻¹), and the widths of all the lines constrained to be equal. The intensity of the peak due to ¹²⁹I⁻ was never greater than 1.5% of the total, but the fits to 9 lines generally gave a significantly better χ^2 value than an 8 peak fit. For example, for the compound trans-[¹²⁹IQ₂Pt(OMe)₃]PF₆, the peak due to Na¹²⁹I accounted for <1% of the total intensity, but the χ^2 improved by 50 from an 8 line to a 9 line fit.

E. References

1. R. L. Mössbauer; *Naturwissenschaften* (1958) 45, 538.
2. O. C. Kistner and A. W. Sunyar; *Phys. Rev. Lett.* (1960) 4, 412.
3. "Mössbauer Effect Data Index (1972)"; edited by J. G. Stevens and V. E. Stevens, Plenum, N. Y. (1973).
4. G. M. Bancroft, M. J. Mays and B. E. Prater; *J. Chem. Soc. (A)* (1970), 956.
5. R. A. Mazak and R. L. Collins; *J. Chem. Phys.* (1969) 51, 3220.
6. R. V. Parish and R. H. Platt; *J. Chem. Soc. (A)* (1969), 2145; *Inorg. Chim. Acta* (1970) 4, 65.
7. M. G. Clark, A. G. Maddock and R. H. Platt; *J. C. S. Dalton* (1972), 281.
8. G. M. Bancroft, K. D. Butler and A. T. Rake; *J. Organomet. Chem.* (1972) 34, 137.
9. G. M. Bancroft and R. H. Platt; *Adv. Inorg. Radiochem.* (1972) 15, 59.
10. M. G. Clark; *Mol. Phys.* (1971) 20, 257.
11. C. H. Townes and D. P. Dailey; *J. Chem. Phys.* (1949) 17, 782.
12. D. W. Hafmeister, G. De Pasquali and H. De Waard; *Phys. Rev.* (1964) 135B, 1089; G. J. Perlow and M. R. Perlow; *J. Chem. Phys.* (1966) 45, 2193.
13. V. Jaccarino, J. G. King, R. A. Satten and H. H. Stroke; *Phys. Rev.* (1954) 94, 1798.
14. J. R. Gabriel and S. L. Ruby; *Nucl. and Instr. Methods* (1965) 36, 23.
15. B. W. Dale, R. J. Dickinson and R. V. Parish; *Chem. Comm.* (1974), 35; *Chem. Phys. Lett.* (1974) 24, 286.
16. P. G. L. Williams and G. M. Bancroft; *Mol. Phys.* (1970) 19, 717; *Mössbauer Effect Methodology* (1971) 7, 39.
17. R. J. Wonnacott and T. H. Wonnacott; "Econometrics", (1970) Wiley, New York; p. 265.
18. A. J. Stone; appendix to G. M. Bancroft, W. K. Ong, A. G. Maddock, R. H. Prince and A. J. Stone; *J. Chem. Soc. (A)* (1967), 1966.

CHAPTER 2

Measurement of Mössbauer Parameters in Four Co-ordinate Compounds Containing a Tin-Transition Metal Bond

A. Introduction

Before the work described in this thesis was undertaken, the 119-tin Mössbauer spectra for compounds containing a tin to transition metal bond had been the subject of a number of papers¹⁻⁴; and other studies of this kind have appeared in the literature more recently⁵⁻¹⁴. These compounds are generally of the type $R_l X_m SnM_n$ ($R = Me, Et, Bu, Ph, C_6F_5$; $X = Cl, Br, I, NCS, CH_3COO$; $M = Cr(CO)_3cp, Mn(CO)_5, Fe(CO)_2cp, Co(CO)_6, Mo(CO)_3cp, Re(CO)_5, W(CO)_3cp$; $l + m + n = 4$).

In this study, the ^{119}Sn Mössbauer spectra of more of these compounds has been undertaken, initially to elucidate some of the bonding characteristics of metal-metal bonds, and to investigate the reason for the large QS values observed^{1,2} for low symmetry four co-ordinate tin compounds. The work was later extended to fill gaps in the series of compounds already reported, and to rationalize and systematize the Mössbauer parameters observed in terms of structure and bonding. This latter objective has been

achieved for QS values in terms of an additivity model, whose application to these systems will be described in Chapter 3.

In order to test the ability of the additivity model to predict other Mössbauer parameters - such as η , and the sign of the QS - the magnetic spectra of three key compounds were also recorded, to augment the limited number of such spectra reported^{7,8} in the literature.

B. Results

The ^{119}Sn Mössbauer parameters which have been measured for 50 compounds containing both a tin atom and at least one transition metal atom are listed in table 2.1. Typical spectra are shown in figure 2.1. Agreement between these results and those which have been reported for several of the compounds in previous^{1,2,4} and subsequent^{5-7,10-13} studies, is generally good. Compound 25, $\text{Ph}_2\text{Sn}[\text{Co}(\text{CO})_4]_2$, has been widely studied, and various CS and QS values reported^{1,4,13}. The parameters given by Parish¹³ agree closely with those measured in this laboratory. For compound 31, $\text{ClSn}[\text{Co}(\text{CO})_4]_2$, the CS (1.93 mm s^{-1}) and QS (1.78 mm s^{-1}) values reported recently¹¹ are not in good agreement with those found in this study.

In the cases of the Ph_3SnM compounds ($\text{M} = \text{Mn}(\text{CO})_5$, $\text{Fe}(\text{CO})_2\text{cp}$), compounds 6 and 11, quadrupole splitting was not reported previously^{1,3,12}. Both one peak and two peak computed fits to the data for $\text{Ph}_3\text{SnMn}(\text{CO})_5$ are shown in figure 2.2. For both the Mn- and Fe-bonded triphenyltin compounds, χ^2 values

table 2.1

^{119}Sn Mössbauer Parameters Observed for some
TIn-Transition Metal Bonded Complexes at ~ 78 K
(mm s^{-1} ; CS relative to BaSnO_3)

Compound	CS ^a	QS ^a	$\Gamma_{1,2}^b$
1. $\text{Me}_2\text{SnMn}(\text{CO})_6$	1.41	0.82	1.13, 1.06
2. $\text{Me}_2\text{ClSnMn}(\text{CO})_6$	1.52	2.60	1.08, 1.09
3. $\text{MeCl}_2\text{SnMn}(\text{CO})_6$	1.62	2.62	1.13, 1.11
4. $\text{Cl}_3\text{SnMn}(\text{CO})_6$	1.65	1.60	1.17, 1.13
5. $\text{Br}_3\text{SnMn}(\text{CO})_6$	1.76	1.53	1.23, 0.98
6. $\text{Ph}_3\text{SnMn}(\text{CO})_6$	1.35	0.41 \pm 0.10	0.97, 1.04
7. $\text{Cl}_3\text{SnMn}(\text{CO})_6(\text{Ph}_3\text{P})$	1.70	1.69	0.91, 0.95
8. $\text{Ph}_3\text{SnMn}(\text{CO})_6(\text{Ph}_3\text{P})$	1.42 \pm 0.05	<0.30	1.26
9. $[\text{Ph}_3\text{As}^+][\text{Cl}_3\text{SnMn}(\text{CO})_6\text{cp}^-]$	2.13 \pm 0.05	1.84 \pm 0.05	1.11, 1.17
10. $[\text{Ph}_3\text{As}^+][\text{Cl}_3\text{SnMn}(\text{CO})_6\text{Me-cp}^-]$	2.13 \pm 0.05	1.88 \pm 0.05	1.12, 1.15
11. $\text{Ph}_3\text{SnFe}(\text{CO})_5\text{cp}$	1.39	0.32 \pm 0.10	0.97, 0.98
12. $\text{Cl}_3\text{SnFe}(\text{CO})_5\text{cp}$	1.75	1.83	1.03, 1.11
13. $\text{Br}_3\text{SnFe}(\text{CO})_5\text{cp}$	1.86	1.63	1.14, 0.92
14. $\text{Cl}_3\text{SnFe}(\text{CO})_5(\text{Ph}_3\text{P})\text{cp}$	1.86	1.83	1.10, 1.04
15. $\text{Cl}_3\text{SnFe}(\text{CO})_5(\text{P}(\text{OPh})_3)\text{cp}$	1.79	1.82	1.14, 0.96
16. $\text{cis}-(\text{Cl}, \text{Sn})\text{ClFe}(\text{p-MeO.C}_6\text{H}_4.\text{NC})_2$	2.02 \pm 0.05	1.77 \pm 0.05	1.05, 1.05
17. $\text{trans}-(\text{Cl}, \text{Sn})_2\text{Fe}(\text{p-MeO.C}_6\text{H}_4.\text{NC})_2$	1.82	1.74	1.05, 1.05
18. $\text{trans}-(\text{Cl}, \text{Sn})_2\text{Fe}(\text{p-MeO.C}_6\text{H}_4.\text{NC})_2$	1.88	1.72	1.10, 1.10
19. $[(\text{Cl}, \text{Sn})\text{Fe}(\text{p-MeO.C}_6\text{H}_4.\text{NC})_2][\text{ClO}_4^-]$	1.85 \pm 0.05	1.70 \pm 0.05	1.15, 1.15

table 2.1 (cont'd)

Compound	CS ^a	QS ^a	$\tau_{1,2}^b$
20. MeSn[Co(CO) ₄] ₂	1.79	1.29	1.01, 1.01
21. Me ₂ Sn[Co(CO) ₄] ₂	1.57	1.53	1.04, 1.02
22. Me ₃ SnCo(CO) ₄	1.39	1.73	1.05, 1.05
23. Me ₂ ClSnCo(CO) ₄	1.49	2.73	1.20, 1.24
24. MeClSn[Co(CO) ₄] ₂	1.74	2.38	1.07, 1.34
25. Ph ₂ Sn[Co(CO) ₄] ₂	1.60	1.27	1.07, 1.07
26. Ph ₃ SnCo(CO) ₄	1.41	1.20	1.01, 1.01
27. Ph ₂ ClSnCo(CO) ₄	1.48	2.18	1.00, 1.02
28. PhClSn[Co(CO) ₄] ₂	1.70	1.88	1.10, 1.05
29. Sn[Co(CO) ₄] ₄	2.04	0.0	1.11
30. FSn[Co(CO) ₄] ₂	1.75	0.97	1.05, 1.05
31. ClSn[Co(CO) ₄] ₂	2.05	1.42	1.02, 0.98
32. Cl ₂ Sn[Co(CO) ₄] ₂	1.75	1.44	1.01, 1.11
33. Cl ₃ SnCo(CO) ₄	1.42	1.20	1.02, 1.02
34. Br ₂ Sn[Co(CO) ₄] ₂	1.75	1.46	1.03, 1.03
35. I ₂ Sn[Co(CO) ₄] ₂	1.86	1.07	1.12, 1.12
36. Me ₂ Sn[Co(CO) ₄][Mn(CO) ₅]	1.55	1.46	0.97, 1.00
37. PhClSn[Co(CO) ₄][Co(CO) ₅ (Ph ₃ P)]	1.67	2.00	1.07, 1.15
38. Ph ₂ Sn[Co(CO) ₄ (NBD)]	1.60	0.83	1.02, 1.03

table 2.1 (cont'd)

Compound	CS ^a	QS ^a	$\Gamma_{1,2}^b$
39. Cl ₂ Sn[M(CO) ₂ cp] ₂	1.87±0.05	2.15±0.05	1.20, 1.27
40. Cl ₂ SnM(Ph ₃ P)cp	1.76	2.01	1.06, 1.06
41. Cl ₂ SnM(Ph ₃ P)cp·CH ₂ Cl ₂	1.80	2.06	1.06, 1.02
42. Cl ₂ SnM(Ph ₃ P)cp·(CH ₃) ₂ CO	1.81	1.97	1.06, 1.01
43. [Cl ₂ Sn ⁻][M(Ph ₃ P) ₂ cp ⁺]	3.15	1.29	1.06, 1.02
44. [Cl ₂ Sn ⁻][M(Ph ₃ P) ₂ cp ⁺].1.3CH ₂ Cl ₂	3.18	1.20	1.11, 1.09
45. [Cl ₂ Sn ⁻][M(Ph ₃ P) ₂ cp ⁺].(CH ₃) ₂ CO	3.19	1.24	1.06, 1.06
46. [Cl ₂ Sn ⁻][M(Ph ₃ P) ₂ cp ⁺].CH ₃ OH	3.21	1.33	1.07, 1.11
47. [Cl ₂ Sn ⁻][M(Ph ₃ P) ₂ cp ⁺].THF	3.11	1.29	1.06, 1.13
48. [Cl ₂ Sn ⁻][M(Ph ₃ P) ₂ cp ⁺].C ₆ H ₆	3.15	1.23	1.01, 0.99
49. [Cl ₂ Sn ⁻][M(dppe)cp ⁺]	3.20	1.49	1.06, 1.07
50. <i>trans</i> -(Me ₂ Sn) ₂ Pt(Ph ₃ P) ₂	1.31	0.57	1.03, 1.03

a ±0.02 unless otherwise shown

b ±0.05

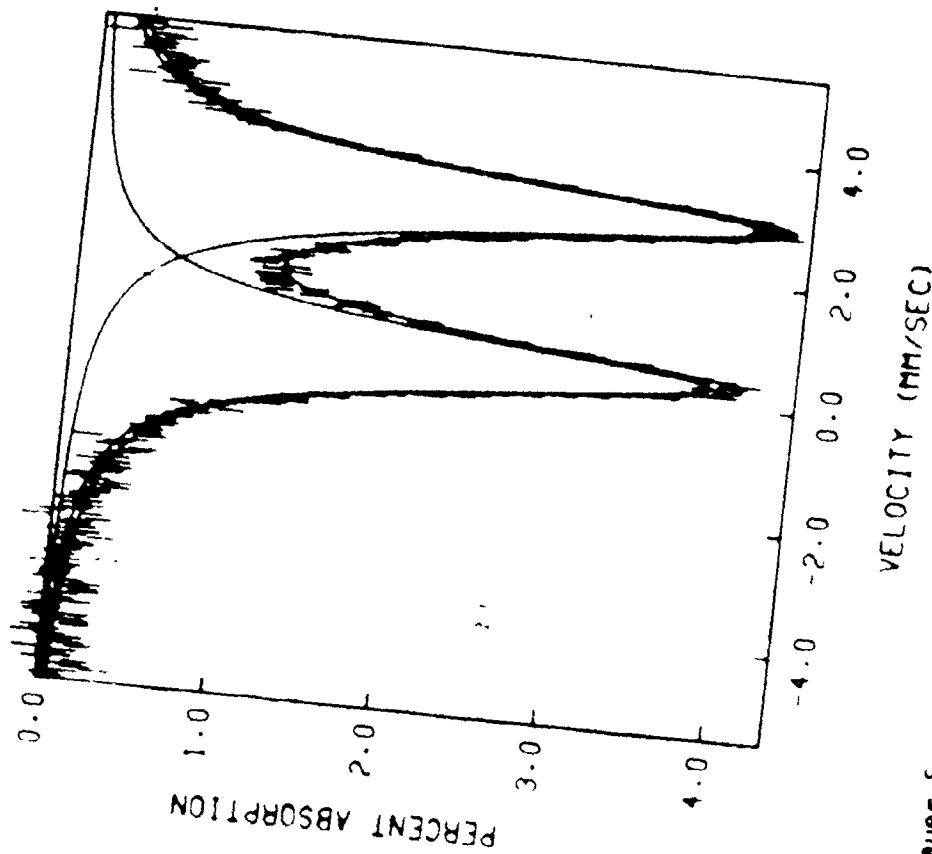
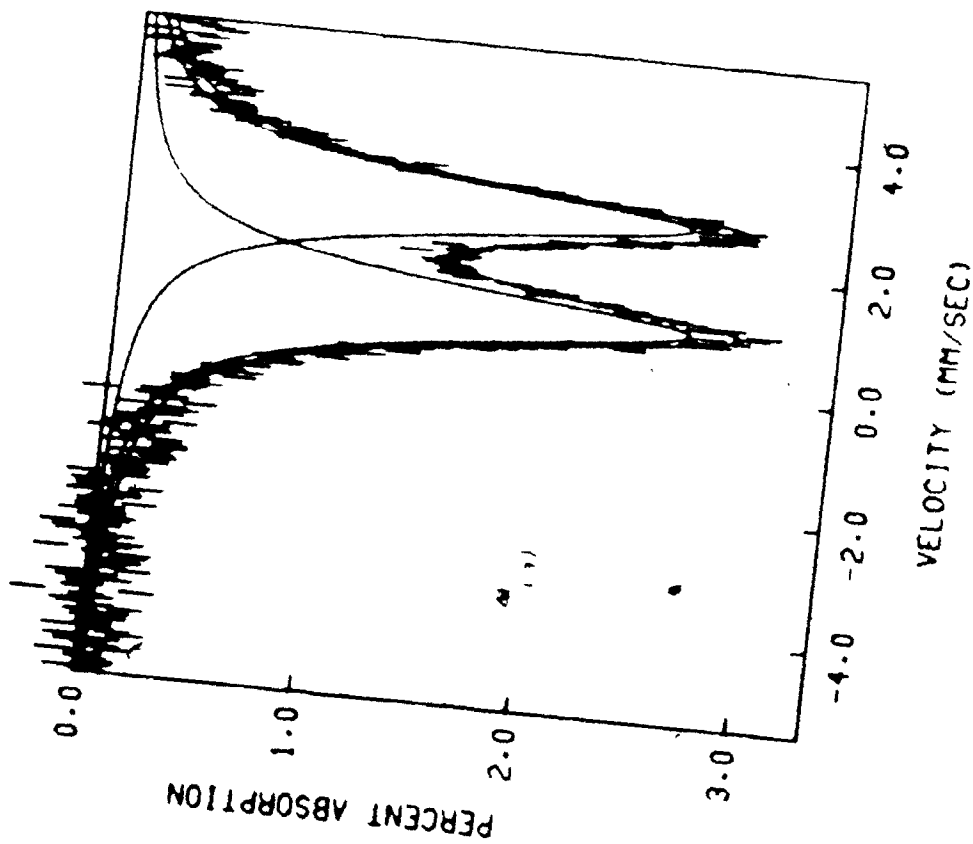


Figure 2.1: ^{119}Sn Mössbauer Spectra of
 (a) $\text{Crans}-(\text{Cl}, \text{Sn})$, $\text{Fe}(\text{p-MeO.C}_6\text{H}_4.\text{NC})_2$, and (b) MeCl , $\text{SnMn}(\text{CO})_6$
 at -78K ; showing computed Lorentzian fits to the data.

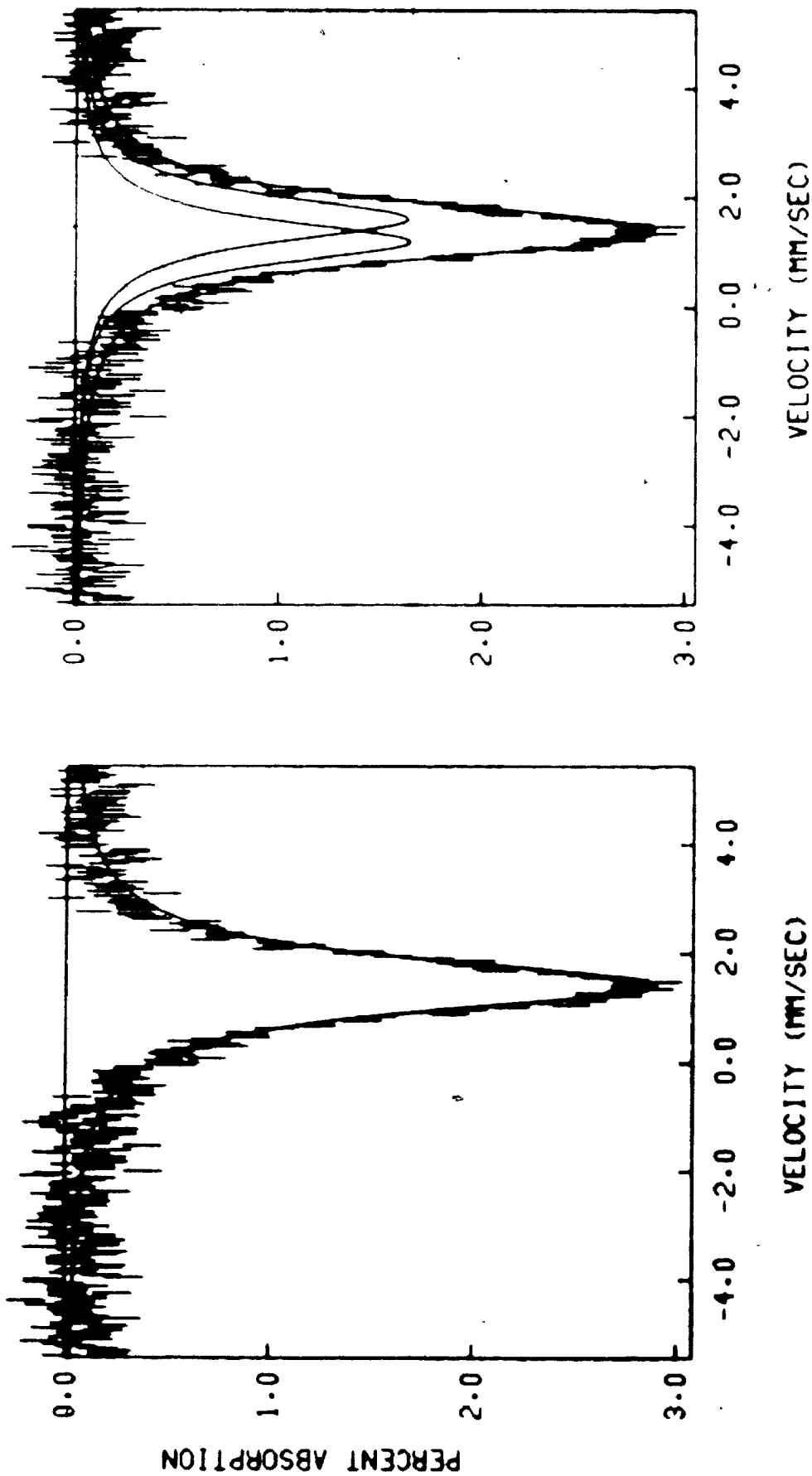


Figure 2.2: ^{119}Sn Mössbauer spectrum of $\text{Ph}_3\text{SnMn(CO)}$, at -78K , showing

(a) one peak and (b) two peak fits to the data.

24

for two peak fits to the spectra were over 50 smaller than for one peak fits. The errors in these small QS values are, of course, relatively large. However, for $\text{Ph}_3\text{SnMn}(\text{CO})_4(\text{Ph}_3\text{P})$, compound 8, one and two peak fits to the spectrum yielded χ^2 values which differed by less than 10. It is likely, though, that the QS is non-zero, since the one peak fit has a width at half height greater than that observed for well resolved individual peaks for the other compounds.

Absorptions for all samples were in the range 2 - 11%. Compounds containing a cobalt atom generally showed lower absorption than those containing manganese, iron and nickel; except where the latter also contained arsenic or iodine. Also, the percent absorption for the ionic tin-nickel compounds (43 - 49) was less than half that for the tin-nickel bonded species (compounds 39 - 42), consistent with the greater sensitivity of Sn(IV) relative to Sn(II) noted previously¹⁵.

One of the most striking features of the QS data concerns the three series of compounds $\text{R}_l\text{X}_m\text{SnM}_n$ (i.e. compounds 1,2,3,4 ; 22,23,24,33 ; 26,27,28,33). The QS values for the compounds in these series where $l, m, n \neq 0$ are much larger than the related compounds where one of l, m or n is zero. It is noticeable, too, that the nickel-containing compounds fall into two distinct groups with respect to CS values. The ionic compounds have $\text{CS} \sim 3.2$, while the neutral complexes have $\text{CS} \sim 1.8$. Parameters for all the phosphine and phosphite substituted compounds are within 0.15 cm^{-1} of those measured for the parent carbonyl

complexes.

The signs of the quadrupole splittings and the values of η for $\text{Me}_2\text{ClSnMn}(\text{CO})_5$, $\text{MeCl}_2\text{SnMn}(\text{CO})_5$ and $(\text{C}_6\text{F}_5)_3\text{SnMn}(\text{CO})_5$ were determined by recording their ^{119}Sn Mössbauer spectra at 4.2K in the presence of a very strong magnetic field. The spectra for two of these compounds are shown in figures 2.3a and b. Best computed fits to the spectra gave the results shown in table 2.2.

table 2.2

Mössbauer Parameters Derived from Magnetic Spectra, at 4.2K

<u>compound</u>	<u>QS (mm s⁻¹)</u>	<u>η</u>
$\text{Me}_2\text{ClSnMn}(\text{CO})_5$	-2.70	0.35
$\text{MeCl}_2\text{SnMn}(\text{CO})_5$	+2.66	0.46
$(\text{C}_6\text{F}_5)_3\text{SnMn}(\text{CO})_5$	+0.99	0.0

The errors in η are considered to be ± 0.05 . It can be seen from figure 2.3 that line intensities, though not line positions, for the observed and computed spectra do not match perfectly. This will not affect the derived parameters, and is probably caused by Goldanskii-Karyagin effects or a small amount of accidental crystal orientation in the randomized samples.

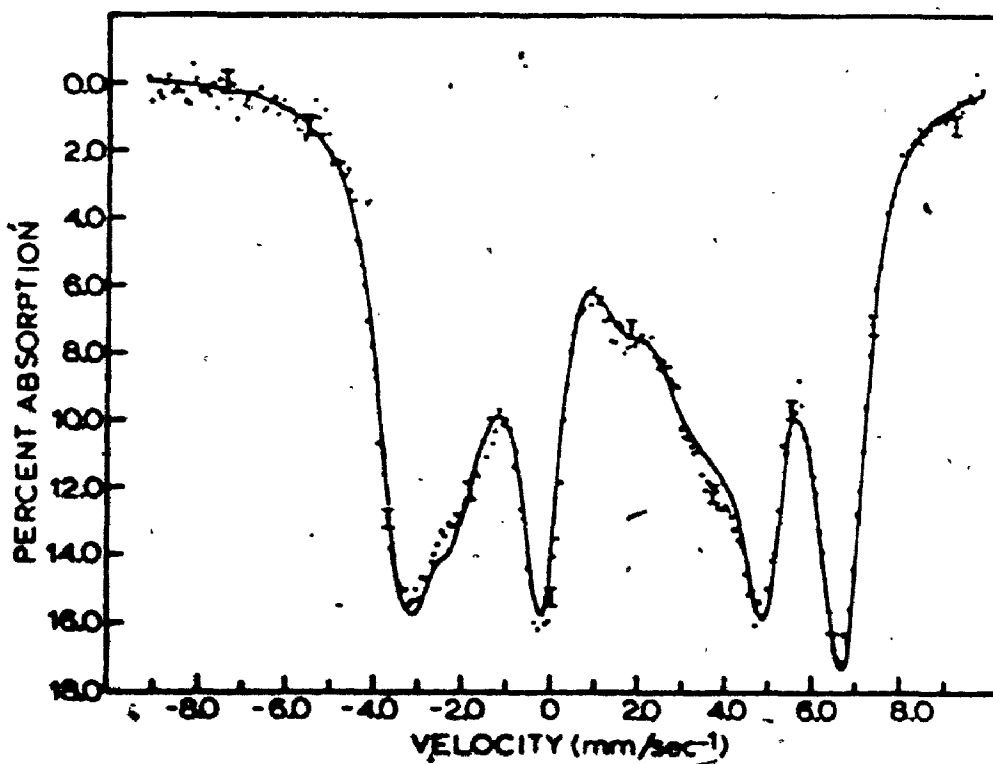
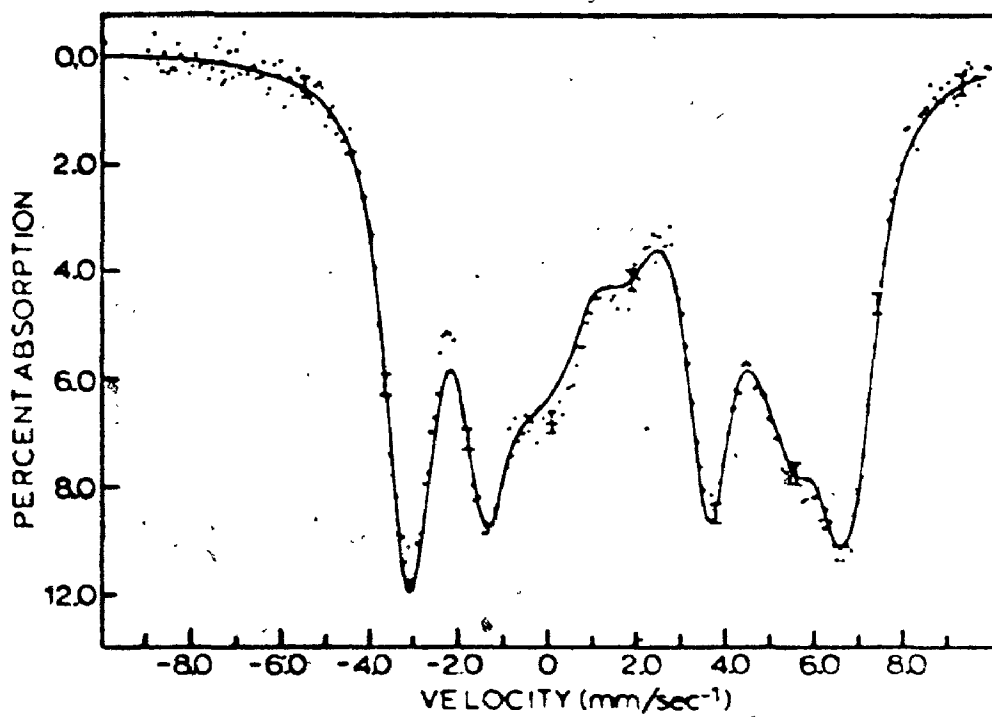


Figure 2.3: ^{119}Sn Mössbauer spectra of (a) $\text{MnCl}_2\cdot\text{SnMn}(\text{CO})_8$ and (b) $\text{Mn}_2\text{ClSnMn}(\text{CO})_8$ at 4.2K in a magnetic field of 42 kG. The solid line gives the best computed fit to the spectral data.

C. Compounds Containing Tin and Nickel

The existence of a covalent tin-nickel bond has not yet been established, in any compound, from X-ray diffraction results. However, a direct bond between nickel and a group IVA element was shown to be present in $\text{Cl}_3\text{GeNi}(\text{Ph}_3\text{P})\text{cp}^{16}$, and a closely related metal-metal bond was also found in $\text{Cl}_3\text{SnPd}(\text{Ph}_3\text{P})(\text{h}^3\text{-C}_5\text{H}_5)^{17}$, both from X-ray crystallographic studies.

The CS values found for the tin and nickel containing compounds being studied here are discussed in chapter 4, and these data indicate that in compounds 39 to 42 (table 2.1), tin and nickel are covalently bonded, while compounds 43 to 49 are ionic, having the general form $[\text{Ni}(\text{L})_2\text{cp}^+][\text{SnCl}_3^-]$.

The presence of the solvent molecules in a number of these compounds is established from elemental analyses, and from infrared and ^1H nmr spectra. The proportion of the solvent molecules in the compounds were established by the same methods, and by weight loss studies by van den Akker and Jellinek¹⁸.

The role of the solvent molecules in these compounds is not clear. In the original report¹⁸ of the synthesis of compounds 44 and 45, the authors formulated the structures of the ionic compounds as $[\text{cpNi}(\text{Ph}_3\text{P})_2]^+[\text{solvent.SnCl}_3^-]$, on the basis of infrared data for acetone and dichloromethane. The $\nu(\text{CO})$ band of acetone in compound 45 was at 1705 cm^{-1} (cf. 1712 cm^{-1} found in this study) compared with 1740 cm^{-1} in gaseous acetone. A similar reduction of 23 cm^{-1} in the (C-Cl) stretching frequency for CH_2Cl_2 was noted¹⁸ for compound 44 compared with gaseous dichloromethane. The

^1H nmr signals due to the solvent molecules were not shifted from those of the free solvent, but that is possibly due to dissociation in solution.

However, the Mössbauer CS and QS parameters are almost invariant for all the compounds containing solvent molecules (which should have widely different potential bonding modes) and for the compound (43) containing no solvent at all; suggesting that the solvent molecules are not bonded to the tin atom. Confirmation of this assertion comes from the compound $[\text{cpNi}(\text{Ph}_3\text{P})_2]^+[\text{PF}_6]^-$.acetone, whose infrared $\nu(\text{CO})$ band is a narrow doublet at $1709/1713\text{ cm}^{-1}$, little different from the position of the band for the corresponding tin-containing compound. In addition, it has been shown¹⁷, from an X-ray diffraction study, that the acetone molecule in the metal-metal bonded compound $(\text{Cl}_2\text{Sn})\text{Pd}(\text{Ph}_3\text{P})(\text{h}^3\text{-C}_6\text{H}_5)0.4$ acetone is not bound to any other atom in the molecule. The $\nu(\text{CO})$ band for acetone in this compound occurs at 1710 cm^{-1} , close to the values observed here for the acetone-containing compounds. Similarly, the structure of the compound $[\text{Co}(\text{dppe})_2\text{Cl}]^+[\text{SnCl}_3]^-$ in solvated form (with $\text{C}_6\text{H}_5\text{Cl}$) is known from a diffraction study¹⁹. It contains a discrete SnCl_3^- ion, and the $\text{C}_6\text{H}_5\text{Cl}$ molecule is not bonded to either the anion or cation, both of which have very similar geometries to the same ions in the unsolvated form of the compound.

The solvent molecules are surprisingly difficult to remove from the ionic compounds if they are not bonded, acetone and dichloromethane only being removed from compounds 45 and 44 at

850 and 1150 $^{\circ}$ C respectively under vacuum¹⁸. On the other hand, it is difficult to prevent the spontaneous loss of dichloromethane from the neutral compound 41 at room temperature. The $\nu(\text{C}-\text{Cl})$ infrared band for the neutral and ionic compounds containing CH_2Cl_2 differ by only 6 cm^{-1} .

The CS observed for compound 49, which has a chelating phosphine co-ordinated to nickel, is not significantly different from the related ionic complexes containing two triphenylphosphine ligands. However, the QS for this compound is somewhat larger than the Ph_3P analogues, which suggests that the geometry of the three chlorine ligands about the tin has altered somewhat. The correlation of CS and QS for Cl_3SnM compounds (M = transition metal complex ligand) by Mays and Sears²⁰ suggests that, for a CS of -3.2, an increase in QS reflects an increase in the $\text{Cl}-\text{Sn}-\text{Cl}$ angles in the $\text{Cl}_3\text{Sn}^{\text{r}}$ moiety.

D. Experimental

Except for the new compounds (numbers 36, 37, 49, 46 and 47 in table 2.1), the tin-transition metal compounds examined in this study were synthesised using methods outlined in references 21 - 24 (Sn/Mn compounds), 21, 25 - 27 (Sn/Fe compounds), 28 (Sn/Co compounds) and 16, 18, 28 - 30 (Sn/Ni compounds). Identity and purity of all compounds was checked from melting points, and infrared and nmr spectra. New compounds were synthesised by the methods described below, and the physical and analytical data for them are shown in table 2.3. Microanalyses were performed

table 2.3

Analytical Data for some TIn-Transition Metal Complexes

Compound	Colour	C		H		Cl	
		Found	calc.	Found	calc.	Found	calc.
$\text{Me}_2\text{Sn}[\text{Co}(\text{CO})_2][\text{Mn}(\text{CO})_5]$	orange	25.9	25.7	1.35	1.20	-	-
$\text{PhClSn}[\text{Co}(\text{CO})_2][\text{Co}(\text{CO})_2(\text{Ph}_3\text{P})]$	yellow	47.1	46.1	2.15	2.50	4.8	4.4
$[\text{Cl}_2\text{Sn}][\text{Ni}(\text{Ph}_3\text{P})_2\text{cp}]$	yellow-green	55.8	56.3	3.81	4.04	12.5	12.2
$[\text{Cl}_2\text{Sn}][\text{Ni}(\text{Ph}_3\text{P})_2\text{cp}] \cdot (\text{CH}_3)_2\text{CO}$	yellow-green	56.0	56.7	4.17	4.44	12.1	11.4
$[\text{Cl}_2\text{Sn}][\text{Ni}(\text{Ph}_3\text{P})_2\text{cp}] \cdot \text{CH}_3\text{OH}$	yellow-green	55.3	55.7	4.09	4.34	11.2	11.8
$[\text{Cl}_2\text{Sn}][\text{Ni}(\text{Ph}_3\text{P})_2\text{cp}] \cdot \text{THF}$	yellow-green	57.2	57.2	4.19	4.58	11.9	11.3
$[\text{Cl}_2\text{Sn}][\text{Ni}(\text{dppe})\text{cp}]$	yellow	50.1	49.8	3.79	3.91	15.3	14.2

by Chemalytics Inc. (Arizona, U.S.A.). All compounds were made and stored under a nitrogen atmosphere, and carefully recrystallised from deoxygenated solvents immediately before Mössbauer spectra were run.

Dimethyl(pentacarbonylmanganese)(tetracarbonylcobalt)tin(IV)

One mole equivalent of $\text{Co}(\text{CO})_4^-$ (formed by dissolving $\text{Co}_2(\text{CO})_8$ in methanol) was added to a solution of $\text{Me}_2\text{ClSnMn}(\text{CO})_5$ in THF, under nitrogen with stirring. The solvent was removed under vacuum, and the orange product, $\text{Me}_2\text{Sn}[\text{Co}(\text{CO})_4][\text{Mn}(\text{CO})_5]$, recrystallised twice from pentane, with cooling. (yield 68%)

Chlorophenyl(tetracarbonylcobalt)(triphenylphosphinetricarbonylcobalt)tin(IV)

One mole equivalent of triphenylphosphine was added to solid $\text{PhClSn}[\text{Co}(\text{CO})_4]_2$ in a flask, and the reactants were heated together on a steam bath, under vacuum, for fifteen minutes. The crude yellow product was extracted with pentane, the volume reduced, and the product, $\text{PhClSn}[\text{Co}(\text{CO})_4][\text{Co}(\text{CO})_3(\text{Ph}_3\text{P})]$, precipitated by cooling. (yield 53%)

Tin-nickel compounds

$\text{Cl}_2\text{Sn}[\text{Ni}(\text{CO})\text{cp}]_2$ was synthesised by insertion of SnCl_2 into $[\text{Ni}(\text{CO})\text{cp}]_2$, as in reference 28; and $\text{Cl}_2\text{SnNi}(\text{Ph}_3\text{P})\text{cp} \cdot \text{CH}_2\text{Cl}_2$ by insertion of SnCl_2 into $\text{cpNi}(\text{Ph}_3\text{P})\text{Cl}$, as in reference 18. Dichloromethane was removed from the latter compound under vacuum at room temperature to yield unsolvated $\text{Cl}_2\text{SnNi}(\text{Ph}_3\text{P})\text{cp}$. Addition of another mole equivalent of Ph_3P to this compound in

dichloromethane precipitated $[\text{Ni}(\text{Ph}_3\text{P})_2\text{cp}^+][\text{SnCl}_3^-] \cdot 1.33 \text{ CH}_2\text{Cl}_2$ in over 90% yield^{18,29}. For this ionic compound, CH_2Cl_2 could be removed under vacuum only when heated to 115°C ¹⁸. The solvent adducts were prepared by recrystallization from the appropriate solvent. In the cases of THF, acetone and methanol, the compound dissociated extensively to $\text{cpNi}(\text{Ph}_3\text{P})\text{cp}$ and SnCl_2 in solution^{18,29,30}, but the required product crystallised on cooling overnight at -20°C . However, because of this reaction, recrystallisation did not appreciably purify these compounds. The acetone and benzene solvates have been previously reported^{16,18,30}.

$[\text{Ni}(\text{dppe})\text{cp}^+][\text{SnCl}_3^-]$ was prepared in 60% yield by mixing one mole equivalent each of 1,2-bis(diphenylphosphino)ethane and $[\text{Ni}(\text{Ph}_3\text{P})_2\text{cp}^+][\text{SnCl}_3^-]$ in acetone. $[\text{Ni}(\text{Ph}_3\text{P})_2\text{cp}][\text{PF}_6] \cdot \text{acetone}$ was synthesised by mixing mole equivalents of $\text{cpNi}(\text{Ph}_3\text{P})\text{Cl}$, Ph_3P and AgPF_6 in acetone. AgCl was removed by centrifugation and decantation, and the yellow product crystallised when the volume of the acetone was reduced under vacuum (yield 85%).

Infrared spectra were recorded on a Perkin-Elmer 621 spectrometer, and calibrated with polystyrene. ^1H nmr spectra were measured using a Varian T-60 spectrometer, generally calibrated with TMS and chloroform. The details of the Mössbauer spectrometer are in chapter 1 of this thesis.

E. References

1. A. N. Karasev, N. E. Kolobova, L. S. Polak, V. S. Shpindel and K. N. Anisimov; *Teor. i Eksp. Khim., Akad. Nauk. Ukr.* (1966) 2, 126.
2. V. I. Gol'danskii, B. V. Borshagovskii, E. F. Makarov, R. A. Stukan, K. N. Anisimov, N. E. Kolobova and V. V. Skripkin; *Teor. i Eksp. Khim., Akad. Nauk. Ukr.* (1967) 3, 478.
3. R. H. Herber and A. Hoffman; *Prog. Inorg. Chem.* (1967) 8, 35; R. H. Herber and Y. Gosciny; *Inorg. Chem.* (1968) 7, 1293.
4. D. E. Fenton and J. J. Zuckermann; *J. Am. Chem. Soc.* (1968) 90, 6226.
5. C. Wynter and L. Chandler; *Bull. Chem. Soc. Japan* (1970) 43, 2115.
6. S. Onaka, Y. Sasaki and H. Sano; *Bull. Chem. Soc. Japan* (1971) 44, 126.
7. B. A. Goodman, R. Greatrex and N. N. Greenwood; *J. Chem. Soc. (A)* (1971), 1868.
8. S. R. A. Bird, J. D. Donaldson, A. F. Le C. Holding, B. J. Senior and M. J. Tricker; *J. Chem. Soc. (A)* (1971), 1616.
9. W. R. Cullen, J. R. Sams and J. A. J. Thompson; *Inorg. Chem.* (1971) 10, 843.
10. S. R. A. Bird, J. D. Donaldson, S. A. Keppie and M. F. Lappert; *J. Chem. Soc. (A)* (1971), 1311.
11. S. Ichiba, M. Katada and H. Negita; *Bull. Chem. Soc. Japan* (1972) 45, 1679.
12. S. R. A. Bird, J. D. Donaldson, A. F. Le C. Holding, B. Ratcliff, and S. Cenini; *Inorg. Chim. Acta* (1972) 6, 379.
13. R. V. Parish; *Progr. Inorg. Chem.* (1972) 15, 101.
14. M. J. Mays and P. L. Sears; *J. C. S. Dalton* (1973), 1873.
15. R. J. H. Clark, L. Maresca and P. J. Smith; *J. Chem. Soc. (A)* (1970), 2687.
16. F. Glockling, A. McGregor, M. L. Schneider and H. M. M. Shearer; *J. Inorg. Nucl. Chem.* (1970) 32, 3101.
17. R. Mason, G. B. Robertson, P. O. Whimp and D. A. White; *Chem. Comm.* (1968), 1655; R. Mason and P. O. Whimp; *J. Chem. Soc. (A)* (1969), 2709.

18. M. van den Akker and F. Jellinek; J. Organomet. Chem. (1967) 10, P37;
M. van den Akker; Ph.D. thesis (Rijksuniversiteit te Groningen) (1970).
19. J. K. Stalick, D. W. Meek, B. Y. K. Ho and J. J. Zöckerman;
Chem. Comm. (1972), 630.
20. M. J. Mays and P. L. Sears; J. C. S. Dalton (1974), in press.
21. R. D. Gorsich; J. Am. Chem. Soc. (1962) 84, 2486.
22. H. C. Clark and J. H. Tsai; Inorg. Chem. (1966) 5, 1407.
23. M. R. Booth, D. J. Cardin, N. A. D. Carey, H. C. Clark and
B. R. Sreenathan; J. Organomet. Chem. (1970) 21, 171.
24. J. K. Ruff; Inorg. Chem. (1971) 10, 409.
25. D. S. Field and M. J. Newlands; J. Organomet. Chem. (1971) 27, 213.
26. A. T. Rake; Ph.D. thesis (1972), University of Western Ontario.
27. M. J. Mays and B. E. Prater, J. Chem. Soc. (A) (1969), 2525.
28. D. J. Patmore and W. A. G. Graham; Inorg. Chem. (1966) 5, 1405,
2222; (1967) 6, 981; (1968) 7, 771.
29. P. A. McArdle and A. R. Manning; Chem. Comm. (1967), 417.
30. F. Glockling and A. McGregor; J. Inorg. Nucl. Chem. (1973) 35, 1481.

CHAPTER 3

The Additivity Model for Quadrupole Splittings, and its Application to Four Co-ordinate Tin Systems

A. Determination of Partial Quadrupole Splittings

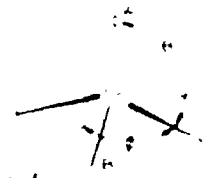
In this thesis, the additivity model, as outlined in chapter 1, is to be applied to four co-ordinate tin compounds. Using the geometric expressions from table 1.1 together with the appropriate θ and ϕ angles for a regular tetrahedral array of ligands about a central tin atom, the formulae for the efg components for all possible four co-ordinate stoichiometries were derived, and are shown in table 3.1. From this table it can be seen that for SnAC_3 molecules, the efg tensor is diagonalized already since, taking the axis system shown in the table, the principal efg V_{ZZ} axis coincides with the highest order symmetry (C_{3v}) axis. For molecules of lower symmetry, the efg tensor must be diagonalized. In fact, for the SnA_2C_2 molecules, V_{ZZ} is always the same magnitude as that for the corresponding SnAC_3 and SnA_3C molecules, but the QS is increased by a factor of 1.15 since η is predicted to be 1.00 (see equation 1.3).

It can be seen from table 3.1 that all the formulae

table 3.1

COMPONENTS OF THE EFG TENSOR FOR FOUR COORDINATE TETRAHEDRAL Sp^3 COMPOUNDS*

[1] are partial field gradients



Components of EFG tensor	Sp^3ABC_3D	Sp^3ABC_2	$Sp^3A_2C_2$	Sp^3AC_4
V_{xx}	$[A] + \frac{1}{2}[B] - \frac{1}{2}[C] + [D]$	$-[A] + \frac{1}{2}[B] - \frac{1}{2}[C]$	$\frac{1}{2}[A] - \frac{1}{2}[C]$	$[A] + [C]$
V_{yy}	$-[A] - [B] + [C] + [D]$	$-[A] - [B] + 2[C]$	$-2[A] + 2[C]$	$[A] + [C]$
V_{zz}	$2[A] - \frac{1}{2}[B] + [C] + [D]$	$2[A] - \frac{1}{2}[B] + 2[C]$	$\frac{1}{2}[A] - [C]$	$2[A] - 2[C]$
$V_{xx} = V_{yy}$	$\frac{1}{2}[C] - [D]$	0	0	0
$V_{yy} = V_{zz}$	$-\frac{1}{2}[-2[B] + [C] + [D]]$	$-\frac{1}{2}[-2[B] + 2[C]]$	$-\frac{1}{2}[-2[A] + 2[C]]$	0
$V_{zz} = V_{xx}$	$\frac{1}{2}[C] - [D]$	0	0	0

* The axes system x, y, z as defined above does not in general coincide with the principal directions X, Y, Z of the EFG tensor. For example, in Sp^3ABC_2 compounds, y coincides with Y but x and z are rotated to coincide with X and Z when the EFG tensor is diagonalized.

involve differences, so that, in fact, absolute pqs values cannot be evaluated. To establish a scale for pqs values Clark et al¹ defined the value of {X} to be 0.00 mm s^{-1} (where X = Cl, Br), so that the pqs value of any other ligand, L, relative to this value can be evaluated from the QS of an appropriate compound containing only L and Cl or Br ligands, using the formulae in table 3.1. For example, as will be mentioned later, the pqs value for the ligand $[\text{Co}(\text{CO})_4]$ is derived here from the QS of the compound $\text{ClSn}[\text{Co}(\text{CO})_4]_2$. Given that the QS is (-)1.42, and $n = 0$, then

$$\begin{aligned}
 -1.42 &= e^2 q Q (1 + n^2/3)^{1/2} \\
 &= e Q V_{zz} \\
 &= -[2\{\text{Cl}\} - 2\{\text{Co}(\text{CO})_4\}] \\
 &= 2\{\text{Co}(\text{CO})_4\} - 0 \\
 \therefore \{\text{Co}(\text{CO})_4\} &= -0.71 \text{ mm s}^{-1}
 \end{aligned}$$

The arbitrary definition of 0.00 mm s^{-1} for {Cl} and {Br} will not affect the QS values calculated for any four co-ordinate molecules since it is only the differences between pqs values for the different ligands which are important when regular tetrahedral geometry is assumed.

Clark et al¹ have recently determined precise four co-ordinate pqs values for several ligands - which are shown in table 3.2 - and more tentative values for a number of others, including C_6F_6 , $\text{Mn}(\text{CO})_5$, $\text{Fe}(\text{CO})_2\text{cp}$ and $\text{Co}(\text{CO})_4$. In this work, better pqs values for these latter four moieties and for

table 3.2

Ligand pqs Values for Four Co-ordinate Tin,
Calculated in reference 1

<u>Ligand</u>	<u>pqs (mm s⁻¹)</u>
Br, Cl, F	0.00
I	-0.17
R(CH ₃ , C ₂ H ₅ , etc.)	-1.37
R _F (CF ₃ , etc.)	-0.63
C ₆ H ₅	-1.26
C ₆ Cl ₅	-0.83
HCOO	-0.18
MeCOO	-0.15
NCS	+0.21
Re(CO) ₅	-0.80

Fe(dppe)cp and Mo(CO)₂cp have been derived, which are somewhat different to those of Clark et al¹, but which give considerably better agreement between calculated and observed QS values. These are shown in table 3.3. Pqs values for other transition metal complex moieties which bond to tin could be derived, but it only seems worthwhile to calculate pqs for those where it can be checked using another compound containing the same moiety.

As has been pointed out¹, it is desirable to derive pqs values from compounds which are relatively little distorted from ideal geometry. From structural considerations, which will be dealt with in chapter 4, we would expect that, of all the compounds containing the desired ligands, the R₃SnM (R = alkyl) compounds would be the least distorted. Thus, these types of compound, as shown in table 3.3, were used to determine pqs values for Mn(CO)₅, Fe(CO)₂cp, Fe(dppe)cp and Mo(CO)₂cp. The analogous Cl₃SnM compounds used by Clark et al¹ will be appreciably more distorted. In fact, the bond angles about the tin atom in Me₃SnMn(CO)₅ were determined⁵ in an X-ray diffraction study and found to deviate by an average of -2° from the regular tetrahedral value of 109.47°, compared with an average deviation of -11° in Cl₃SnFe(CO)₂cp⁶. Similarly, the R_nSn(C₆F₅)_{4-n} (R = Me, Ph; n = 1, 2, 3) compounds should have near regular T_d geometry. There is good internal consistency in the C₆F₅ pqs values calculated from these compounds, and the average value is -0.76 cm s⁻¹.

In the case of Co(CO)₄, the QS value for Me₃SnCo(CO)₄ is

table 3.3

Ligand pqs Values for Four Co-ordinate Tin₄
and Compounds from which they were Derived in this Study

<u>L</u>	<u>Compound</u>	<u>QS (mm s⁻¹)</u>	<u>reference</u>	<u>pqs (mm s⁻¹)</u>
Mn(CO) ₅	Me ₃ SnMn(CO) ₅	(-)0.80	this work	-0.97
Fe(CO) ₂ cp	Bu ₃ SnFe(CO) ₂ cp	-0.59	2	-1.08
Fe(dppe)cp	Me ₃ SnFe(dppe)cp	(-)0.70	3	-1.02
Co(CO) ₄	ClSn[Co(CO) ₄] ₂	(-)1.42	this work	-0.71
Mo(CO) ₃ cp	Me ₃ SnMo(CO) ₃ cp	(-)1.25	4	-0.75
C ₆ F ₅	Me ₃ Sn(C ₆ F ₅)	-1.35	1	-0.70
	Me ₂ Sn(C ₆ F ₅) ₂	1.51	1	
	MeSn(C ₆ F ₅) ₃	(+)1.14	1	
	Ph ₃ Sn(C ₆ F ₅)	±0.95	1	
	Ph ₂ Sn(C ₆ F ₅) ₂	1.11	1	
	PhSn(C ₆ F ₅) ₃	(+)0.92	1	

anomalous for a number of reasons (see next section, this chapter). The structure of the compound $\text{ClSn}[\text{Co}(\text{CO})_4]$, has been determined⁷ using diffraction methods, and shows angles about the tin atom little different from regular tetrahedral values. Consequently the QS value for this compound was used to calculate the pqs for $\text{Co}(\text{CO})_4$ instead.

The signs of QS for the Me_3SnM compounds are almost certainly negative, in view of the negative sign determined² for the QS of $\text{Bu}_3\text{SnFe}(\text{CO})_2\text{cp}$. Similarly, the sign of the QS for $\text{ClSn}[\text{Co}(\text{CO})_4]$, will be negative in view of the positive signs determined^{2,8} for the $\text{Cl}_3\text{SnFe}(\text{CO})_2\text{cp}$ and $\text{Cl}_3\text{SnMn}(\text{CO})_5$ QS parameters.

In addition to their use in predicting QS, pqs values also give useful information on the bonding between tin and the ligands. Since it has been shown¹ that, for ^{119}Sn , any π bonding involving Sn 5d orbitals would have no observable effect on the QS, only σ interactions need be considered here. The more negative the pqs value, the greater is the Sn $5p_z$ orbital population⁹. This population depends on both the donor strength of the ligand and the p character of the metal hybrid orbital. For example, if we consider a molecular orbital, α_L , to be a linear combination of a metal orbital, h_L , and a ligand orbital, χ_L , then

$$\alpha_L = c_1 h_L + c_2 \chi_L$$


Clark et al¹ showed that the pqs values are proportional to c_2^2 , which increases, as the donor ability of the ligand increases. In addition, however, the tin $5p_z$ orbital population will depend

on the p character of the tin hybrid orbital involved in the tin-ligand bond - i.e. h_L could be expressed as the sum of s and p electron contributions.

The competition of these two effects is illustrated by the pqs values of Me and Ph relative to those for the transition metal complex moieties. As will be seen in chapter 4, CS values for these compounds indicate that the transition metal complex ligands are at least as good or better donors to tin than are alkyl or aryl ligands. The CS values also show that the tin hybrid orbital used in tin-transition metal bonding has a very high tin s character, and thus a very low p character, compared with Me or Ph. This latter effect, then, makes the pqs values of the transition metal complex ligand less negative, so that $\{M\} > \{R\}$ (where $M = Mn(CO)_5, Fe(CO)_2cp, Fe(dppe)cp, Co(CO)_4, Mo(CO)_3cp$; $R = Me, Ph$) in spite of the fact that the M groups are as good or better donors than R groups.

B. Application of the Additivity Model to Four Co-ordinate Tin

The structures of a number of tin-transition metal compounds have been determined using diffraction techniques. The details of these structures will be discussed in chapter 4; but the seventeen compounds whose structures are known, and which are marked with an asterisk in table 3.4, appear to be unambiguously four co-ordinate about the tin atom, with no abnormally short non-bonded distances. With the possible exceptions of compounds 56, 60, 66 and 78 (in table 3.4), there is no reason to suppose



that the remainder of the compounds in table 3.4 contain other than four co-ordinate tin. The angles between the tin-ligand bonds are distorted, in varying amounts, away from the regular tetrahedral value of 109.47° .

Using the pqs values from tables 3.2 and 3.3, and the appropriate formulae from table 3.1, QS and η values for 135 compounds were calculated, and are listed together with all appropriate measured values in table 3.4.

Clark et al¹ have proposed that, considering the approximations inherent in the additivity model, agreement between calculated and observed QS values within $\pm 0.4 \text{ mm s}^{-1}$ can be considered to be satisfactory. Using this criterion, only 8 of the 122 compounds, for which comparison is possible, are not in acceptable agreement. Indeed, a large number of the compounds in table 3.4 show agreement within $\pm 0.2 \text{ mm s}^{-1}$. (It is likely that compounds 33, 34, 44, 45, 94 - 96, and 103 - 105 have small, as yet unresolved splittings). For illustrative purposes, observed and calculated values are plotted against each other in figure 3.1. A linear least-squares fit to this data indicates a line of best fit having a slope of 1.02 and intercept on the vertical axis of 0.04, very close to the expected values of 1.00 and 0.00 respectively. The correlation coefficient $R = 0.992$.

Because of the more complex techniques involved, only a small number of ^{119}Sn spectra have been recorded^{2,8} with the sample in the strong field of a superconducting magnet, to allow the determination of the sign of the QS, and the value of η .

table 3.4

119-Tin Quadrupole Splittings (χe^2qQ)(Observed, and Predicted
from Partial Quadrupole Splittings) for Four Co-ordinate Tin Compounds

<u>Compound</u>	<u>observed</u>	<u>Quadrupole Splitting calculated</u>	<u>reference</u>	<u>n calculated</u>
1. $Me_3SnMn(CO)_5$	0.82	(-ve)††	b	0.00
2. $Et_3SnMn(CO)_5$	0.88	-0.82	10	0.00
3. $Me_2Sn[Mn(CO)_5]_2$	0.92	0.92	11	1.00
4. $MeSn[Mn(CO)_5]_3$	0.95	+0.82	11	0.00
5. $Me_2ClSnMn(CO)_5$	-2.60	-2.59	b	0.41
6. $Me_2BrSnMn(CO)_5$	2.54	-2.59	12	0.41
7. $MeCl_2SnMn(CO)_5$	+2.62	+2.79	b	0.89
8. $MeBr_2SnMn(CO)_5$	2.51	+2.79	12	0.89
9. $MeClSn[Mn(CO)_5]_2$	a	-2.33	-	0.49
10. $Cl_3SnMn(CO)_5$	+1.60	+1.94	b	0.00
11. $Br_3SnMn(CO)_5$	1.53	+1.94†	b	0.00
12. $I_3SnMn(CO)_5$	1.32	+1.60	13	0.00
13. $Cl_2Sn[Mn(CO)_5]_2$	2.10	2.24	14	1.00
14. $Br_2Sn[Mn(CO)_5]_2$	2.12	2.24	14	1.00

table 3.4 (cont'd)

Compound	Quadrupole Splitting		reference	$\frac{n}{\text{calculated}}$
	observed	calculated		
15. $\star\text{Cl Sn}[\text{Mn}(\text{CO})_5]_3$	1.55	-1.94	15	0.00
16. $\text{Br Sn}[\text{Mn}(\text{CO})_5]_3$	a	-1.94	-	0.00
17. $\star\text{Ph}_3\text{SnMn}(\text{CO})_5$	0.41	-0.58	b	0.00
18. $\star\text{Ph}_2\text{Sn}[\text{Mn}(\text{CO})_5]_2$	a	0.67	-	1.00
19. $\text{PhSn}[\text{Mn}(\text{CO})_5]_3$	a	+0.58	-	0.00
20. $\text{Ph}_2\text{ClSnMn}(\text{CO})_5$	2.50	-2.39	b	0.32
21. $\text{Ph}_2\text{BrSnMn}(\text{CO})_5$	2.31	-2.39	b	0.32
22. $\text{Ph}_2\text{ISnMn}(\text{CO})_5$	a	-2.06	-	0.37
23. $\text{PhCl}_2\text{SnMn}(\text{CO})_5$	2.52	+2.62	b	0.94
24. $\text{PhBr}_2\text{SnMn}(\text{CO})_5$	2.65	+2.62	b	0.94
25. $\text{PhI}_2\text{SnMn}(\text{CO})_5$	2.19	2.23	13	0.91
26. $\text{PhClSn}[\text{Mn}(\text{CO})_5]_2$	a	-2.20	-	0.37
27. $\text{Ph}_2(\text{C}_6\text{F}_5)\text{SnMn}(\text{CO})_5$	0.95	-0.97	b	0.78
28. $\text{Ph}(\text{C}_6\text{F}_5)_2\text{SnMn}(\text{CO})_5$	1.06	+0.95	b	0.58
29. $(\text{C}_6\text{F}_5)_3\text{SnMn}(\text{CO})_5$	+0.99	+0.42†	b	0.00
30. $\text{Sn}[\text{Fe}(\text{CO})_2\text{cp}]_6$	0.0	0.00	14	0.00
31. $\text{Me}_3\text{SnFe}(\text{CO})_2\text{cp}$	0.46	-0.58	16	0.00

table 3.4 (cont'd)

Compound	Quadrupole Splitting		reference	$\frac{n}{\text{calculated}}$
	observed	calculated		
32. $\text{Bu}_2\text{SnFe}(\text{CO})_2\text{cp}$	-0.59	(-ve)††	17	0.00
33. $\text{Me}_2\text{Sn}[\text{Fe}(\text{CO})_2\text{cp}]_2$	0	0.67	10	1.00
34. $\text{Et}_2\text{Sn}[\text{Fe}(\text{CO})_2\text{cp}]_2$	0	0.67	10	1.00
35. $\text{MeSn}[\text{Fe}(\text{CO})_2\text{cp}]_2$	a	+0.58	-	0.00
36. $\text{Cl}_2\text{SnFe}(\text{CO})_2\text{cp}$	+1.83	+2.16	b	0.00
37. $\text{Br}_2\text{SnFe}(\text{CO})_2\text{cp}$	1.63	+2.16†	b	0.00
38. $\text{I}_2\text{SnFe}(\text{CO})_2\text{cp}$	1.50	+1.82	8	0.00
39. $\text{Cl}_2\text{Sn}[\text{Fe}(\text{CO})_2\text{cp}]_2$	+2.39	2.50	8, 17	1.00
40. $\text{Br}_2\text{Sn}[\text{Fe}(\text{CO})_2\text{cp}]_2$	2.42	2.50	14	1.00
41. $\text{I}_2\text{Sn}[\text{Fe}(\text{CO})_2\text{cp}]_2$	2.25	2.09	8	1.00
42. $\text{ClSn}[\text{Fe}(\text{CO})_2\text{cp}]_2$	a	-2.16	-	0.00
43. $\text{Ph}_2\text{SnFe}(\text{CO})_2\text{cp}$	0.32	-0.36	b	0.00
44. $\text{Ph}_2\text{Sn}[\text{Fe}(\text{CO})_2\text{cp}]_2$	0	0.42	18	1.00
45. $\text{PhSn}[\text{Fe}(\text{CO})_2\text{cp}]_2$	0	+0.36	18	0.00
46. $\text{Ph}_2\text{ClSnFe}(\text{CO})_2\text{cp}$	2.54	-2.42	b	0.20
47. $\text{Ph}_2\text{BrSnFe}(\text{CO})_2\text{cp}$	2.52	-2.42	b	0.20

table 3.4 (cont'd)

Compound	Quadrupole Splitting		reference	η
	observed	calculated		
48. $\text{PhCl}_2\text{SnFe}(\text{CO})_2\text{cp}$	2.84	+2.72	b	0.98
49. $\text{PhBr}_2\text{SnFe}(\text{CO})_2\text{cp}$	2.65 ^a	+2.72	b	0.98
50. $\text{PhClSn}[\text{Fe}(\text{CO})_2\text{cp}]_2$	a	-2.31	-	0.21
51. $\text{Ph}_2(\text{C}_6\text{F}_5)\text{SnFe}(\text{CO})_2\text{cp}$	0.93	-0.94	b	0.50
52. $\text{Ph}(\text{C}_6\text{F}_5)_2\text{SnFe}(\text{CO})_2\text{cp}$	1.37	+0.99	b	0.84
53. $(\text{C}_6\text{F}_5)_3\text{SnFe}(\text{CO})_2\text{cp}$	1.21	+0.64 ⁺	b	0.00
54. $\text{ClSn}[\text{Mn}(\text{CO})_5][\text{Fe}(\text{CO})_2\text{cp}]_2$	2.02	-2.10	18	0.14
55. $(\text{NCS})_2\text{SnFe}(\text{CO})_2\text{cp}$	2.24	+2.58	8	0.00
56. $(\text{NCS})_2\text{Sn}[\text{Fe}(\text{CO})_2\text{cp}]_2$	+2.56	2.97 ⁺	8,17	1.00
57. $(\text{HCOO})_2\text{SnFe}(\text{CO})_2\text{cp}$	1.45	+1.80	8	0.00
58. $(\text{HCOO})_2\text{Sn}[\text{Fe}(\text{CO})_2\text{cp}]_2$	2.19	2.07	8	1.00
59. $(\text{CH}_3\text{COO})_2\text{SnFe}(\text{CO})_2\text{cp}$	1.87	+1.86	8	0.00
60. $(\text{CH}_3\text{COO})_2\text{Sn}[\text{Fe}(\text{CO})_2\text{cp}]_2$	2.60	2.14 ⁺	8	1.00
61. $\text{Me}_2\text{SnFe}(\text{dppe})\text{cp}$	0.70	(-ve) ⁺⁺	3	0.00
62. $\text{Cl}_2\text{SnFe}(\text{dppe})\text{cp}$	1.76	+2.04	3	0.00
63. $\text{Br}_2\text{SnFe}(\text{dppe})\text{cp}$	1.60	+2.04	3	0.00

table 3.4 (cont'd)

Compound	Quadrupole Splitting		reference	η calculated
	observed	calculated		
64. $I_2SnFe(dppe)_2$ cp	1.53	+1.70	3	0.00
65. $Sn[Co(CO)_4]_2$	0.0	0.00	b	0.00
66. $Me_2SnCo(CO)_2$	1.73	-1.32†	b	0.00
67. $Me_2Sn[Co(CO)_4]_2$	1.53	1.52	b	1.00
68. $MeSn[Co(CO)_4]_2$	1.29	+1.32	b	0.00
69. $Me_2ClSnCo(CO)_2$	2.73	-2.62	b	0.66
70. $MeCl_2SnCo(CO)_2$	4	+2.63	-	0.71
71. $MeClSn[Co(CO)_4]_2$	2.38	-2.27	b	0.99
72. $Cl_2SnCo(CO)_2$	1.20	+1.42	b	0.00
73. $Br_2SnCo(CO)_2$	1.29	+1.42	14,19	0.00
74. $I_2SnCo(CO)_2$	0.71	+1.08	19	0.00
75. $Cl_2Sn[Co(CO)_4]_2$	1.44	1.64	b	1.00
76. $Br_2Sn[Co(CO)_4]_2$	1.46	1.64	b	1.00
77. $I_2Sn[Co(CO)_4]_2$	1.07	1.25	b	1.00
78. $FSn[Co(CO)_4]_2$	0.97	-1.42†	b	0.00
79. $*ClSn[Co(CO)_4]_2$	1.42	(-ve)††	b	0.00

table 3.4 (cont'd)

Compound	Quadrupole Splitting		reference	$\frac{n}{\text{calculated}}$
	observed	calculated		
80. BrSn[Co(CO) ₄] ₂	1.06	-1.42	19	0.00
81. ISn[Co(CO) ₄] ₂	0.95	-1.08	19	0.00
82. Ph ₃ SnCo(CO) ₄	1.20	-1.10	b	0.00
83. Ph ₂ Sn[Co(CO) ₄] ₂	1.27	1.27	b	1.00
84. PhSn[Co(CO) ₄] ₂	1.28	+1.10	20	0.00
85. Ph ₂ ClSnCo(CO) ₄	2.18	-2.39	b	0.60
86. PhCl ₂ SnCo(CO) ₄	a	+2.45	-	0.76
87. PhClSn[Co(CO) ₄] ₂	1.88	-2.07	b	0.83
88. Me ₂ Sn[Mn(CO) ₅][Co(CO) ₄]	e 1.46	-1.30	b	0.80
89. *Ph ₂ Sn[Mn(CO) ₅][Co(CO) ₄]	1.15	-1.06	15	0.72
90. Cl ₂ Sn[Mn(CO) ₅][Co(CO) ₄]	a	-1.83	-	0.37
91. Me ₂ SnMo(CO) ₅ ,cp	1.25	(-ve)††	4	0.00
92. *ClSn[Fe(CO) ₂ ,cp] ₂ [Mo(CO) ₅ ,cp]	a	-2.04	-	0.43
93. Cl ₂ Sn[Mn(CO) ₅][Mo(CO) ₅ ,cp]	2.0	+1.90	15	0.66
94. Ph ₃ SnRe(CO) ₅	0	-0.92	15	0.00
95. Ph ₂ Sn[Re(CO) ₅] ₂	0	1.06	15	1.00

table 3.4 (cont'd)

Compound	Quadrupole Splitting		reference	η calculated
	observed	calculated		
96. $\text{PhSn}[\text{Re}(\text{CO})_5]_2$	0	+0.92	15	0.00
97. $\text{ClSn}[\text{Re}(\text{CO})_5]_2$	1.60	(+ve)††	18	0.00
98. $\text{BrSn}[\text{Re}(\text{CO})_5]_2$	1.60	+1.60	15	0.00
99. $\text{Cl}_2\text{Sn}[\text{Mn}(\text{CO})_5][\text{Re}(\text{CO})_5]$	2.48	+2.06	15	0.96
100. $\text{R}_2\text{Sn}(\text{R}=\text{Me}, \text{Et}, \text{Pr}, \text{Bu}, \text{Neo}, \text{cyH})$	0	0.00	21, 22	0.00
101. $^*\text{Ph}_2\text{Sn}$	0	0.00	21	0.00
102. $(\text{C}_6\text{X}_5)_2\text{Sn}$ (X=F, Cl)	0	0.00	21	0.00
103. Me_2SnPh	0	-0.22	21	0.00
104. Me_2SnPh_2	0	0.25	21	1.00
105. MeSnPh_3	0	+0.22	21	0.00
106. Neo_2SnF	2.79	(-2.74)††	22	0.00
107. Neo_2SnCl	2.65	(-2.74)††	22	0.00
108. $(\text{PhCH}_2)_2\text{SnCl}$	2.80	-2.74	23	0.00
109. $(\text{PhCH}_2)_2\text{SnCl}_2$	2.84	3.15	23	1.00
110. Neo_2SnBr	2.65	(-2.74)††	22	0.00
111. Bu_2SnI	2.65	-2.40	21	0.00

table 3.4 (cont'd)

Compound	Quadrupole Splitting		reference	$\frac{n}{\text{calculated}}$
	observed	calculated		
112. Neo ₃ SnI	2.40	(-ve)††	22	0.00
113. Neo ₃ Sn(O ₂ CH ₃)	2.45	(-ve)††	22	0.00
114. *Ph ₃ SnCl	-2.54	(-2.52)††	23	0.00
115. Ph ₃ SnBr	2.50	(-2.52)††	23	0.00
116. Ph ₃ SnI	2.15	-2.18	23	0.00
117. Ph ₂ SnCl ₂	2.82	2.90	23	1.00
118. Ph ₂ SnBr ₂	2.54	2.90	23	1.00
119. Ph ₂ SnI ₂	2.38	2.51	23	1.00
120. Me ₃ Sn(C ₆ F ₅)	-1.35	(-1.34)††	23	0.00
121. Me ₂ Sn(C ₆ F ₅) ₂	1.51	(1.54)††	23	1.00
122. MeSn(C ₆ F ₅) ₃	1.14	(+1.34)††	24	0.00
123. Ph ₃ Sn(C ₆ F ₅)	-0.95	(-1.12)††	23	0.00
124. Ph ₂ Sn(C ₆ F ₅) ₂	1.11	(1.29)††	23	1.00
125. (4-MeC ₆ H ₄) ₂ Sn(C ₆ F ₅) ₂	1.18	1.29	24	1.00
126. Ph Sn(C ₆ F ₅) ₃	0.92	(+1.12)††	24	0.00
127. (4-MeC ₆ H ₄)Sn(C ₆ F ₅) ₃	1.02	+1.12	24	0.00

table 3.4 (cont'd)

Compound	Quadrupole Splitting		reference	η calculated
	observed	calculated		
128. $\text{ClSn}(\text{C}_6\text{F}_5)_3$	1.56	-1.40	24	0.00
129. $\text{BrSn}(\text{C}_6\text{F}_5)_3$	1.60	-1.40	24	0.00
130. $\text{Me}_3\text{Sn}(\text{C}_6\text{Cl}_5)$	1.09	(-ve)††	25	0.00
131. $\text{Ph}_3\text{Sn}(\text{C}_6\text{Cl}_5)$	0.84	-0.86	25	0.00
132. $\text{Ph}_2\text{Sn}(\text{C}_6\text{Cl}_5)_2$	1.14	0.99	25,26	1.00
133. $\text{Ph Sn}(\text{C}_6\text{Cl}_5)_3$	0.80	+0.86	26	0.00
134. Me_3SnCF_3	1.48	(-ve)††	25,27	0.00
135. $\text{Me}_3\text{SnCF}_2\text{CF}_3$	1.63	1.48	27	0.00

†† Compound used to derive a ligand pqs value. The sign assumed is shown; and the predicted value is also shown if the ligand pqs value was averaged from more than one compound.

a not reported

b this work

* structures shown to be four co-ordinate by diffraction studies (see chapter 3 for details).

† difference between observed and calculated QS values is $>0.4 \text{ nm s}^{-1}$.

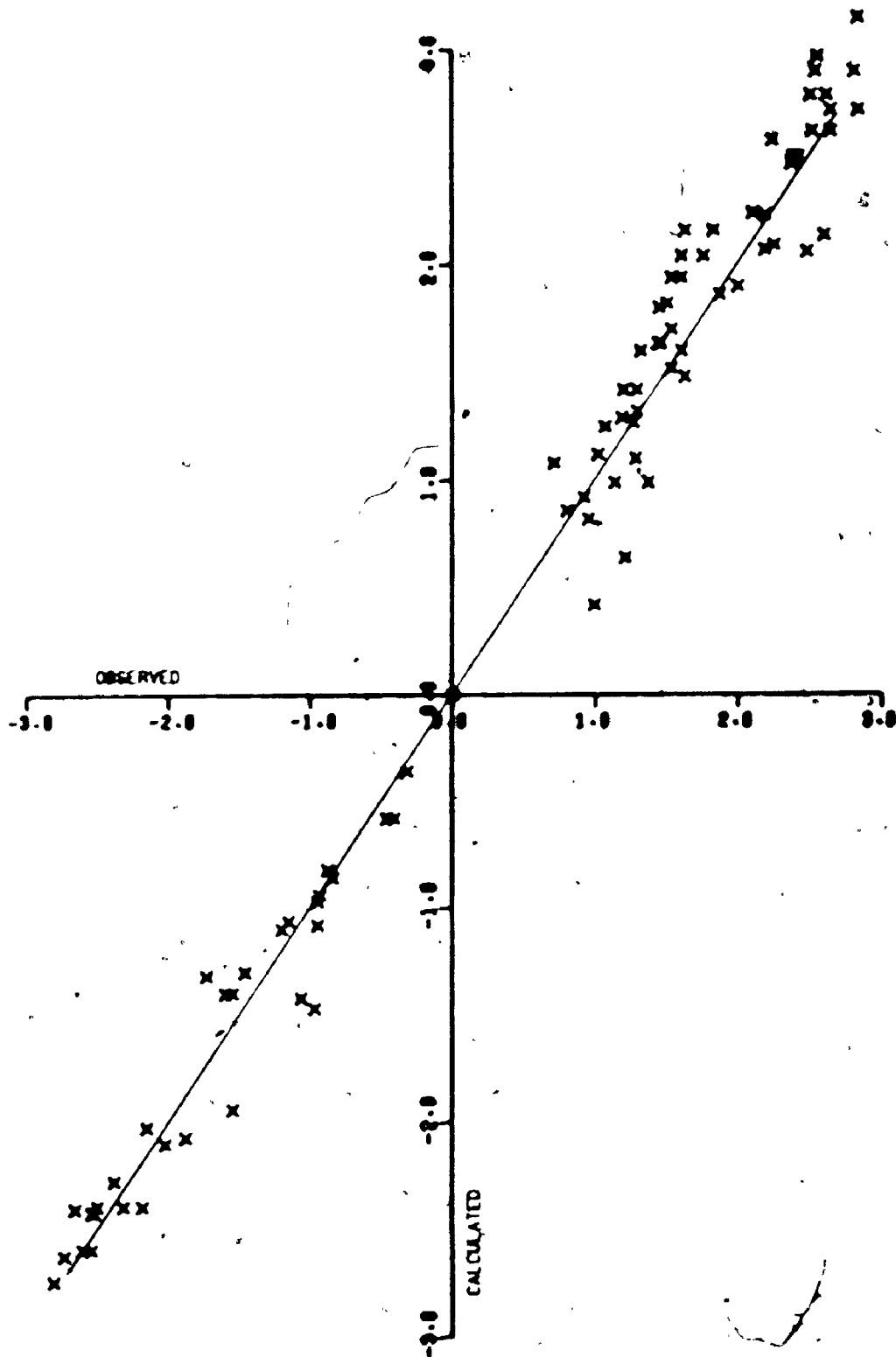


figure 3.1: Calculated vs Observed ^{119}Sn Quadrupole Splittings for Four Co-ordinate Tin Compounds; with linear least-squares fit ($Y = 1.02 X + 0.04$)

However, for all 11 cases where the sign of the QS was determined (see table 3.4), including the three compounds reported here, it is correctly predicted.

The QS values for any series of compounds $R_l X_m SnM_n$ ($R = Me, Ph; X = Cl, Br, I, C_6F_5; M =$ transition metal complex moiety; $l + m + n = 4$) follow a striking pattern. Observed QS values for the compounds with $l, m, n \neq 0$ are much greater than those with one of l, m or $n = 0$. (If more than one of l, m or n is zero, then $QS = 0$, of course). This pattern is correctly predicted in each case.

The additivity model also predicts that the QS for molecules of the type SnA_2C_2 should be 15% larger than the QS values for the corresponding $SnAC_3$ and SnA_3C compounds, as mentioned in the previous section. In practice, the QS values for the $SnAC_3$ and SnA_3C compounds are generally similar, though not precisely equal; and QS for the SnA_2C_2 compound is generally 10 - 15% greater, (though the increase is as much as 30 - 40% in a few cases).

A number of other trends in related series of compounds can be explained quite simply in terms of relative magnitudes of pqs. For example, the QS values for the $R_{4-n} Sn[Co(CO)_5]_n$ compounds are considerably larger, and the QS values for the $X_{4-n} Sn[Co(CO)_5]_n$ compounds substantially smaller than for the $Mn(CO)_5$ and $Fe(CO)_5$ analogues, due to the much less negative $Co(CO)_5$ pqs value ($R = Me, Ph; X = Cl, Br$).

The QS for the compound $Me_3SnCo(CO)_5$ is certainly abnormally

large when compared with the corresponding Ph derivatives and the other $\text{Me}_n\text{Sn}[\text{Co}(\text{CO})_4]_{4-n}$ compounds. For example, as has been pointed out, the $|\text{QS}|$ of the compounds $\text{MeSn}[\text{Co}(\text{CO})_4]_3$ and $\text{Me}_3\text{Sn}[\text{Co}(\text{CO})_4]$ should be equal, and that of $\text{Me}_2\text{Sn}[\text{Co}(\text{CO})_4]_2$ 15% larger. It is possible that the anomalously large value for the $\text{Me}_3\text{SnCo}(\text{CO})_4$ compound is due to large distortions from tetrahedral geometry.

The small QS for the compound $\text{FSn}[\text{Co}(\text{CO})_4]_3$ could be due to distortion or association. Clark et al¹ decided that the pqs of F was very close to those of Cl and Br, and assigned all three a zero value. Thus we would expect that the compounds $\text{ClSn}[\text{Co}(\text{CO})_4]_3$ and $\text{FSn}[\text{Co}(\text{CO})_4]_3$ would have very similar QS values. Indeed for the compound $(\text{Neo})_3\text{SnF}$ ($\text{Neo} = \text{PhC}(\text{Me})_2\text{CH}_2$), which should contain four co-ordinate Sn because of the steric barrier to fluorine bridging presented by the bulky neophyl groups, the observed QS is larger by $0.14 \text{ cm}^{-1} \text{ s}^{-1}$ than those for the analogous chloride and bromide compounds²². This is consistent with a slightly positive pqs value for F, while the QS observed here for a four co-ordinate $\text{FSn}[\text{Co}(\text{CO})_4]_3$ species would suggest a pqs value for F of $-0.23 \text{ cm}^{-1} \text{ s}^{-1}$. These results strongly suggest either that the compound $\text{FSn}[\text{Co}(\text{CO})_4]_3$ has a very distorted four co-ordinate structure, or that there is intermolecular fluorine bridging. Clark²⁹ has shown that a five co-ordinate bridging structure involving one axial and one equatorial F atom would lead to a smaller QS (of $1.14 \text{ cm}^{-1} \text{ s}^{-1}$) than the four co-ordinate structure. This might suggest that fluorine

50

bridging, a common feature of organotin chemistry²⁹, is present in this compound.

Similarly, bridging via acetate and thiocyanate ligands is well-known³⁰ in organotin chemistry, and some degree of association could account for the disagreement between observed and calculated QS values for $(\text{NCS})_2\text{Sn}[\text{Fe}(\text{CO})_2\text{cp}]_2$ and $(\text{CH}_3\text{COO})_2\text{Sn}[\text{Fe}(\text{CO})_2\text{cp}]_2$ (compounds 56 and 60).

The reason for the low observed QS for $\text{Br}_2\text{SnFe}(\text{CO})_2\text{cp}$ is not readily apparent, since the structure of this compound has been determined³¹ by X-ray crystallography, and seems to have no abnormally short interatomic formally non-bonded distances, which could be interpreted as association; though the bond angles about the tin atom are somewhat distorted from regular tetrahedral geometry. In view of disagreements such as this, it is dangerous to infer degrees of association from small changes in QS, in the absence of confirmatory data from other techniques. However, serious disagreement can probably be attributed with confidence to unexpected stoichiometry about the tin atom (e.g. due to polymerization) or to gross distortion from ideal geometry.

One of the most useful applications of this last argument is in the elucidation of the structures of simple organotin halides, which have been the subject of controversy in the literature (for reviews see references 14 and 23). The QS values observed for the compounds $\text{R}_n\text{SnX}_{4-n}$ ($\text{R} = \text{Me}, \text{Neo}, \text{Ph}$; $\text{X} = \text{F}, \text{Cl}, \text{Br}, \text{I}$; $n = 2, 3$), together with the values predicted from the additivity model for a four co-ordinate structure, are shown

in table 3.5. Clearly, unassociated tetrahedral structures can be assigned to Neo_3SnX ($X = \text{F}, \text{Cl}, \text{Br}, \text{I}$), Ph_3SnX ($X = \text{Cl}, \text{Br}, \text{I}$) and Ph_2SnX_2 ($X = \text{Cl}, \text{Br}, \text{I}$) on the basis of good agreement between observed and predicted QS values. This has been confirmed from diffraction studies in the cases of Ph_3SnCl ³² and Ph_2SnCl_2 ³³. The structure of the related compound $\text{Ph}_2\text{ISn}(\text{CH}_2)_6\text{SnIPh}_2$ has also been reported³⁴, and shows four co-ordination around the tin atoms, with angles close to 109.47° . The QS for this compound is reported³⁵ as 2.37 cm^{-1} , in good agreement with the predicted value of $(-)2.26$. The Neo_3SnX compounds would all be expected to be four co-ordinate, though somewhat distorted, because of the very bulky nature of the Neo ligand.

Diffraction studies of Me_3SnF ^{29a} and Me_3SnCl ³⁶ show that these compounds have associated, five co-ordinate structures. On the basis that most of the other compounds in table 3.5 which do not show good agreement between predicted and observed QS values have similar QS to Me_3SnF and Me_3SnCl , it is tempting to suggest that they too have associated five co-ordinate structures. However, though association is suggested for Me_2SnCl_2 by an X-ray crystal structure determination³⁷, the mode is not clearly defined, and the nature of the association is the subject of some disagreement^{33,37}, mainly because the van der Waals radius for Sn is not well established. The much larger QS value for Me_2SnF_2 is consistent with the known^{29b} six co-ordinate associated structure.

table 3.5

 ^{119}Sn Quadrypole Splitting Data for some OrganotinHalide Complexes(mm s⁻¹ at -80 K; values from reference 23)Observed

	F	Cl	Br	I
Me ₃ SnX	3.82	3.44	3.40	3.10
Neop ₃ SnX	2.79	2.65	2.65	2.40
Ph ₃ SnX	3.58	-2.54	2.50	2.15
Me ₂ SnX ₂	+4.38	+3.55	3.36	-
Ph ₂ SnX ₂	3.43	2.82	2.54	2.38

Calculated from pqs values

	F, Cl, Br	I
R ₃ SnX	-2.74	-2.40
Ph ₃ SnX	-2.52	-2.18
R ₂ SnX ₂	3.15	2.76
Ph ₂ SnX ₂	2.90	2.51

Partial quadrupole splittings and the additivity model appear to be somewhat less successful in predicting η values for four co-ordinate tin compounds. The calculated and observed values of η , where they have been measured, are listed in table 3.6. This is, perhaps, not surprising in view of the study of Clark³⁸, where he considered the effect of a minor perturbation on metal-ligand bond lengths - and thus on pqs values - and concluded that η would be changed substantially, while the QS would be virtually unaffected.

The point may also be illustrated by considering the behaviour of η and QS for a compound such as $\text{Me}_2\text{ClSnMn}(\text{CO})_5$, as the pqs value of each ligand is varied, in turn, through the range of pqs values likely to be encountered for real ligands. The appropriate plots are shown in figures 3.2 and 3.3. For $\text{Me}_2\text{ASnMn}(\text{CO})_5$ and Me_2ClSnA , the magnitude of the QS is a minimum when the variable pqs becomes equal to that of the other singly present ligand, so that the stoichiometry of the system effectively becomes SnAB_3 . On the $\text{A}_2\text{ClSnMn}(\text{CO})_5$ curves, this situation occurs twice, but the point of minimum magnitude of QS occurs at a point where the variable ligand pqs is equal to the average of the other two ligand pqs values. It is interesting to note that a change of sign of QS occurs at this point, causing a discontinuity in the curve; and, from figure 3.2, that $\eta = 1$ there. ~~It~~ would be expected, $\eta = 0$ at all points on

table 3.6

Measured Values of the Asymmetry Parameter, η ,
for Tin-Transition Metal Compounds

<u>Compound</u>	<u>η</u>		<u>Reference</u>
	<u>Calculated</u>	<u>Observed</u>	
$\text{Me}_2\text{ClSnMn}(\text{CO})_5$	0.41	0.35	this work
$\text{MeCl}_2\text{SnMn}(\text{CO})_5$	0.89	0.46	this work
$\text{Cl}_3\text{SnMn}(\text{CO})_5$	0.00	-0	2
$\text{Cl}_3\text{SnFe}(\text{CO})_2\text{cp}$	0.00	-0	2,8
$\text{Cl}_2\text{Sn}[\text{Fe}(\text{CO})_2\text{cp}]_2$	1.00	0.65	2
$\text{Bu}_3\text{SnFe}(\text{CO})_2\text{cp}$	0.00	-0	2
$(\text{C}_6\text{F}_5)_3\text{SnMn}(\text{CO})_5$	0.00	-0.0	this work
$(\text{NCS})_2\text{Sn}[\text{Fe}(\text{CO})_2\text{cp}]_2$	1.00	<0.6	2

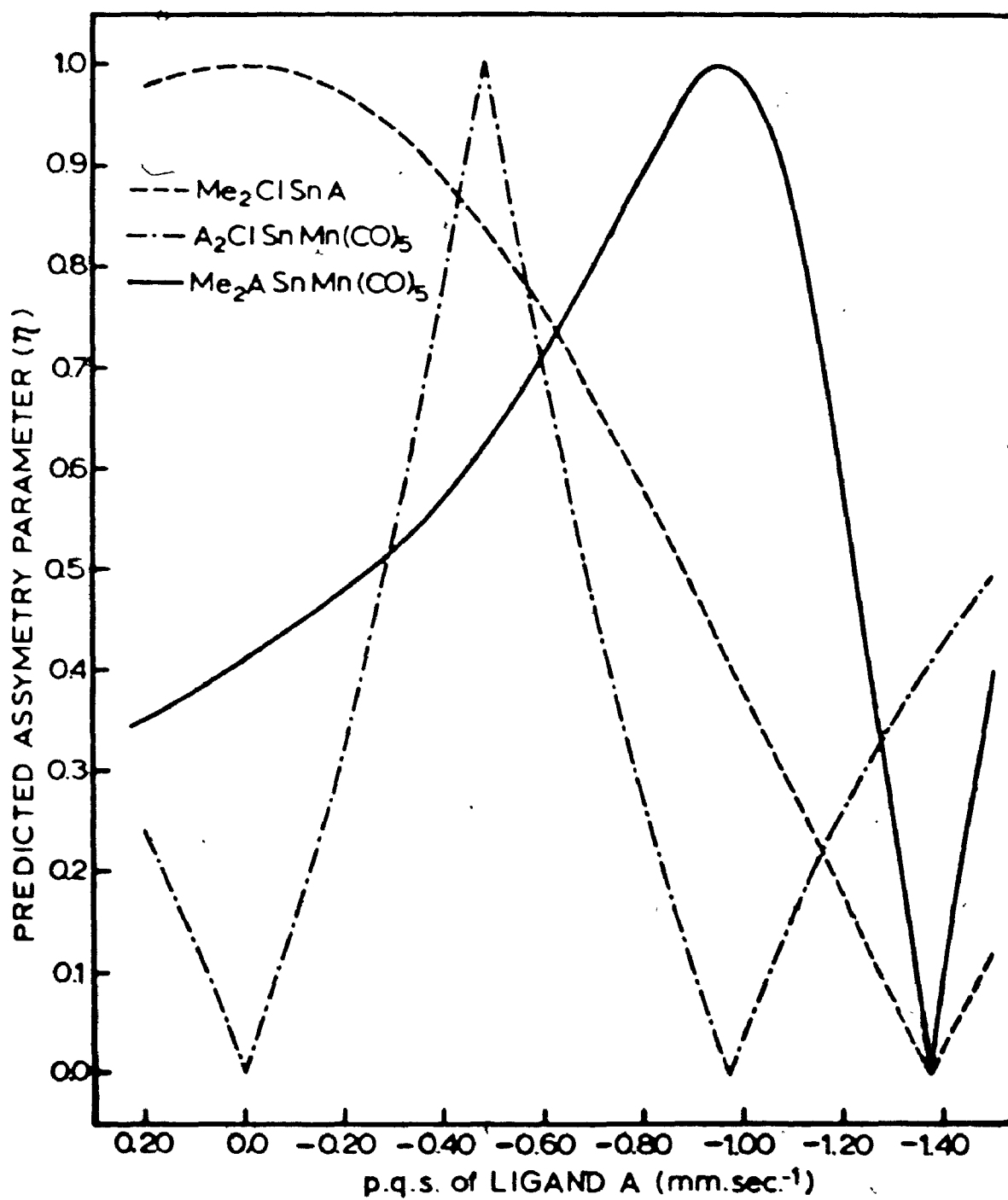


figure 3.2: Variation of calculated η values with pqs of the ligands for Me₂ClSnMn(CO)₅.

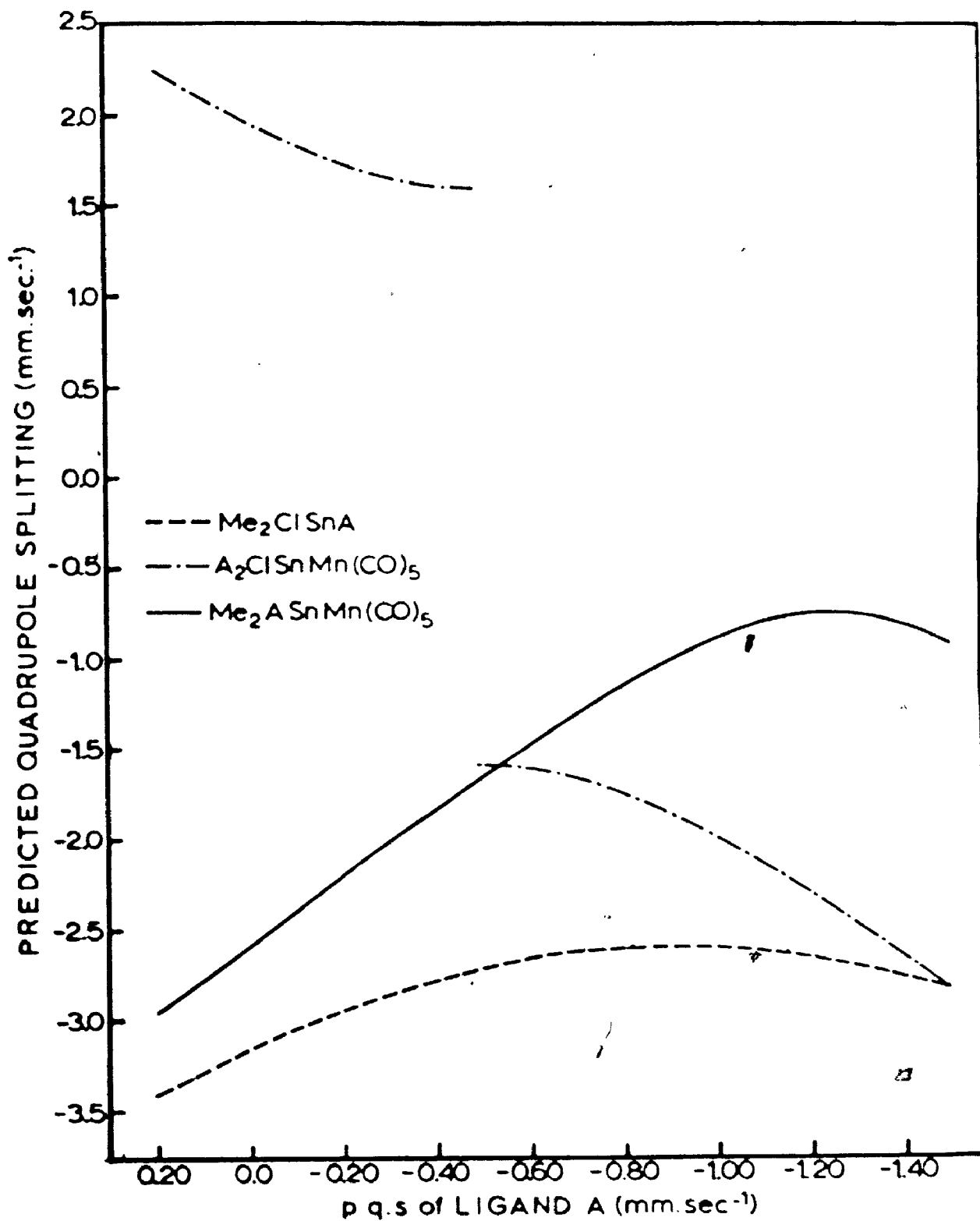


figure 3.3: Variation of calculated QS values with pqs of the ligands for Me₂ClSnMn(CO)₅.

the graph where the variable pqs causes the stoichiometry to become effectively SnAB_3 , and $n = 1$ wherever the stoichiometry is effectively SnA_2B_2 . From the very steep slopes of the n curves compared with the QS curves, it is apparent that n changes much more rapidly than QS for small changes in pqs values, and the large discrepancy between some predicted and observed n values is not surprising.

C. Consideration of Structural Distortions

In the foregoing application of the additivity model, regular tetrahedral geometry was assumed for all molecules, and the efg components were calculated using the regular tetrahedral angle of 109.47° . However, a number of four co-ordinate tin structures have been determined by diffraction methods, and the bond angles deviate significantly from this value in a number of cases. Thus an attempt is made here to apply the additivity model using crystallographically measured bond angles to derive the appropriate equations and pqs values.

When applying the formulae from table 1.1 for the components of the efg using non-regular tetrahedral angles, it is no longer sufficient to utilise relative pqs values, and absolute pqs values must be derived. One possible way of deriving these absolute values is to apply the equations defining QS and n (from V_{XX} , V_{YY} and V_{ZZ}) to a molecule where the QS (and its sign) and n have been measured (and $n \neq 0$). The only appropriate compound so far reported² is $\text{Cl}_2\text{Sn}[\text{Fe}(\text{CO})_2\text{cp}]_2$, which has the parameters $\text{QS} = +2.35 \text{ s}^{-1}$,

and $\eta = 0.65$. Considering the axis system shown below table 3.7, V_{11} , V_{jj} , and V_{kk} are the principal efg axes V_{XX} , V_{YY} and V_{ZZ} - but not necessarily in that order. From the reported crystallographic study³⁹ of this compound, $\alpha = 128.6$ and $\beta = 94.1$; so that the efg components are given by

$$-eQV_{11} = -0.8716\{\text{Fe}\} + 0.7855\{\text{Cl}\} \quad \dots(3.1a)$$

$$-eQV_{jj} = -2.0000\{\text{Fe}\} + 1.2145\{\text{Cl}\} \quad \dots(3.1b)$$

$$-eQV_{kk} = +2.8716\{\text{Fe}\} - 2.0000\{\text{Cl}\} \quad \dots(3.1c)$$

where $\{\text{Fe}(\text{CO})_2\text{cp}\}$ is abbreviated as $\{\text{Fe}\}$.

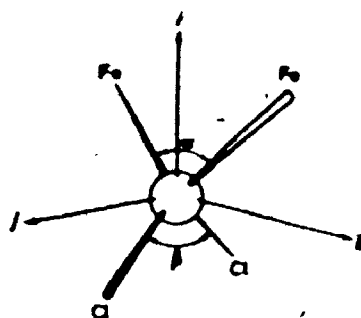
Clearly, there are six ways in which axes i , j , k can be assigned to X , Y , Z ; but there seems to be no simple way in which they can be identified. Thus, the above equations (3.1a-c) were solved against $\eta = (V_{YY} - V_{XX})/V_{ZZ}$ for $\{\text{Fe}\}$ and $\{\text{Cl}\}$ for each possible assignment, and the results are shown in table 3.7. The most straightforward test of these derived absolute pqs values is to use them, together with the measured⁶ crystallographic angles, to calculate the QS for $\text{Cl}_2\text{SnFe}(\text{CO})_2\text{cp}$; using the relevant equations from table 1.1. V_{ZZ} is unambiguously defined for this molecule and η is known to be zero^{2,8}.

The $|\text{QS}|$ of $\text{Cl}_2\text{SnFe}(\text{CO})_2\text{cp}$ is 1.83 (table 2.1) and its sign is positive^{2,8}. Thus solutions 1, 3 and 4 in table 3.7 do not predict the correct sign, and can be neglected. Of the other solutions, solution 2 shows the best agreement; but this is not as good as the $+2.16 \text{ cm}^{-1}$ predicted using regular tetrahedral angles.

table 3.7

Calculated Absolute pqs Values for Cl and Fe(CO)₂cp
(method 1)

Assignment	{Cl} (mm s ⁻¹)	{Fe(CO) ₂ cp} (mm s ⁻¹)	OS. {Cl, SnFe(CO) ₂ cp} (calculated) (mm s ⁻¹)
1. i = x j = y k = z	+0.70	+3.90	-2.05
2. i = y j = x k = z	-1.86	-2.06	+2.53
3. i = x j = z k = y	+11.0	+7.79	-6.14
4. i = y j = z k = x	+5.05	+4.17	-4.01
5. i = z j = x k = y	-11.8	-3.07	+6.02
6. i = z j = y k = x	-9.16	-5.73	+3.60



A possible problem with the above analysis is the fact that the uncertainty in the n value measured for $\text{Cl}_2\text{Sn}[\text{Fe}(\text{CO})_2\text{cp}]_2$ is relatively large $(0.05)^2$. Consequently, an alternative (and possibly more accurate) approach is to solve for $\{\text{Cl}\}$ and $\{\text{Fe}(\text{CO})_2\text{cp}\}$ using the V_{ZZ} expressions for $\text{Cl}_2\text{Sn}[\text{Fe}(\text{CO})_2\text{cp}]_2$ and $\text{Cl}_2\text{SnFe}(\text{CO})_2\text{cp}$. For the latter compound,

$$-eQV_{ZZ} = 0.8589\{\text{Cl}\} - 2.0000\{\text{Fe}\} \quad \dots, (3.2)$$

; and V_{ZZ} for the former compound is defined by one of equations 3.1a-c. Consequently, there are three possible solutions as, once again, it is possible that V_{ii} , V_{jj} or V_{kk} for $\text{Cl}_2\text{Sn}[\text{Fe}(\text{CO})_2\text{cp}]_2$ could be assigned to V_{ZZ} . However, of the three possible solutions, only the one for $V_{kk} = V_{ZZ}$ correctly reproduces the correct QS and n for $\text{Cl}_2\text{Sn}[\text{Fe}(\text{CO})_2\text{cp}]_2$.

The $\{\text{Cl}\}$ and $\{\text{Fe}(\text{CO})_2\text{cp}\}$ thus derived were used to also derive $\{\text{Ph}\}$, $\{\text{Mn}(\text{CO})_5\}$ and $\{\text{Co}(\text{CO})_5\}$ from the compounds listed in table 3.8, once again applying crystallographically determined bond angles^{7,40,41} in the equations in table 1.1. It can be seen that these pqs values are not greatly different from those calculated using regular tetrahedral angles, and the order of the ligand pqs values is similar (except for $\text{Mn}(\text{CO})_5$ and $\text{Co}(\text{CO})_5$, whose pqs values are now nearly equal).

The number of compounds to which these pqs values can be applied is limited by the number whose structural parameters have been measured. These compounds, together with the predicted and observed QS and n values, are listed in table 3.9. It can

table 3.8

Calculated Absolute Ligand pqs Values for Four
Co-ordinate Tin
(method 2)

L	pqs (mm s^{-1})	derived from (QS; mm s^{-1})
$\text{Fe}(\text{CO})_2\text{cp}$	-1.15	$\text{Cl}_n\text{Sn}[\text{Fe}(\text{CO})_2\text{cp}]_{4-n}$
Cl	-0.556	($n = 2, 3$)
Ph	-1.66	$\text{Ph}_3\text{SnFe}(\text{CO})_2\text{cp}$
$\text{Mn}(\text{CO})_5$	-0.996	$\text{ClSn}[\text{Mn}(\text{CO})_5]_3$
$\text{Co}(\text{CO})_4$	-1.02	$\text{ClSn}[\text{Co}(\text{CO})_4]_3$

table 3.9

Calculated and Observed QS Values for some
Four Co-ordinate Tin Compounds;
Using Crystallographically Measured Bond Angles

Compound	QS (mm s^{-1})		
	Observed	Calculated from crystallographic data	Calculated assuming regular tetrahedral geometry
Ph_3SnCl	-2.54 ($\eta=0.0$)	-2.68 ($\eta=0.00$)	-2.52 ($\eta=0.00$)
$\text{Ph}_3\text{SnMn}(\text{CO})_5$	0.41	-0.76 ($\eta=0.00$)	-0.58 ($\eta=0.00$)
$\text{PhCl}_2\text{SnFe}(\text{CO})_2\text{cp}$	2.84	-3.10 ($\eta=0.30$)	+2.72 ($\eta=0.98$)
$\text{Ph}_2\text{Sn}[\text{Mn}(\text{CO})_5][\text{Co}(\text{CO})_4]$	1.15	+1.30 ($\eta=0.95$)	-1.06 ($\eta=0.72$)

be seen that QS values calculated using either relative pqs values and regular tetrahedral geometry, or absolute pqs values and crystallographically measured bond angles agree almost equally well with measured values.

Thus, the use of these absolute pqs values rather than the relative values does not seem justified in general, since the calculations are less straightforward, and are limited to the small number of compounds whose structural parameters have been determined from diffraction studies.

D. References

1. M. G. Clark, A. G. Maddock and R. H. Platt; J. C. S. Dalton; (1972), 281.
2. B. A. Goodman, R. Greatrex and N. N. Greenwood; J. Chem. Soc. (A) (1971), 1868; T. C. Gibb, R. Greatrex and N. N. Greenwood; J. C. S. Dalton (1972), 238.
3. M. J. Mays and P. L. Sears; J. C. S. Dalton (1973), 1873.
4. S. R. A. Bird, J. D. Donaldson, S. A. Keppie and M. F. Lappert; J. Chem. Soc. (A) (1971), 1311.
5. R. F. Bryan; Chem. Comm. (1967), 355; J. Chem. Soc. (A) (1968), 696.
6. P. J. Greene and R. F. Bryan; J. Chem. Soc. (1970), 1696.
7. B. P. Bir'yukov, E. A. Kukhtenkova, Yu. Y. Struchkov, K. N. Anisimov, N. E. Kolobova and V. I. Khandozhko; J. Organomet. Chem. (1971) 27, 337.
8. S. R. A. Bird, J. D. Donaldson, A. F. Le C. Holding, B. J. Senior and M. J. Tricker; J. Chem. Soc. (A) (1971), 1616.
9. G. M. Bancroft, M. J. Mays and B. E. Prater; Discuss. Faraday Soc. (1969) 47, 136; J. Chem. Soc. (A) (1970), 956.
10. R. H. Herber and A. Hoffman; Progr. Inorg. Chem. (1967) 8, 36.
11. C. Wynter and L. Chandler; Bull. Chem. Soc. Japan (1970) 43, 2115.
12. S. Onaka, Y. Sasaki and H. Sano; Bull. Chem. Soc. Japan (1971) 44, 126.
13. S. R. A. Bird, J. D. Donaldson, A. F. Le C. Holding, B. Ratcliff, and S. Cenini; Inorg. Chim. Acta (1972) 6, 379.
14. R. V. Parish; Progr. Inorg. Chem. (1972) 15, 101.
15. A. N. Karasev, N. E. Kolobova, L. S. Polak, V. S. Shpinel and K. N. Anisimov; Teor. i Eksp. Khim., Akad. Nauk. Ukr. (1966) 2, 126.
16. W. R. Cullen, J. R. Sams and J. A. J. Thompson; Inorg. Chem. (1971) 10, 843.
17. B. A. Goodman, R. Greatrex and N. N. Greenwood; J. Chem. Soc. (A) (1971), 1868.
18. V. I. Gol'danskii, B. V. Borshagovskii, E. F. Makarov, R. A. Stukan, K. N. Anisimov, N. E. Kolobova and V. V. Skripkin;

Teor. i Eksp. Khim., Akad. Nauk. Ukr. (1967) 3, 478.

19. S. Ichiba, M. Katada and H. Negita; Bull. Chem. Soc. Japan (1972) 45, 1679.
20. D. E. Fenton and J. J. Zuckermann; J. Amer. Chem. Soc. (1968) 90, 6226.
21. Average value from several sources, or private communication, listed in P. J. Smith; Organometal. Chem. Rev. (A) (1970) 5, 373.
22. R. H. Herber, H. A. Stöckler and W. T. Reichle; J. Chem. Phys. (1965) 42, 2447.
23. Average value from several sources, or private communication, listed in G. M. Bancroft and R. H. Platt; Adv. Inorg. Radiochem. (1972) 15, 59.
24. H. A. Stöckler and H. Sano; Trans. Faraday Soc. (1968) 64, 577.
25. R. V. Parish and R. H. Platt; J. Chem. Soc. (A) (1969), 2145.
26. M. Cordey Hayes, R. D. W. Kemmitt, R. D. Peacock and G. Rimmer; J. Inorg. Nucl. Chem. (1969) 31, 1515.
27. W. R. Cullen, J. R. Sams and M. C. Waldman; Inorg. Chem. (1970) 9, 1682.
28. M. G. Clark; private communication.
29. For example: (a) H. C. Clark, R. J. O'Brien and J. Trotter; J. Chem. Soc. (1964), 2332;
(b) E. O. Schlemper and W. C. Hamilton; Inorg. Chem. (1966) 5, 995.
30. For example: R. A. Forder and G. M. Sheldrick; J. Organomet. Chem. (1970) 21, 115;
N. W. Alcock and R. E. Timms; J. Chem. Soc. (A) (1968), 1873.
31. G. A. Melson, P. F. Stokely and R. F. Bryan; J. Chem. Soc. (A) (1970), 2247.
32. N. G. Bokii, G. N. Zakharova and Yu. T. Struchkov; J. Struct. Chem. (USSR) (1970) 11, 828.
33. P. T. Greene and R. F. Bryan; J. Chem. Soc. (A) (1971), 2549.
34. V. Cody and E. R. Corey; J. Organomet. Chem. (1969) 19, 359.

35. A. G. Maddock and R. H. Platt; J. Chem. Soc. (A) (1971), 1191.
36. P. J. Smith; personal communication to R. H. Platt.
37. A. G. Davies, H. J. Milledge, D. C. Puxley and P. J. Smith; J. Chem. Soc. (A) (1970), 2862.
38. M. G. Clark; Chem. Phys. Lett. (1972) 13, 316.
39. J. E. O'Connor and E. R. Corey; Inorg. Chem. (1967) 6, 968.
40. R. F. Bryan; J. Chem. Soc. (A) (1967), 192.
41. J. H. Tsai, J. J. Flynn and J. P. Boer; Chem. Comm. (1967), 702.

CHAPTER 4

Centre Shifts for Compounds Containing a Tin-Transition Metal Bond

A. Introduction

The interpretation of organo-tin centre shift (CS) values has met with difficulties (for reviews see references 1 and 2). CS values for octahedral and tetrahedral Sn(IV) halide complexes decrease with increasing ligand electronegativity³⁻⁷. Both 5s and 5p electron density are withdrawn from the tin atom by electronegative ligands; but, since the CS is most sensitive to changes in 5s electron density⁸, and $\delta R/R$ is positive, a net withdrawal of s electrons by an electronegative ligand decreases the CS. For example, the order of CS values found¹ for the series SnX_3^- is $X = \text{F} < \text{Cl} < \text{Br} < \text{I}$.

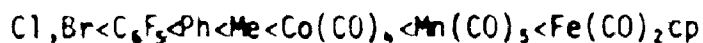
However, for compounds containing a tin-transition metal bond, expected trends in terms of the above argument are not borne out by experimental results. For example, in each of the series of compounds $\text{R}_n \text{X}_{3-n} \text{SnM}$ and $\text{R}_n \text{X}_{2-n} \text{SnM}_2$ ($\text{R} = \text{Me}, \text{Ph}; \text{X} = \text{Cl}, \text{Br}; \text{M} = \text{Mn}(\text{CO})_5, \text{Fe}(\text{CO})_2\text{cp}, \text{Co}(\text{CO})_4$), the CS increases as n increases (table 4.1), despite the much greater electronegativity of X

relative to R. Such trends have been interpreted⁹⁻¹³ in terms of a large tin 5s character in the Sn-M bond relative to the other tin-ligand bonds. Thus, if the Sn-Cl bond in one of these compounds involves little tin 5s character, Cl would be expected to increase $|\Psi(0)_{5s}|^2$ by removal of p electron density (i.e. by deshielding), and the CS increases - in contrast to the decrease in CS noted earlier if the Sn-Cl bond involves appreciable tin 5s character. This interpretation is similar to that used to explain ^{129}Xe and ^{129}I CS parameters in the square-planar complexes XeX_4 and IX_4^- (X = halide). Because the bonds have essentially pure p character, $|\Psi(0)_s|^2$ also increases as the electronegativity of the halide ligand increases^{1,14,15}.

This approach is used and extended here for a range of tin-transition metal bonded complexes.

b. The s-character Series and n.m.r. Coupling Constants

The relative amount of tin 5s character present in tin-ligand bonds for a number of ligands may be established to increase in the order



directly from Mossbauer CS data. This order is derived by considering the following results, using data shown in table 4.1.

The trend of CS values in the series of four co-ordinate compounds $\text{X}_n\text{SnM}_{4-n}$, $\text{R}_n\text{SnM}_{4-n}$ and $\text{R}_n\text{SnX}_{4-n}$ (X = Cl, Br, I; R = Me, Ph, C₆F₅; M = Mn(CO)₅, Fe(CO)₂cp, Co(CO)₆) establishes that the general ordering of s character in tin-ligand bonds is X < R < M. The generally larger CS values for compounds containing the

table 4.1

 ^{119}Sn Mossbauer Centre Shift Data for someFour Co-ordinate Tin Complexes(mm s⁻¹; relative to BaSnO_3 ; -77 K)

M =	<u>$\text{Co}(\text{CO})_4$</u>	<u>$\text{Mn}(\text{CO})_5$</u>	<u>$\text{Fe}(\text{CO})_5$</u> ,cp
SnM_4	2.04 *		2.14 a
MeSnM_3	1.79 *	1.83 a	
PhSnM_3	1.54 a		2.00 a
ClSnM_3	2.05 *	1.92 a	
BrSnM_3	1.97 c		
Me_2SnM_2	1.57 *	1.68 a	1.68 a
MeClSnM_2	1.74 *		
Ph_2SnM_2	1.60 *		1.74 a
PhClSnM_2	1.70 *		
Cl_2SnM_2	1.75 *	1.90 b	1.99 a
Br_2SnM_2	1.75 *	2.04 b	1.99 a
Me_3SnM	1.39 *	1.41 *	1.35 d
Me_2ClSnM	1.49 *	1.52 *	
Me_2BrSnM		1.54 a	
MeCl_2SnM		1.62 *	
MeBr_2SnM		1.69 a	
Cl_3SnM	1.42 *	1.65 *	1.75 *
Br_3SnM	1.49 c	1.76 *	1.86 *
Ph_3SnM	1.41 *	1.35 *	1.39 *
Ph_2ClSnM	1.48 *	1.61 a	1.58 a
Ph_2BrSnM		1.58 a	1.61 a
PhCl_2SnM		1.63 a	1.70 a
PhBr_2SnM		1.75 a	1.73 a

* this work

a from various workers, listed in reference 1

b reference 7b

c reference 16

d reference 13

$\text{Fe}(\text{CO})_2\text{cp}$ moiety compared with the analogous $\text{Mn}(\text{CO})_5$ compounds strongly indicate that the $\text{Sn}-\text{Fe}$ bond has a greater $5s$ character than the $\text{Sn}-\text{Mn}$ bond; especially since OS results (see chapter 2) indicate that $\text{Fe}(\text{CO})_2\text{cp}$ is a better p electron donor than $\text{Mn}(\text{CO})_5$, which would tend to decrease the relative CS values. A similar argument indicates that the s character of the $\text{Sn}-\text{Me}$ bond is greater than that of the $\text{Sn}-\text{Ph}$ bond (eg. CS of Me_4Sn and Ph_4Sn are 1.31 and 1.22 mm s^{-1} respectively¹). Again the p donor strengths from pqs values would give the opposite trend.

The fact that CS increases markedly with n in the series $\text{R}_{4-n}\text{Sn}[\text{Co}(\text{CO})_4]_n$ ($\text{R} = \text{Me}, \text{Ph}$), as it does for the analogous $\text{Mn}(\text{CO})_5$ and $\text{Fe}(\text{CO})_2\text{cp}$ series, shows that $\text{Co}(\text{CO})_4$ lies above Me and Ph in the s -character series. However, the CS values for most of the $\text{Co}(\text{CO})_4$ compounds are smaller than for the $\text{Mn}(\text{CO})_5$ and $\text{Fe}(\text{CO})_2\text{cp}$ analogues, which would indicate that the order of s character in the $\text{Sn}-\text{M}$ bonds is $\text{M} = \text{Co}(\text{CO})_4 < \text{Mn}(\text{CO})_5, \text{Fe}(\text{CO})_2\text{cp}$. For example; considering the halide complexes, CS for the $\text{X}_n\text{Sn}[\text{Co}(\text{CO})_4]_{4-n}$ compounds is generally less than for the $\text{X}_n\text{SnM}_{4-n}$ ($\text{M} = \text{Mn}(\text{CO})_5, \text{Fe}(\text{CO})_2\text{cp}$; $\text{X} = \text{Cl}, \text{Br}$) compounds. This is largely due to the higher tin $5s$ character in the $\text{Sn}-\text{X}$ bonds of the cobalt compounds, and therefore lower $5s$ character in the $\text{Sn}-\text{Co}$ bonds. The electronegative halogens therefore withdraw more s electron density in the cobalt compounds than in the manganese or iron analogues, and thus decrease the CS.

One consequence of this relative order of s character

7

in the tin-transition metal bonds can be seen in the CS values for the series of compounds $R_{3-n}X_nSnM$. For $M = Co(CO)_4$, the CS only increases marginally with increase in n , and then decreases, in contrast to the situation for $M = Mn(CO)_5$ and $M = Fe(CO)_2cp$. For example, the CS values for the compounds $Ph_3SnCo(CO)_4$, $Ph_2ClSnCo(CO)_4$ and $Cl_3SnCo(CO)_4$ are 1.41, 1.48 and 1.42 $mm\ s^{-1}$ respectively; while the values for the analogous $Fe(CO)_2cp$ compounds are 1.39, 1.58 and 1.75 $mm\ s^{-1}$. This difference can be attributed, again, to an increase in s character of the Sn—Cl bonds in the $Co(CO)_4$ compounds.

Thus, the s character of the Sn—Cl bond is significant enough so that the CS is affected by direct s electron withdrawal, as well as p electron deshielding. The Sn—Cl bonds in the $Fe(CO)_2cp$ halide compounds contain so little s character that the CS is dominated by the effect on nuclear s density of p electron deshielding effects.

C_6F_5 lies below Ph in the tin-ligand bond s -character series, since CS values¹⁷ in the series $Ph_{4-n}Sn(C_6F_5)_n$ decrease from 1.22 $mm\ s^{-1}$ for Ph_4Sn to 1.04 $mm\ s^{-1}$ for $(C_6F_5)_4Sn$. Again, the p -donor strengths from pqs values would give the opposite trend.

The above s -character series is entirely consistent with $|^2J(^{119}Sn-C^1H_3)|$ parameters reported for Me_nSnL compounds (table 4.2). (The treatment described here is an extension of

table 4.2

 ^1H nmr and ^{119}Sn Mössbauer Data for some Me_3SnL Compounds

Compound	$ ^2J(^{119}\text{Sn}-\text{C}^1\text{H}_3) $ (Hz)	CS (mm s^{-1})
$\text{Me}_3\text{Sn}(\text{C}_6\text{F}_5)$	58.8 a	1.27 f
$\text{Me}_3\text{Sn}(\text{C}_6\text{Cl}_5)$	56.8 a	1.32 f
Me_3SnPh	54.6 a	1.21 f
Me_4Sn	54.0 a	1.31 f
$\text{Me}_3\text{SnCo}(\text{CO})_4$	52.0 b	1.39 *
$\text{Me}_3\text{SnMn}(\text{CO})_5$	48.8 c	1.41 *
$\text{Me}_3\text{SnMo}(\text{CO})_3\text{cp}$	48.3 d	1.43 g
$\text{Me}_3\text{SnW}(\text{CO})_3\text{cp}$	48.2 d	1.36 g
$\text{Me}_3\text{SnCr}(\text{CO})_3\text{cp}$	48.1 d	1.41 q
$\text{Me}_3\text{SnFe}(\text{CO})_2\text{cp}$	47.2 e	1.35 e
$\text{Me}_3\text{SnFe}(\text{CO})(\text{PhO})_3\text{Pcp}$	44.0 e	1.39 e
$\text{Me}_3\text{SnFe}(\text{CO})(\text{Ph}_3\text{P})\text{cp}$	40.4 ^a e	1.41 e

* this work

a reference 18

b reference 19

c reference 20

d reference 21

e reference 13

f average values; from reference 1

g reference 22

the ideas of Fenton et al⁹, Cullen et al¹³ and other workers^{11,23,24}). Assuming that the main contribution to $^2J(^{119}\text{Sn}-\text{C}^1\text{H}_3)$ is from the Fermi-contact term, then for a series of closely related compounds such as those listed in table 4.2, Pidcock et al²⁵ have proposed that the two bond tin-methyl coupling constant, 2J , is affected by $|\psi(0)_{\text{Sn}5s}|^2$, α^2 (the s character of the tin-carbon bond) and c_s (the degree of covalency due to s electron overlap in the tin carbon bond). Pidcock has pointed out²⁰ that the nmr $|\psi(0)_s|^2$ term refers to the square of the amplitude of the atomic wave function at the nucleus, and the α^2 and c_s terms represent the extent to which this orbital is populated in bonding. In contrast, the Mössbauer $|\psi(0)_s|^2$ term has, in past treatments, been taken to include all three of these terms. However, when comparing 2J and CS parameters, it seems convenient to separate the terms for the CS in the same way, i.e.

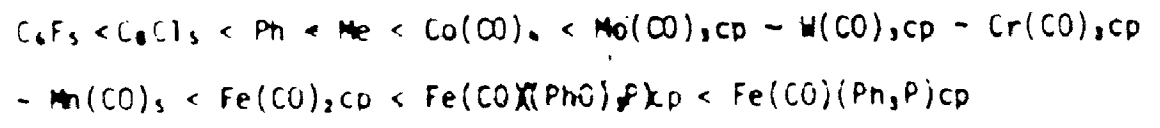
$$CS = |\psi(0)_{\text{Sn}5s}|^2 \times \prod_{\text{all bonds}} \alpha_s^2 \times \prod_{\text{all bonds}} c_s \quad \dots (4.1)$$

Thus $|\psi(0)_{\text{Sn}5s}|^2$ will only vary in response to shielding effects - i.e. changes in tin 5p orbital populations.

From table 4.2, it is apparent that there is no correlation between CS and $|^2J(^{119}\text{Sn}-\text{C}^1\text{H}_3)|$; and that the variation in CS from compound to compound is relatively small. In the Me_2SnL compounds, α_s^2 in the tin-methyl bond would be expected to vary considerably as the L ligand is varied through a series of moieties with widely varying bonding modes. In contrast, changes in $|\psi(0)_{5s}|^2$ and c_s should be small, and in opposition to one another.

However, the total α_s^2 over all the ligands will be almost invariant; so that, if the CS varies little in a series of related compounds, then the changes in the total $|\psi(0)_{5s}|^2$ and c_s must be equal, and in opposition.

As a consequence, the trend in the $^2J(^{119}\text{Sn}-\text{C}^1\text{H}_3)$ values will reflect the relative order of tin s character in the tin-methyl bonds. Conversely, the order of increasing s character in the tin-ligand (L) bond will be the reverse of the order of coupling constants: i.e. (from table 4.2)



- consistent with the order of s character derived previously.

Although the difference in 2J coupling constants between Me_2SnPh and Me_2Sn is not great, their relative order in the tin s-character series is unambiguous since the compound with the larger 2J value also has the smaller CS value. Hence the coupling constant increases despite the decrease in s electron density at the tin nucleus. The relative positions of $\text{Mn}(\text{CO})_5$, $\text{Mo}(\text{CO})_3\text{cp}$ and $\text{W}(\text{CO})_3\text{cp}$ are illustrated by the 2J values for the compounds $\text{Me}_2\text{Sn}[\text{Mn}(\text{CO})_5]_2$ (36.7 Hz), $\text{Me}_2\text{Sn}[\text{Mn}(\text{CO})_5][\text{Mo}(\text{CO})_3\text{cp}]$ (36.9 Hz) and $\text{Me}_2\text{Sn}[\text{Mn}(\text{CO})_5][\text{W}(\text{CO})_3\text{cp}]$ (37.3 Hz)²⁷. These parameters show that in the s-character series, $\text{Mn}(\text{CO})_5 \sim \text{Mo}(\text{CO})_3\text{cp}$, but that $\text{Mn}(\text{CO})_5$ is slightly below $\text{W}(\text{CO})_3\text{cp}$ (though this latter difference did not show up so strongly in the Me_2SnL series).

It is interesting to note the surprisingly large increase in s character in the Sn—Fe bond from the parent carbonyl to the phosphite- and phosphine-substituted compounds, as reflected in the nmr 2J values. However, the CS values do not change appreciably, so that the donor ability of the ligand is little changed.

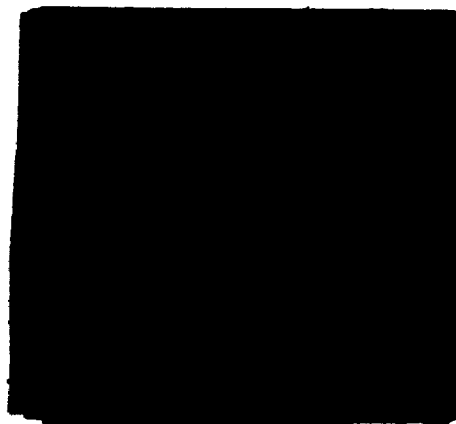
Figure 4.1 shows a correlation between $^2J(^{119}\text{Sn}-\text{CH}_3)$ and CS for the related series of compounds $\text{Me}_n\text{SnM}_{4-n}$ ($M = \text{Co}(\text{CO})_4$, $\text{Mn}(\text{CO})_5$, $\text{Fe}(\text{CO})_2\text{cp}$). Data were collected from references 1, 13, 18-20 and 28, as well as this work. The changes in CS for these series of compounds will be due to a change in the total c_s term - since $|\psi(0)_{\text{Sn}5s}|$ and the total $\alpha_s^2(\text{Sn})$ are constant - due to the different donor abilities of the transition metal complex ligands compared with Me. Since the CS increases systematically from Me_4Sn to M_4Sn ($M = \text{Co}(\text{CO})_4$, $\text{Mn}(\text{CO})_5$, $\text{Fe}(\text{CO})_2\text{cp}$), then the transition metal moieties must be better donors than Me. The 2J values vary in the series in figure 4.1 because of changes in $\alpha_s^2(\text{Sn}-\text{Me})$ and $c_s(\text{Sn}-\text{Me})$, which reinforce. Greater covalency of the Sn—M bonds will be at the expense of the Sn—Me bonds, and the increasing demand for s character for Sn—M bonds as the number of M groups increases implies the negative $^2J/CS$ plot which is observed.

Finally, it is interesting to compare the isoelectronic complexes $[\text{Cl}_3\text{SnFe}(\text{CO})_2\text{cp}]^-$ and $[\text{Cl}_3\text{SnMn}(\text{CO})_2\text{cp}]^-$. The CS values for these two (table 2.1) are similar, which implies that the donor-acceptor properties of the $\text{Fe}(\text{CO})_2\text{cp}$ and $\text{Mn}(\text{CO})_2\text{cp}$ groups

2

OF/DE

2



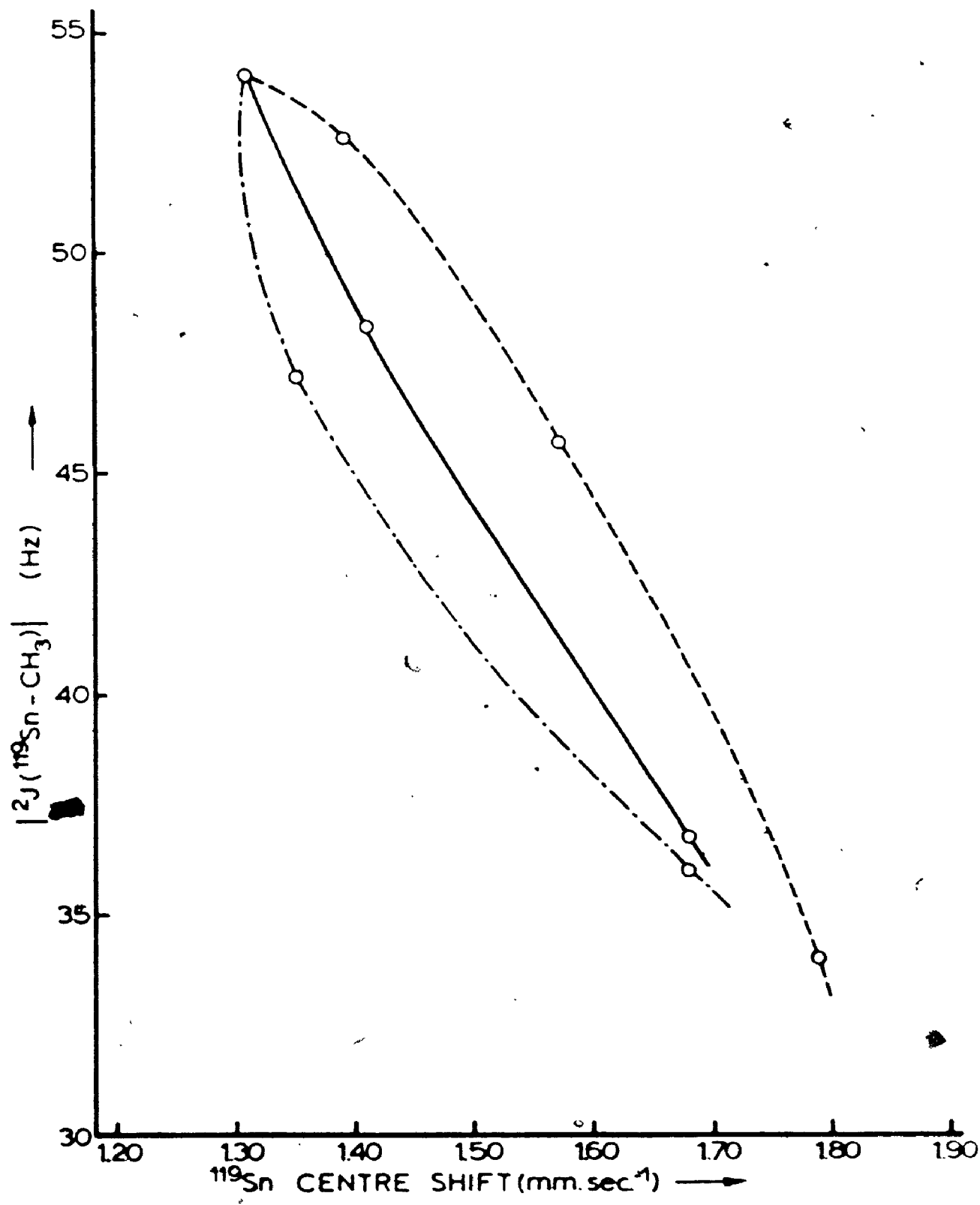


figure 4.1

Plot of $|^2J(^{119}\text{Sn}-\text{CH}_3)|$ versus ^{119}Sn Centre Shift for $\text{Me}_n\text{SnM}_{4-n}$ Compound
(---) Co(CO)_4 ; (—) Mn(CO)_5 ; (- - - -) $\text{Fe(CO)}_2\text{cp}$.

to tin are quite similar. However, the significantly different CS values indicate that in these cases, the Sn—Mn bond has a greater s character than the Sn—Fe bond.

C. Molecular Geometry in Four Co-ordinate Tin Compounds

The s-character series just derived may be used to rationalize the published structural data for four co-ordinate tin compounds which contain tin-transition metal bonds. From the re-hybridisation concepts of Bent²⁹, it would be expected that the greater the difference in s characters of the tin-ligand bonds in tetrahedral compounds, the greater would be the deviation from regular geometry; and the L—Sn—L bond angles will be smallest for the Sn—L bonds of lowest s character. These expectations are borne out by the data in tables 4.3 a - d. Thus $\text{Me}_3\text{SnMn}(\text{CO})_5$ is only slightly distorted from regular T_d geometry, and Me and $\text{Mn}(\text{CO})_5$ are almost adjacent in the s-character series. By contrast, $\text{Cl}_3\text{SnFe}(\text{CO})_2\text{cp}$ is the most distorted of the A_3SnB -type compounds in table 4.3a, and Cl and $\text{Fe}(\text{CO})_2\text{cp}$ are far apart in the s-character series. The distortions of the other A_3SnB compounds qualitatively agree with that which would be predicted from the s-character series: i.e.

$\text{Me}_3\text{SnMn}(\text{CO})_5 < \text{Ph}_3\text{SnMn}(\text{CO})_5 - \text{Ph}_3\text{SnCl} < \text{Ph}_3\text{SnFe}(\text{CO})_2\text{cp} < \text{Me}_3\text{SnFe}(\text{CO})(f_6\text{fos})\text{cp} < \text{Br}_3\text{SnFe}(\text{CO})_2\text{cp} < \text{Cl}_3\text{SnFe}(\text{CO})_2\text{cp}$ ($f_6\text{fos}$ is a diphenyl fluoroalkyl phosphine ligand).

Similarly, for the series of compounds ClSnA_3 (table 4.3b), bond angles deviate more and more from 109.47° (as in SnCl_4)

table 4.3

Bond Angle Data* for some Tetrahedral Organo-tin Compounds.

4.3	<u>compound</u>	<u>bond angles (°)</u>		<u>reference</u>
		<u>A-Sn-A</u>	<u>A-Sn-B</u>	
	<u>A₃SnB</u>			
	Me ₃ SnMn(CO) ₅	107.3	111.6	30
	Ph ₃ SnMn(CO) ₅	106.0	112.7	31
	Ph ₃ SnCl	112.4	106.4	32
	Ph ₃ SnFe(CO) ₂ cp	105.2	113.4	33
	Me ₃ SnFe(CO)(f ₆ f _{os})cp	102.3	115.8	34
	Br ₃ SnFe(CO) ₂ cp	100.2	117.7	35
	Cl ₃ SnFe(CO) ₂ cp	98.3	119.2	36

4.3b	<u>compound</u>	<u>bond angles (°)</u>		<u>reference</u>
		<u>A-Sn-A</u>	<u>A-Sn-Cl</u>	
	<u>A₃SnCl</u>			
	[Mn(CO) ₅] ₂ SnCl	116.5	101.0	37
	[Co(CO) ₄] ₂ SnCl	114	104	38
	Ph ₃ SnCl	112.3	106.4	32
	Cl ₄ Sn	109.5	109.5	39

table 4.3 (cont'd)

4.3c	<u>compound</u>	<u>bond angles (°)</u>		<u>reference</u>
		<u>A-Sn-A</u>	<u>B-Sn-B</u>	
	<u>A₂SnB₂</u>			
	Me ₂ Sn[Fe(CO) ₂ cp] ₂	104	123	40
	Ph ₂ Sn[Fe(CO) ₂ cp] ₂	95	116	41
	Cl ₂ Sn[Fe(CO) ₂ cp] ₂	94.1	128.6	42
	Cl ₂ SnPh ₂	100	125.5	43
	Ph ₂ Sn[Mn(CO) ₅] ₂	100	117	44
	Ph ₂ Sn[Co(CO) ₂ (NBD)] ₂	99.6	118.3	45
	Cl ₂ Sn[Co(CO) ₂ (NBD)] ₂	98.1	128.3	45
<hr/>				
4.3d	<u>compound</u>	<u>bond angles (°)</u>		<u>reference</u>
		<u>Mn-Sn-A</u>		
	<u>Ph₂Sn[Mn(CO)₅]A</u>			
	Ph ₂ Sn[Mn(CO) ₅] ₂	117		44
	Ph ₂ Sn[Mn(CO) ₅][Co(CO) ₄]	114		46
	Ph ₃ Sn[Mn(CO) ₅]	112.7		31

*Average values given where there is more than one such angle in the compound

in the order $A = \text{Cl} < \text{Ph} < \text{Co}(\text{CO})_4 < \text{Mn}(\text{CO})_5$ - ie. as Cl and the ligand A are increasingly further apart in the s-character series.

For the A_2SnB_2 compounds listed in table 4.3c, the order of increasing distortion is, once again, that expected from the s-character series; though the degree of distortion is greatly increased from the A_1SnB compounds. As the difference between the s characters of the Sn—A and Sn—B bonds increases, the p character of the Sn—A bonds increases. Thus the A—Sn—A angle will deviate towards the "pure p" angle of 90° . In addition, the decreasing p character of the Sn—B bond will cause the B—Sn—B angle to become larger than the sp^3 value of 109.47° . Thus, in the A_2SnB_2 series, $\text{Ph}_2\text{Sn}[\text{Mn}(\text{CO})_5]_2$ is the least distorted, and $\text{Cl}_2\text{Sn}[\text{Fe}(\text{CO})_2\text{cp}]_2$ the most distorted. It is difficult to assess qualitatively the other distortions, but it is interesting to note that the distortion in Ph_2SnCl_2 is similar to that in such compounds as $\text{Me}_2\text{Sn}[\text{Fe}(\text{CO})_2\text{cp}]_2$ which also contain two non-nearest neighbour ligands in the s-character series.

For the A_2SnB_2 compounds with the same B ligands (B = $\text{Fe}(\text{CO})_2\text{cp}$ for A = Me, Ph, Cl; B = $\text{Co}(\text{CO})_2(\text{NBD})$ for A = Ph, Cl), the A—Sn—A angle decreases progressively as the ligand A falls lower in the s-character series. It can be noted, too, that the Ph—Sn—Ph angle is $>109.47^\circ$ in Ph_2SnCl_2 , but $<109.47^\circ$

in $\text{Ph}_2\text{Sn}[\text{Mn}(\text{CO})_5]_2$, as Cl and $\text{Mn}(\text{CO})_5$ are on opposite sides of Ph in the s-character series.

The data in tables 4.3a, b and c are thus consistent with Ph_2SnCl_2 and Ph_3SnCl being four co-ordinate, with the s character concentrated in the Sn—Ph bond, and with no inter-molecular association; consistent with the conclusions from the additivity model (see chapter 3), and X-ray diffraction studies^{32,43}.

Finally, from table 4.3d, the Mn—Sn—A angle in $\text{Ph}_2\text{Sn}[\text{Mn}(\text{CO})_5]_2\text{A}$ compounds increases in the order $\text{A} = \text{Ph} < \text{Co}(\text{CO})_5 < \text{Mn}(\text{CO})_5$ as would be expected. Patmore and Graham¹⁹ have also proposed, on the basis of intensity ratios of the A_1 and B_1 $\nu(\text{CO})$ bands for the series of compounds $\text{Ph}_n\text{Cl}_{2-n}\text{Sn}[\text{Co}(\text{CO})_5]_2$, that the Co—Sn—Co angle increases from $n = 2$ to $n = 0$ (ie. as Ph ligands are successively replaced by Cl). This trend is, once more, consistent with the s-character series derived in this study.

Consistent with another of Bent's "rules" for re-hybridisation²⁹, the Fe—Sn bond length can be observed to decrease as the proposed s character of the bond increases. Thus the measured Fe—Sn bond length decreases from 2.536(3) Å for $\text{Ph}_3\text{SnFe}(\text{CO})_2\text{cp}$ ³³, to 2.504(3) Å for $\text{Ph}_2\text{ClSnFe}(\text{CO})_2\text{cp}$ ⁴⁷, and to 2.467(2) for $\text{PhCl}_2\text{SnFe}(\text{CO})_2\text{cp}$ ³⁶ and 2.467(1) for $\text{Cl}_3\text{SnFe}(\text{CO})_2\text{cp}$ ³⁶. The bond length, like the CS, levels off for the latter two complexes. Similarly, for the $\text{A}_2\text{Sn}[\text{Fe}(\text{CO})_2\text{cp}]_2$ complexes, the Sn—Fe bond decreases in the order $\text{A} = \text{Me}$ (2.605(4) Å⁴⁰) > Ph (2.537 Å⁴¹) > Cl (2.492(8) Å⁴²), as would be expected for increasing s character

in the Sn—Fe bond. The same phenomenon is observed for the Sn—Co bond in the complexes $A_2Sn[Co(CO)_2(NBD)]_2$, where Sn—Co is 2.571(3) Å for A = Ph, and 2.499(1) Å for A = Cl⁴⁵.

D. 59-Cobalt e^2qQ Values

Several recent papers^{48,49} have reported ⁵⁹Co e^2qQ values, from nuclear quadrupole resonance (nqr) spectra, for some $X_nSn[Co(CO)_4]_{4-n}$ compounds (X = Me, Ph, Br, Cl; n = 1, 2, 3), and it is useful to correlate these with the ¹¹⁹Sn Mössbauer centre shifts measured in this study. As will be shown in chapter 5, the e^2qQ value for a hypothetical $Co(CO)_4^+$ species should be ca. +180 MHz. When the CO ligand along the Z principal efg axis is replaced by a ligand L, e^2qQ will become more negative if L is a better σ donor than CO, and more positive if it is a better π acceptor than CO. Thus $e^2qQ(^{59}Co)$ is proportional to $\Delta\pi - \Delta\sigma$.

For the three series of compounds $X_nSn[Co(CO)_4]_{4-n}$ (n = 1, 2 or 3), $e^2qQ(^{59}Co)$ increases as CS increases, as shown in figure 4.2. This correlation can be readily rationalised in terms of σ effects, if the controlling factor in the CS variation is the large s character in the Sn—Co bond, compared with the other tin-ligand bonds. Thus the CS becomes more negative as σ donation by X ligands, largely to the tin 5p orbitals, increases. (It would become more positive if the π acceptance of X increased). Thus the $(^{119}Sn)CS/(^{59}Co)e^2qQ$ correlations represent a plot of $(-\sigma_p + \pi)$ against $(\Delta\pi - \Delta\sigma)$, and gradients

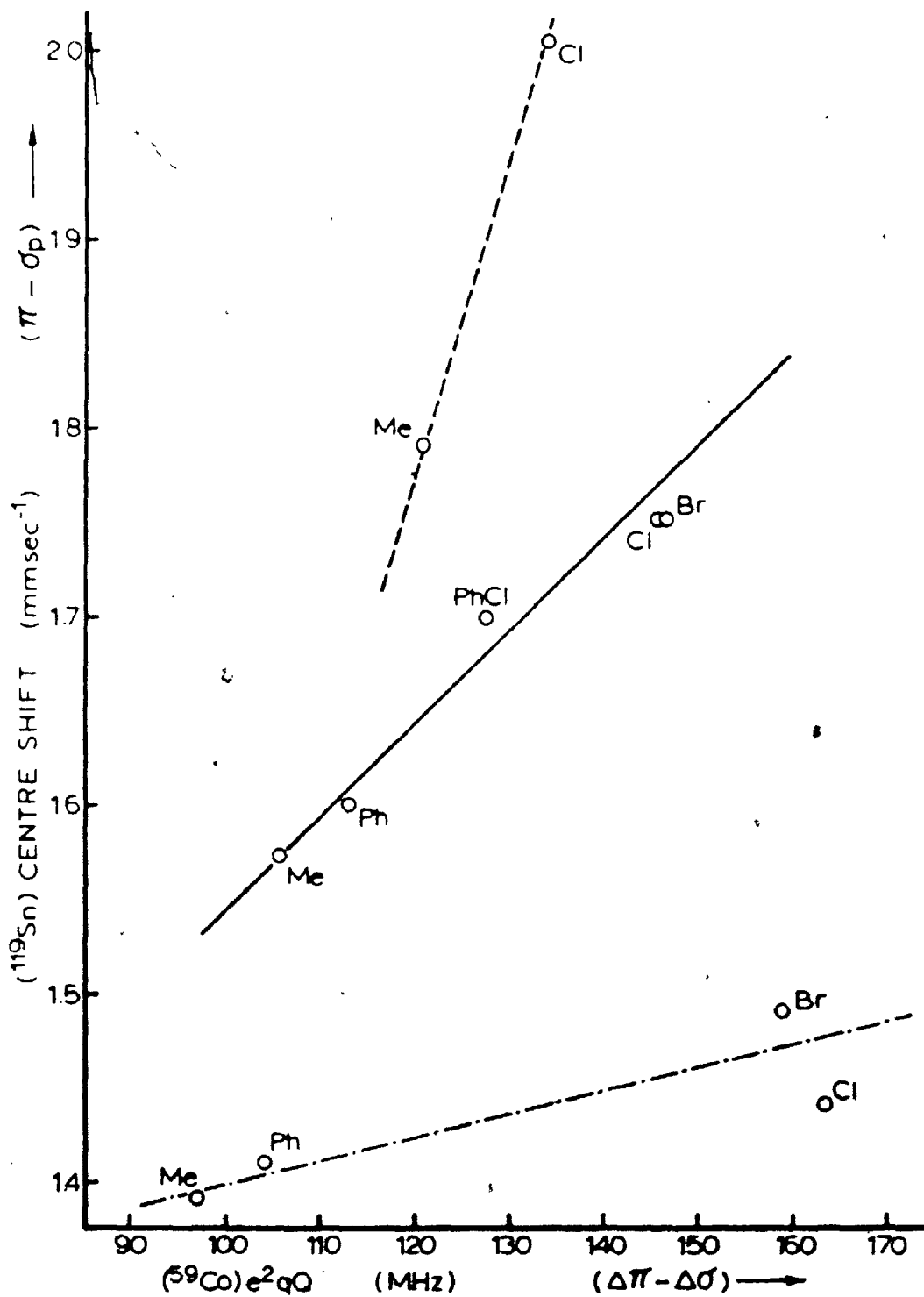


figure 4.2

Plot of ^{119}Sn Mössbauer Centre Shift versus $(^{59}\text{Co}) e^2qQ$ (from nqr) for some $X_n\text{Sn}[\text{Co}(\text{CO})_n]_{4-n}$ Compounds.

(--- n = 1, — n = 2, - · - · - n = 3)

should be positive, as is observed. Thus the plots in figure 4.2 cannot distinguish σ and π effects, but both $e^2qQ(^{59}\text{Co})$ nqr results⁴⁸ and $CS(^{119}\text{Sn})$ values^{1,9} indicate that both parameters are probably much more sensitive to σ effects.

The greater sensitivity of the ^{119}Sn CS for small n (figure 4.2) can also be explained using the s character arguments given above. As n decreases, more tin $5s$ character is used in the larger number of $\text{Sn}-\text{Co}$ bonds, and the $\text{Sn}-\text{X}$ bonds will thus have greater $5p$ character. This will, of course, make the CS more sensitive to variation in σ properties of X as n decreases, as is observed. The variation in $\text{Sn}-\text{Co}$ bonding with variation in X is also felt by the carbonyl ligands, as indicated by the $\nu(\text{CO})$ against $e^2qQ(^{59}\text{Co})$ correlation for $X_n\text{Sn}[\text{Co}(\text{CO})_2]_{4-n}$ compounds, given previously⁴⁸.

It might be expected that a similar correlation of $CS(^{119}\text{Sn})$ with $e^2qQ(^{57}\text{Fe})$ from ^{57}Fe Mössbauer spectra for $X_n\text{Sn}[\text{Fe}(\text{CO})_2\text{cp}]_{4-n}$ would yield conclusions similar to those for the tin-cobalt compounds above. However, insufficient ^{57}Fe Mössbauer data for such compounds has been published for a meaningful analysis to be made. In addition, as has been pointed out⁵⁰, the range of ^{57}Fe e^2qQ values for all $\text{LFe}(\text{CO})_2\text{cp}$ compounds so far observed is small, and variations for closely related compounds are generally not much greater than the experimental errors.

E. The Oxidation State and Valency of Tin

The concept of oxidation state is one which has proved very useful in rationalising experimental results in a number of areas of inorganic chemistry, particularly in connection with complexes of transition metals. However, the concept is a formal one only, and difficulties can arise when trying to assign oxidation states in other than simple bonding situations. For example, Parshall⁵¹ recently reported the ESCA spectra of some tin-platinum cluster compounds, and attempted to assign formal oxidation states to the Sn and Pt atoms. However, for a number of these compounds, the calculated oxidation states were non-integral; and it was concluded that the bonding in these systems could only be adequately represented by a molecular orbital description.

More relevant to the present work is the postulate of Fenton and Zuckerman⁵² that ^{119}Sn Mössbauer CS values can be used to assign formal oxidation state to tin atoms in various tin compounds. The CS values measured in this study for the compounds *cis*- and *trans*- $[(\text{Cl}, \text{Sn})_2\text{Fe}(\text{RNC})_4]$, *cis*- $[\text{Cl}(\text{Cl}, \text{Sn})\text{Fe}(\text{RNC})_4]$ and $[(\text{Cl}, \text{Sn})\text{Fe}(\text{RNC})_3]\text{ClO}_4$ (RNC = *p*-MeO.C₆H₄.NC) (see table 4.4) are the first reported exceptions to the criterion of Fenton and Zuckerman⁵², that Sn(II) compounds have CS values greater than 2.65 mm s^{-1} (relative to BaSnO₃), while CS for Sn(IV) compounds will fall below this value. Clearly the formal oxidation state of the tin atom in these compounds is 2+, since the oxidation state of the iron atom can be shown⁵³ from electronic

table 4.4

CS Values for some Tin-Transition Metal Complexes(mm s⁻¹; relative to BaSnO₃)

	<u>Compound</u>	<u>CS (mm s⁻¹)</u>	<u>Reference</u>
1.	<i>cis</i> -Cl(Cl ₂ Sn)Fe(RNC) ₄	2.02	this work
2.	<i>cis</i> -(Cl ₂ Sn) ₂ Fe(RNC) ₄	1.82	this work
3.	<i>trans</i> -(Cl ₂ Sn) ₂ Fe(RNC) ₄	1.88	this work
4.	[(Cl ₂ Sn)Fe(RNC) ₅]ClO ₄	1.85	this work
5.	<i>cis</i> -Cl(Cl ₂ Sn)Fe(CO) ₄	1.55	56
6.	<i>cis</i> -(Cl ₂ Sn) ₂ Fe(CO) ₄	1.53	56
7.	<i>trans</i> -(Cl ₂ Sn) ₂ Fe(CO) ₄	1.53	56
8.	<i>cis</i> -Cl(Cl ₂ Sn)Fe(P(OMe) ₃) ₄	1.93	57
9.	[(Cl ₂ Sn)Fe(P(OMe) ₃) ₅]Ph ₄ B	1.98	57
10.	Cl ₂ Sn[Ni(CO)cp] ₂	1.87	this work
11.	Cl ₂ SnNi(Ph ₃ P)cp	1.76	this work
12.	[Ni(Ph ₃ P) ₂ cp][SnCl ₃]	3.15	this work
13.	[Ni(dppe)cp][SnCl ₃]	3.20	this work
14.	[Co(dppe) ₂ Cl][SnCl ₃]	3.10	58

and ^{57}Fe Mössbauer spectra to be 2+ in each case; yet the ^{119}Sn CS is $\ll 2.65 \text{ mm s}^{-1}$. Both the ^{57}Fe QS and CS are additive functions of ligand parameters (i.e. pqs and pcs) in these compounds⁵⁴. If the tin was present as Sn(IV), the oxidation state of iron would change from Fe(II) in $\text{Cl}_2\text{Fe}(\text{RNC})_4$, to Fe(0) in $\text{Cl}(\text{Cl}_3\text{Sn})\text{Fe}(\text{RNC})_4$, to Fe(-II) in $(\text{Cl}_3\text{Sn})_2\text{Fe}(\text{RNC})_4$, and the CS and QS would not be additive. Consequently, CS values for such tin compounds cannot be used to define the oxidation state of Sn; and it is probably more reasonable to use the CS as a measure of the valency of the tin atom, as suggested by Lappert et al⁵⁵. The CS values for the recently reported CO ⁵⁶ and $\text{P}(\text{OMe})_3$ ⁵⁷ analogues of these compounds (5 - 9 in table 4.4) can be treated in the same way.

Some very recently reported compounds which also seem to be exceptions to the Sn(II)/Sn(IV) CS criterion are the so-called "stannylenes" complexes⁵⁹, of the type $(t\text{-Bu})_2(\text{S})\text{SnM}$ ($\text{S} = \text{THF}, \text{py}, \text{DMSO}$; $\text{M} = \text{Fe}(\text{CO})_4, \text{Cr}(\text{CO})_5$), which formally contain Sn(II). However, once again a direct tin-transition bond is present^{59b}, and the measured CS values are in the range $1.82 - 2.11 \text{ mm s}^{-1}$.

The very low CS observed for such compounds does not seem unreasonable. The lone pair in the $\text{Sn}(\text{II})\text{Cl}_2^-$ ion has a high s character^{7b,52,55}, and donation of this lone pair on bonding to Fe or other metals will thus decrease the s electron density at the tin nucleus considerably, and thus the CS, from that observed in the free SnCl_2^- ion (e.g. 3.54 mm s^{-1} in

$[\text{Et}_3\text{N}^+][\text{SnCl}_3^-]^{52}$). Any π back-donation to tin would also decrease the CS.

In recent publications, CS values up to 2.54 cm^{-1} for directly bonded tin-transition metal complexes have been reported^{60,61}, and rationalised in terms of the relative donor-acceptor strengths of the transition metal complex ligands.

For compounds 1 - 9 in table 4.4, the order of CS values for analogous complexes is $\text{P}(\text{OMe})_3 > \text{RNC} > \text{CO}$. In terms of a bonding scheme where decreasing CS is a reflection of increasing σ donation of the SnCl_3^- lone pair, the observed order is probably a measure of the greater electron acceptor ability of iron arising from the increasing ligand π acceptor ability $\text{CO} > \text{RNC} > \text{P}(\text{OMe})_3$.

Thus the formal oxidation state is poorly defined for Cl_3Sn -transition metal complexes, but all these systems contain four-valent tin.

The structures of tin/nickel compounds 10-13 (table 4.4), in the solid state, may be assigned using this criterion. The nature of the complexes containing Ph_3P , when in solution, have been established⁶²⁻⁶⁴ from conductivity studies. Complexes of the type $\text{Cl}_3\text{SnNi}(\text{L})\text{cp}$ were non-electrolytes, while the $\text{Cl}_3\text{SnNi}(\text{L})_2\text{cp}$ compounds were 1:1 electrolytes (L = neutral ligand). Mass spectrometric studies of the same complexes^{62,63}, and of compound 10 (table 4.4) and closely related carbonyl

complexes^{65,66}, indicated that these structures persisted in the solid state - ie. $\text{Cl}_2\text{SnNi}(\text{L})\text{cp}$ ($\text{L} = \text{Ph}_3\text{P}, \text{CO}$) are neutral molecules, while $\text{Cl}_2\text{SnNi}(\text{Ph}_3\text{P})_2\text{cp}$ is ionic.

The Mössbauer CS values for these complexes confirm the above structural conclusions. Thus the CS values of 1.87 mm s^{-1} and 1.76 mm s^{-1} for $\text{Cl}_2\text{Sn}[\text{Ni}(\text{CO})\text{cp}]_2$ and $\text{Cl}_2\text{SnNi}(\text{Ph}_3\text{P})\text{cp}$ respectively indicate the presence of a covalent tin-nickel bond and four-valent tin, while the much larger CS values of 3.15 mm s^{-1} and 3.20 mm s^{-1} for $\text{Cl}_2\text{SnNi}(\text{Ph}_3\text{P})_2\text{cp}$ and $\text{Cl}_2\text{SnNi}(\text{dppe})\text{cp}$ indicate the presence of a discrete Cl_2Sn^- species, containing divalent tin.


There have been no published reports of crystallographically determined structures for any tin-nickel compounds, but some confirmatory evidence for the above structural conclusions can be obtained from X-ray diffraction studies of related compounds. Thus, the presence of a group IVA-nickel bond was established⁶⁷ in the compound $\text{Cl}_2\text{GeNi}(\text{Ph}_3\text{P})\text{cp}$, and a metal-metal bond was also found⁶⁸ in the compound $\text{Cl}_2\text{SnPd}(\text{Ph}_3\text{P})(\text{h}^3\text{-C}_3\text{H}_5)$. In contrast, the presence of a discrete SnCl_2^- ion was established⁶⁸ in the compound $\text{Cl}_2\text{SnCo}(\text{dppe})_2\text{Cl}$, which has a CS value similar to that of the ionic nickel compounds reported here (see table 4.4). Further details of the structures of the tin-nickel compounds, including those for the solvated species, are in chapter 2.

F. References

1. G. M. Bancroft and R. H. Platt; *Adv. Inorg. Radiochem.* (1972) 15, 59.
2. R. V. Parish; *Prog. Inorg. Chem.* (1972) 15, 101.
3. R. H. Herber and H. S. Cheng; *Inorg. Chem.* (1969) 8, 2145.
4. C. A. Clausen and M. L. Good; *Inorg. Chem.* (1970) 9, 817.
5. A. G. Davies, L. Smith and P. J. Smith; *J. Organomet. Chem.* (1970) 23, 135.
6. R. V. Parish and P. Rowbotham; *Chem. Phys. Lett.* (1971) 11, 137.
- 7(a) R. V. Parish and R. H. Platt; *Inorg. Chim. Acta* (1970) 4, 589;
7(b) R. V. Parish; *Prog. Inorg. Chem.* (1972) 15, 101.
8. J. K. Lees and P. A. Flinn; *J. Chem. Phys.* (1968) 48, 882.
9. D. E. Fenton and J. J. Zuckermann; *J. Am. Chem. Soc.* (1968) 90, 6226.
10. C. Wynter and L. Chandler; *Bull. Chem. Soc. Japan* (1970) 43, 2115.
11. S. Onaka, Y. Sasaki and H. Sano; *Bull. Chem. Soc. Japan* (1971) 44, 726.
12. S. R. A. Bird, J. D. Donaldson, A. F. Le C. Holding, B. J. Senior and M. J. Tricker; *J. Chem. Soc. (A)* (1971), 1616.
13. W. R. Cullen, J. R. Sams and J. A. J. Thompson; *Inorg. Chem.* (1971) 10, 843.
14. M. Pasternak and T. Sonnino; *J. Chem. Phys.* (1968) 48, 1997, 2009.
15. G. J. Perlow and H. Yoshida; *J. Chem. Phys.* (1968) 49, 1474.
16. S. Ichiba, M. Katada and H. Negita; *Bull. Chem. Soc. Japan* (1972) 45, 1679.
17. H. A. Stöckler and H. Sano; *Trans. Faraday Soc.* (1968) 64, 577.
18. T. Chivers and J. R. Sams; *J. Chem. Soc. (A)* (1970), 928.
19. D. J. Patmore and W. A. G. Graham; *Inorg. Chem.* (1966) 5, 222; (1967) 6, 981; (1968) 7, 771.
20. H. C. Clark and J.-H. Tsai; *Inorg. Chem.* (1966) 5, 1407.
21. D. J. Cardin, S. A. Keppie and M. F. Lappert; *J. Chem. Soc. (A)* (1970), 2594.

22. S. R. A. Bird, J. D. Donaldson, S. A. Keppie and M. F. Lappert; *J. Chem. Soc. (A)* (1971), 1311.
23. J. R. Holmes and H. D. Kaesz; *J. Am. Chem. Soc.* (1961) 83, 3903.
24. T. F. Boles and R. S. Drago; *J. Am. Chem. Soc.* (1966) 88, 5730.
25. A. Pidcock, R. E. Richards and L. M. Venanzi; *J. Chem. Soc. (A)* (1966), 1707.
26. A. Pidcock; private communication.
27. H. R. H. Patil and W. A. G. Graham; *J. Am. Chem. Soc.* (1965) 87, 673.
28. R. H. Herber and A. Hoffmann; *Prog. Inorg. Chem.* (1967) 8, 35.
29. H. A. Bent; *Chem. Rev.* (1961) 61, 275.
30. R. F. Bryan; *J. Chem. Soc. (A)* (1968), 696.
31. H. P. Weber and R. F. Bryan; *Chem. Comm.* (1966), 443.
32. N. G. Bokii, G. N. Zakharova and Yu. T. Struchkov; *Zhur. Strukt. Khim.* (1970) 11, 895.
33. R. F. Bryan; *J. Chem. Soc. (A)* (1967), 192.
34. F. W. B. Einstein and R. Restivo; *Inorg. Chim. Acta* (1971) 5, 501.
35. G. A. Melson, P. F. Stokely and R. F. Bryan; *J. Chem. Soc. (A)* (1970), 2247.
36. P. J. Greene and R. F. Bryan; *J. Chem. Soc. (A)* (1970), 1696.
37. J. H. Tsai, J. J. Flynn and J. P. Boer; *Chem. Comm.* (1967), 702.
38. B. P. Bir'yukov, E. A. Kukhtenkova, Yu. T. Struchkov, K. N. Anisimov, N. E. Kolobova and V. I. Khandozhko; *J. Organomet. Chem.* (1971) 27, 337.
39. R. L. Livingston and C. N. R. Rao; *J. Chem. Phys.* (1959) 30, 339.
40. B. P. Bir'yukov, Yu. T. Struchkov, K. N. Anisimov, N. E. Koloba and V. V. Skripkin; *Chem. Comm.* (1968), 159.
41. B. P. Bir'yukov, Yu. T. Struchkov, K. N. Anisimov, N. E. Kolobova and V. V. Skripkin; *Chem. Comm.* (1968), 1193.
42. J. E. O'Connor and E. R. Corey; *Inorg. Chem.* (1967) 6, 968.
43. P. T. Greene and R. F. Bryan; *J. Chem. Soc. (A)* (1971), 2549.

44. B. T. Kilbourn and W. M. Powell; Chem. and Ind. (1964), 1578.
45. F. P. Boer and J. J. Flynn; J. Am. Chem. Soc. (1971) 93, 6495.
46. B. P. Bir'yukov, Yu. T. Struchkov, K. N. Anisimov, N. E. Kolobova, O. P. Osipova and M. Ya. Zakharov; Chem. Comm. (1967), 749.
47. P. J. Greene and R. F. Bryan; J. Chem. Soc. (A) (1970), 2261.
48. T. L. Brown, P. A. Edwards, C. B. Harris and J. L. Kirsch; Inorg. Chem. (1969) 8, 763;
D. D. Spencer, J. L. Kirsch and T. L. Brown; Inorg. Chem. (1970) 9, 235.
49. J. D. Graybeal, S. D. Ing and M. W. Hsu; Inorg. Chem. (1970) 9, 678.
50. G. M. Bancroft, K. D. Butler, L. E. Manzer, A. Shaver and J. E. H. Ward; Can. J. Chem. (1974) 52, 782.
51. G. W. Parshall; Inorg. Chem. (1972) 11, 433.
52. E. E. Fenton and J. J. Zuckerman; Inorg. Chem. (1969) 8, 1771;
J. Am. Chem. Soc. (1968) 90, 6226.
53. G. M. Bancroft and K. D. Butler; J. C. S. Dalton (1972), 1209.
54. G. M. Bancroft, M. J. Mays and B. E. Prater; J. Chem. Soc. (A) (1970), 956.
55. S. R. A. Bird, J. D. Donaldson, S. A. Keppie and M. F. Lappert; J. Chem. Soc. (A) (1971), 1311.
56. N. Dominelli, E. Wood, P. Vasudev and C. H. W. Jones; Inorg. Nucl. Chem. Lett. (1972) 8, 1077.
57. E. T. Libbey and G. M. Bancroft; J. C. S. Dalton (1974), 87.
58. J. K. Stalick, D. W. Meek, B. Y. K. Ho and J. J. Zuckerman; Chem. Comm. (1972), 630.
- 59(a) T. J. Marks; J. Am. Chem. Soc. (1971) 93, 7090;
T. J. Marks and A. R. Newman; J. Am. Chem. Soc. (1973) 95, 769;
G. W. Grynkewich, B. Y. K. Ho, T. J. Marks, D. L. Tomaja and J. J. Zuckerman; Inorg. Chem. (1973) 12, 2522;
(b) M. D. Brice and F. A. Cotton; J. Am. Chem. Soc.; (1973) 95, 529.
60. M. J. Mays and P. L. Sears; J. C. S. Dalton (1974), in press.
61. R. V. Parish and P. J. Rowbotham; J. C. S. Dalton (1973), 37.
62. M. van den Akker and F. Jellinek; J. Organomet. Chem. (1967) 10, P37;
M. van den Akker; Ph.D. thesis (Rijksuniversiteit te Groningen) (1970).

63. F. Glockling and A. McGregor; J. Inorg. Nucl. Chem. (1973) 35, 1481.
64. P. A. McArdle and A. R. Manning; Chem. Comm. (1967), 417.
65. K. Yasufuku and H. Yamazaki; J. Organomet. Chem. (1972) 38, 367.
66. L. K. Thompson, E. Eisner and M. J. Newlands; J. Organomet. Chem. (1973) 56, 327.
67. F. Glockling, A. McGregor, M. L. Schneider and H. M. Shearer; J. Inorg. Nucl. Chem. (1970) 32, 3101.
68. R. Mason, G. B. Robertson, P. O. Whimp and D. A. White; Chem. Comm. (1968), 1655; R. Mason and P. O. Whimp; J. Chem. Soc. (A) (1969), 2709.
- 

CHAPTER 5

Ratios of Quadrupole Splittings

A. Introduction

One of the principal limitations to the chemical usefulness of the Mössbauer effect is the fact that the number of elements which can be readily studied using this technique is limited. However useful information on structure and bonding can be obtained for compounds of "non-Mössbauer" elements by correlating Mössbauer data for closely related nuclei with information obtained using other techniques. One such correlation - first suggested by Harris¹ and further developed by Bancroft¹ - utilized ⁵⁹Co nuclear quadrupole resonance and ⁵⁷Fe Mössbauer parameters to yield previously unobtainable information, such as the sign of the electric field gradient in cobalt compounds, and the sign and magnitude of the ⁵⁷Fe nuclear quadrupole moment. This method has been applied to analogous compounds for the pairs of elements Co(III)/Fe(II)^{1,2}, Fe(II)/Mn(I)³ and Fe(II)/Ru(II)⁴. In this study the method is tested using two Mössbauer-active isotopes (¹²¹Sb and ¹¹⁹Sn) to compare Sb(V) and Sn(IV) compounds; and is also used to derive bonding information for analogous Fe(II), Mn(I) and Re(I) compounds.

using results from ^{57}Fe Mössbauer and ^{55}Mn , ^{185}Re and ^{187}Re nuclear quadrupole resonance spectral data.

B. Theory

Consider any pair of isoelectronic and isostructural compounds of two closely related elements M1 and M2. If we assume

- a) that the bonding in the two compounds is identical
- b) that contributions to e^2qQ from the small occupation of orbitals not formally occupied, and from the presence of counter-ions are negligible, and
- c) that the Sternheimer antishielding factors $(1 - R)$ are the same for both compounds, we may write

$$[e^2qQ]_{M2} = \frac{e^2 q'_{M2} Q_{M2}}{e^2 q'_{M1} Q_{M1}} \cdot [e^2qQ]_{M1} \quad \dots(5.1)$$

where

$[e^2qQ]_M \equiv$ measured quadrupole splitting for compound of element M

$e \equiv$ electronic charge

$eq'_M \equiv$ field gradient due to one valence electron
(p or d)

$Q_M \equiv$ nuclear quadrupole moment for nucleus M.

There are several ways in which this equation can be used. Often it is convenient to plot $(e^2qQ)_{M1}$ against $(e^2qQ)_{M2}$ for a number of pairs of analogous compounds of M1 and M2. The intercept

should be zero, and the slope given by $(e^2q'_{M2} Q_{M2}) / (e^2q'_{M1} Q_{M1})$. From such a graph the signs of $(e^2qQ)_{M2}$ can be obtained if those of $(e^2qQ)_{M1}$ are known; and the slope can be used to obtain the magnitude and/or sign of Q_{M2} if they have been established for Q_{M1} .

C. 119-Sn and 121-Sb Quadrupole Splittings

Figure 5.1 shows such a correlation for a series of isoelectronic and isostructural antimony⁵⁻⁸ and tin⁹⁻¹⁴ compounds.² The signs of the non-zero antimony e^2qQ values are all known^{5,7,8} to be negative. Among the tin compounds, the signs of $[\text{Me}_3\text{SnCl}_2]^-$ and $[\text{Ph}_3\text{SnCl}_2]^-$ have been determined¹¹, and are negative. Points 4, 5 and 6 on the graph in figure 5.1 do not correspond to exact stoichiometric analogues, but rather to pairs of compounds of the type $\text{Cl}_3\text{SbL} / \text{cis-Cl}_2\text{SnL}_2$. However the partial quadrupole splitting treatment for octahedral compounds predicts¹⁵ that for any pair of compounds $X_3\text{ML} / \text{cis-X}_2\text{ML}_2$, the QS values will be the same magnitude, but of opposite sign. The opposite sign has been confirmed for the compounds where $L = \text{MeCN}$, since the sign of $\text{cis}-(\text{MeCN})_2\text{SnCl}_2$ is positive¹⁶, while that of $(\text{MeCN})\text{SbCl}_3$ is negative⁸. All the pairs of compounds in figure 5.1 give a positive correlation. (The sign of SnCl_3^- will be discussed later).

Both SbCl_3 and $[\text{SnCl}_3]^-$ have regular trigonal bipyramidal structures at room temperature, with metal-chlorine bond lengths of $2.34 \pm 0.1 \text{ \AA}$ ¹⁷. Several studies have shown¹⁸ that SbCl_3 undergoes

figure 5.1

Plot of Antimony and Tin $|e^2qQ|$ values
for the following pairs of Complexes

1.	SbCl_6^-	SnCl_6^-
2.	SbBr_6^-	SnBr_6^-
3.	SbCl_5	SnCl_5
4.	$(\text{Ph}_3\text{PO})\text{SbCl}_5$	<i>cis</i> - $(\text{Ph}_3\text{PO})_2\text{SnCl}_6$
5.	$(\text{MeCN})\text{SbCl}_5$	<i>cis</i> - $(\text{MeCN})_2\text{SnCl}_6$
6.	$(\text{Cl}_3\text{PO})\text{SbCl}_5$	<i>cis</i> - $(\text{Cl}_3\text{PO})_2\text{SnCl}_6$
7.	Ph_3SbBr_2	$\text{Ph}_3\text{SnBr}_2^-$
8.	Ph_3SbCl_2	$\text{Ph}_3\text{SnCl}_2^-$
9.	Me_3SbBr_2	$\text{Me}_3\text{SnBr}_2^-$
10.	Me_3SbCl_2	$\text{Me}_3\text{SnCl}_2^-$

Linear least-squares fit gives $y = 3.38x + 0.34$

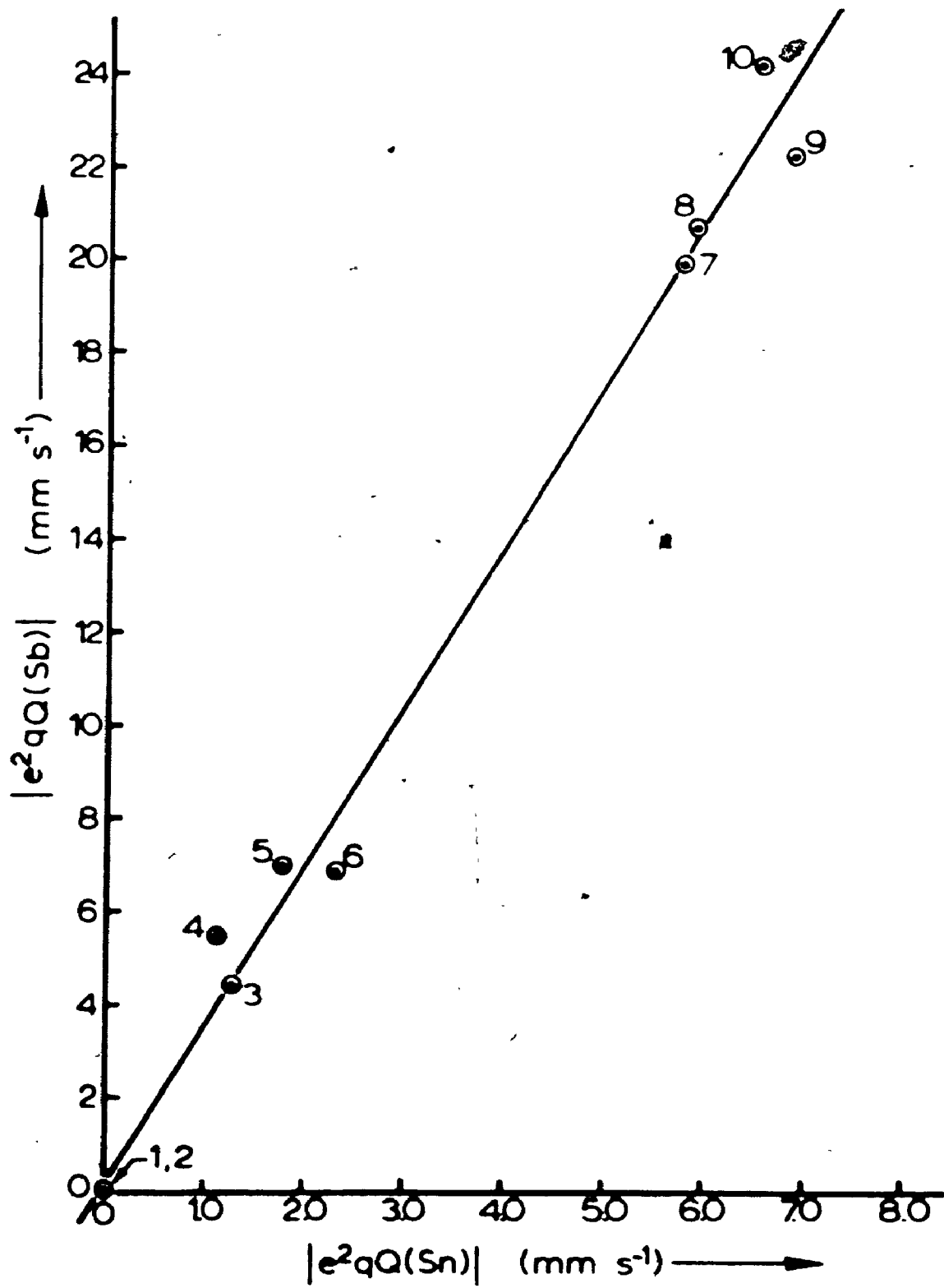


figure 5.1

structural changes at low temperatures, though the nature of this change is not definitely established^{15,19}. Consequently, the e^2qQ value measured by nqr at room temperature, where the molecule certainly has C_{3v} symmetry¹⁷, is used in this correlation. The structure of the $[\text{SnCl}_6]^{2-}$ ion in K_2SnCl_6 ²⁰ and $(\text{NH}_4)_2\text{SnCl}_6$ ²¹ has been determined in diffraction studies, and is octahedral in both cases. Mössbauer¹⁵ and infrared²² spectra of the $[\text{SnBr}_6]^{2-}$ ion clearly indicate that it is also based on a regular octahedron, as would be expected. The structures of the $[\text{SbX}_6]^-$ ions ($X = \text{Cl}, \text{Br}$) has not been established by diffraction methods, but the observed single-line ^{121}Sb Mössbauer spectra⁷, with narrow line-widths, for the RbSbX_6 compounds indicate that the antimony atom is in an octahedral environment.

Cis-octahedral structures have been established crystallographically for the Cl_4SnL_2 ($L = \text{POCl}_3, \text{MeCN}$) compounds^{23,24}. In addition, the crystallographic evidence indicates that the bonding in these Sn and Sb compounds is similar. Thus, the Sn—Cl bond lengths in $\text{Cl}_4\text{Sn}(\text{POCl}_3)_2$ and $\text{Cl}_4\text{Sn}(\text{MeCN})_2$ range from 2.31 - 2.36 Å²³ and 2.339 - 2.356 Å²⁴ respectively, while the Cl_4SbL analogues show very similar Sb—Cl bond lengths of 2.32 - 2.35 Å for $L = \text{POCl}_3$ ²³ and 2.33 - 2.40 Å for $L = \text{MeCN}$ ²⁵. Thus the assumption of identical bonding which is inherent in this treatment is a reasonable one.

The Me_3SbX_2 and Ph_3SbX_2 ($X = \text{Cl}, \text{Br}, \text{I}$) structures are known^{26,27}, and all are based on a trigonal bipyramid, with axial halogens and equatorial organic ligands. Of the related tin

compounds, the structure of only the $[\text{Me}_3\text{SnCl}_2]^-$ ion has been established²⁸ by single crystal X-ray diffraction. Its symmetry, like that of Me_3SbCl_2 , is C_{3v} . Infrared evidence²⁹ for $[\text{Ph}_3\text{SnCl}_2]^-$ suggests that its structure is similar to that of the methyl analogue.

The linear least-squares fit to the data for the pairs of compounds is also shown in figure 5.1. The slope of the line is +3.38, and the intercept is very close to zero (+0.34 mm s^{-1}). The good fit to the data is shown by the correlation co-efficient (r) of 0.995, which strongly suggests that the assumptions inherent in the ratio treatment are reasonable.

A number of useful deductions can be made using this correlation. The most obvious use of the graph is that, given the e^2qQ value for any complex of one of the elements (Sn or Sb), then the e^2qQ for the isoelectronic and isostructural complex of the other element may be derived. This is particularly useful in estimating quadrupole splittings for antimony compounds, which commonly exhibit poorly resolved ^{121}Sb Mössbauer spectra. Computation of antimony compounds with small e^2qQ values is difficult, as will be mentioned later. In addition, the determination of the sign of e^2qQ for tin compounds is experimentally much more complex than running routine ^{119}Sn Mössbauer spectra. Consequently, if e^2qQ for an antimony compound has been measured, then the sign of the tin e^2qQ is immediately obvious using figure 5.1, since the

multiline Mössbauer ^{121}Sb spectra allow the determination of the sign for the antimony compound without using special techniques. For SnCl_3^- , the sign of e^2qQ cannot be determined, in any case, even using magnetic spectra, since the quadrupole splitting is too small for the peaks in the magnetic spectrum to be resolved. However, the sign of e^2qQ for SbCl_3 is known^{5,6} to be negative, so that, from figure 5.1, e^2qQ (SnCl_3^-) must also be negative. This is the sign originally assumed for the ion by Parish and Platt⁹, but a recent MO treatment of tin quadrupole splittings³⁰ left this sign in some doubt. It is very important for the additivity treatment of five co-ordinate complexes that this sign be known. Using the pqs model, the quadrupole splitting ($QS = \frac{1}{2}e^2qQ$) for $[\text{SnX}_3]^-$ is given by:

$$QS(\text{SnX}_3^-) = -4\{X\}_{\text{tba}} + 3\{X\}_{\text{tbe}} \quad \dots(5.2)$$

where $\{X\}_{\text{tba}} \equiv$ pqs value for axial X ligands

and $\{X\}_{\text{tbe}} \equiv$ pqs value for equatorial X ligands,

in a trigonal bipyramidal complex.

Hence, if e^2qQ (SnCl_3^-) is negative, then it follows that

$$\{Cl\}_{\text{tba}} > \{Cl\}_{\text{tbe}}$$

Despite the large body of data that has been published on 119-tin quadrupole splittings, some of the quadrupole parameters

for the ^{119}Sn nucleus are not yet well established. For example, the sign and magnitude of the 119-tin nuclear quadrupole moment, $Q(^{119}\text{Sn})$, have been reported^{31,32}, but the uncertainty in the magnitude is very large. In addition, confirmatory evidence for the negative sign of $Q(^{119}\text{Sn})$ would be welcome³³, since its determination³¹ was based on bonding schemes too empirical to be entirely reliable. From figure 5.1 and equation 5.1 it can be seen that, since $Q(^{121}\text{Sb})$ is known to be negative³⁴, then $Q(^{119}\text{Sn})$ must also be negative. Substituting the data in the following table

parameter	value	reference
$Q(^{121}\text{Sb})_{\text{gr}}$	$-0.28(\pm 0.1) \times 10^{-28} \text{ m}^2$	34
$q_{5p}(\text{Sn})$	11.2 a_0^{-1}	35
$q_{5p}(\text{Sb})$	13.0 a_0^{-1}	35
$E_{\gamma}(\text{Sb})/E_{\gamma}(\text{Sn})$	1.556	36

and the slope of the graph into equation 5.1, then $Q(^{119}\text{Sn})$ is calculated to be $-0.062 \times 10^{-28} \text{ m}^2$. This value is in very good agreement with that of $-0.065(\pm 0.005) \times 10^{-28} \text{ m}^2$ determined in a Mössbauer study of atomic tin dimers in rare gas matrices at 4.2 K, and published³⁷ since the completion of the work reported here. With the large error in $Q(^{121}\text{Sb})$ and q_{5p} values³⁴, the absolute error in the derived $Q(^{119}\text{Sn})$ value is probably about $\pm 0.02 \times 10^{-28} \text{ m}^2$, but the error in the $Q(^{121}\text{Sb})/Q(^{119}\text{Sn})$ ratio (= 17.31) will be

considerably smaller.

For correlations using equation 5.1 to be completely valid, it is important that pairs of Sb/Sn compounds be strictly isostructural. For example, it might be expected that the e^2qQ values for $SbCl_3$ and $[SnCl_3]^-$ would lie on the line in figure 5.1. However, their structures are quite dissimilar; the antimony atom in $SbCl_3$, being in a distorted octahedral environment³⁸, while the $SnCl_3^-$ ion is pyramidal in ionic $MSnCl_3$ ($M = Cs^+$, $Cu(dppe)_2Cl^+$) compounds^{39,40}. Furthermore, the e^2qQ values observed for ionic $MSnCl_3$ compounds vary widely, and are very sensitive to small changes in the $Cl-Sn-Cl$ angles⁴¹.

However it is interesting to consider the species $[Ph_3SnF_2]^-$, which has not yet been reported. Using the published e^2qQ value for Ph_3SbF_2 ⁵, and figure 5.1, the e^2qQ for $Ph_3SnF_2^-$ is predicted to be 3.22 mm s^{-1} . The e^2qQ value reported¹⁵ for Ph_3SnF is 3.58 mm s^{-1} , which is considerably greater than the value (2.74 mm s^{-1}) predicted from the additivity model for an unassociated four co-ordinate molecule, but in better agreement with the e^2qQ value predicted above for $Ph_3SnF_2^-$. This is probably good confirmation of the conclusion drawn from other studies⁹, that Ph_3SnF is a highly associated compound, with a structure analogous to that in Ph_3SbF_2 ²⁷ - i.e. with axial fluorine atoms and equatorial phenyl groups - and also analogous to that determined for Me_3SnF ⁴². Similarly, the quadrupole splittings for Me_3SnCl (3.44 mm s^{-1}) and Me_3SnBr (3.40 mm s^{-1}) are similar

to those observed for $\text{Me}_3\text{SnCl}_2^-$ (3.28 mm s^{-1}) and $\text{Me}_3\text{SnBr}_2^-$ (3.45 mm s^{-1}) respectively¹⁵, suggesting that the Me_3SnX ($X = \text{Cl}, \text{Br}$) compounds are also polymeric, with C_{3v} symmetry about the tin atom once again. This suggestion has been confirmed by a single crystal X-ray diffraction determination of the structure of Me_3SnCl ⁴³; though the related Sn—Cl distances, unfortunately, have not been reported.

A very recent report⁴⁴ of e^2qQ values for compounds of the type $[\text{R}_{3-n}\text{SbM}_n]^+$ ($R = \text{CF}_3, \text{Me}, \text{Bu}, \text{Ph}, \text{Cl}, \text{Br}, \text{I}; M = \text{Fe}(\text{CO})_2\text{cp}$) should permit a correlation with the neutral Sn(IV) analogues. However, a plot of the antimony and tin e^2qQ values yields a line with a slope similar to that in figure 5.1, but with an intercept on the vertical axis of -6 mm s^{-1} ⁴⁵. The structures of the complexes $[\text{Cl}_2\text{SbM}_2]^+$ and Cl_2SnM_2 ($M = \text{Fe}(\text{CO})_2\text{cp}$) are both known^{46,47} to be tetrahedral about the metal atom, with very similar distortions from regular geometry, so that bonding differences would not seem to account for the discrepancy. However, there is some difficulty in computing ^{121}Sb Mössbauer spectra for complexes with small quadrupole splittings, and it is possible that the anomalously large ^{121}Sb e^2qQ values for these compounds are at least partially due to not using the transmission integral in the analysis of the spectra⁸. This problem does not arise for points 4, 5, and 6 in figure 5.1, since, in those cases, the transmission integral was used, and the e^2qQ values were in good agreement with the more accurate values obtained from nqr spectra⁸.

D. Quadrupole Splittings in $[\text{cpM}(\text{CO})_2\text{L}]$ Complexes (M = Fe, Mn, Re)

(i) Introduction

^{57}Fe Mössbauer data has been reported for a large number of neutral complexes of the type $\text{cpFe}(\text{CO})_2\text{X}$ ($\text{cp} = \text{h}^5\text{-C}_5\text{H}_5$, X = anionic ligand)⁴⁸⁻⁵³, though few of the related $[\text{cpFe}(\text{CO})_2\text{L}]^+$ cations (L = neutral ligand) have been investigated^{50,51}. While useful bonding information has been derived from the centre shift parameters, the quadrupole splittings have proved difficult to interpret, mainly because they are all in the range $1.8 \pm 0.1 \text{ mm s}^{-1}$ for X or L ligands with widely varying bonding properties.

The ground state quadrupole splittings for a number of analogous $\text{cpM}(\text{CO})_2\text{L}$ (M = Mn, Re) compounds have been measured using ^{55}Mn ^{54,55}, and ^{185}Re and ^{187}Re ^{56,57} nuclear quadrupole resonance spectroscopy. However, without a knowledge of the signs of the appropriate e^2qQ values, discussion of bonding in the Mn and Re compounds, based on the nqr evidence, must necessarily be speculative.

The range of $[\text{cpFe}(\text{CO})_2\text{L}]^+$ complexes studied by ^{57}Fe Mössbauer spectroscopy has been extended here in an attempt to better understand the bonding in these systems, and, by comparison, in the related manganese and rhenium systems. The measured Mössbauer parameters are shown in table 5.2, together with values for the related values reported in the literature.

(ii) Centre Shifts

As has been shown previously for Fe(II) compounds⁵⁸, the centre shift, which has comparable sensitivity to both

table 5.2

 ^{57}Fe Mössbauer Parameters* for the Derivatives

<u>$[\text{cpFe}(\text{CO})_2\text{L}]^+\text{X}^-$</u>					
	<u>L</u>	<u>X</u>	<u>$\text{CS}^{\S\dagger}$</u>	<u>QS^\dagger</u>	<u>reference</u>
1.	CS	PF_6^-	0.21	1.89	51
2.	CO	PF_6^-	0.29	1.90	this work
3.			0.27	1.78	51
			0.31	1.88	50
3.	Ph_3P	PF_6^-	0.34	1.81	this work
		Cl^-	0.31	1.92	51
4.	py	PF_6^-	0.41	1.86	this work
5.	C_2H_6	PF_6^-	0.43	1.77	this work
		BF_4^-	0.42	1.71	this work
6.	MeCN	PF_6^-	0.44	1.95	this work

* Full peak widths at half height were between 0.25 and 0.31 mm s^{-1} in all cases.

† $\pm 0.01 \text{ mm s}^{-1}$; -78K.

§† With respect to $\text{Na}_2\text{Fe}(\text{CN})_5(\text{NO}) \cdot 2\text{H}_2\text{O}$

σ -donor and π -acceptor properties, decreases as the σ -donor and π -acceptor ability ($\sigma + \pi$) of the ligand(s) increases. Thus, H^- (a strong σ -donor) and NO^+ (a strong π -acceptor) give comparable decreases in iron(II) centre shifts.

In the present series of compounds the centre shifts (table 5.2) vary substantially as L is changed. Hence, we may arrange the compounds in an order of increasing ($\sigma + \pi$) properties of the ligands:



The ordering of CH_3CN , and CO ligands is the same as that obtained from iron(II) six coordinate compounds^{59,60}. The position of C_2H_4 is of special interest. In terms of its ($\sigma + \pi$) ability, C_2H_4 appears to be a very similar ligand to pyridine and acetonitrile. The carbonyl infrared stretching frequencies are also consistent with this observation⁶¹. From previous Mössbauer work, it is interesting to note that N_2 is also a very similar ($\sigma + \pi$) ligand to nitriles, although the quadrupole splitting data indicates that the former is an appreciably better π -acceptor and poorer σ -donor than the latter⁶⁰. However, as will be discussed below, the quadrupole splittings are not helpful in separating σ and π effects in this series of compounds.

(iii) Quadrupole Splittings

In comparison with the QS values for six co-ordinate Fe(II) low spin compounds of the type $trans-[(depe)_2FeHL]Ph_4B^{60}$, the quadrupole splittings in the present series of compounds are

very insensitive to the nature of L, and are in a similar range to that for the neutral complexes mentioned earlier. It appears that the bonding properties of both CO and h^5 -cp change substantially with variations in L to effectively neutralise the changes in electron asymmetry about the iron atom. Thus it has not been possible to rationalise the trends for either the neutral or cationic h^5 -cyclopentadienyliron dicarbonyl derivatives in terms of bonding properties of the ligands.

However, the ^{57}Fe QS values are very useful for assigning the signs of the quadrupole splittings for the analogous neutral manganese and rhenium compounds of the type $\text{cpM}(\text{CO})_2\text{cp}$ ($\text{M} = \text{Mn}, \text{Re}$)⁵⁴⁻⁵⁷. From equation 5.1, we can write:

$$\begin{aligned} (e^2qQ)_{s^{55}\text{Mn}} &= \frac{q_{3d}(\text{Mn})}{q_{3d}(\text{Fe})} \frac{Q(^{55}\text{Mn})}{Q(^{57}\text{Fe})} - (e^2qQ)_{s^{57}\text{Fe}} \\ &= K_1 (e^2qQ)_{s^{57}\text{Fe}} \end{aligned} \quad \dots (5.3)$$

Using literature values for the parameters in equation 5.3^{2,62,63}, the value of K_1 was calculated to be +1.39, in a previous study of some octahedral Mn(I) and Fe(II) analogues³. The sign of the ^{57}Fe QS in $(\text{Bu}_3\text{Sn})\text{Fe}(\text{CO})_2\text{cp}$ is known to be positive⁶⁴, and the very small range of QS values found for all h^5 -cyclopentadienyliron dicarbonyl compounds strongly suggests that all of these neutral and cationic compounds will have positive e^2qQ values. Thus, it is immediately apparent, from equation 5.3, that q and e^2qQ are also positive for the h^5 -cyclopentadienylmanganese dicarbonyl compounds. This is opposite

to the negative sign assumed in earlier ^{55}Mn nqr work^{54,55}. Consequently this result indicates that the bonding model chosen previously, and the ensuing discussion of variations in bonding, were incorrect^{54,55}. It is also apparent that, if $Q(^{185}\text{Re})$ and $Q(^{187}\text{Re})$ are positive, then the e^2qQ values^{56,57} for the rhenium compounds are also positive.

More quantitatively, if we take the measured e^2qQ value for $[\text{cpFe}(\text{CO})_5]^+$ of $(+)$ 3.80 mm s^{-1} (\equiv $(+)$ 44.2 MHz), and assume $\eta = 0$ (as measured in the manganese analog), the predicted value of $(e^2qQ)_{\text{Mn}}$, using $K = 1.39$ and equation (5.3), is $+61.4 \text{ MHz}$. This is in surprisingly good agreement with the measured value of 64.29 MHz , considering the assumptions inherent in the method, and possible errors in the Q and q_{3d} values.

In order to use the above method in a predictive sense, and to indicate that variations in η cause a substantial part of the variations in both Mössbauer quadrupole splittings, $\frac{1}{2}e^2qQ(1 + \eta^2/3)^{1/2}$, and in $\nu(\pm 5/2 \leftrightarrow \pm 3/2)$ values from ^{55}Mn nqr spectra, the multiplying factor K_1 is recalculated, using the measured values of e^2qQ for $[\text{cpFe}(\text{CO})_5]^+$ and $\text{cpMn}(\text{CO})_5$. This is the first pair of analogous iron and manganese compounds where $|e^2qQ|$ values have been measured for both. (Previously³, $\frac{1}{2}e^2qQ$ values for the appropriate iron compounds were calculated from partial quadrupole splittings). The calculated K_1 becomes $+1.45$, which should be more accurate than the earlier value of $+1.39$. This change in K_1 will, in fact, have a very small effect on the previously calculated³ $(e^2qQ)_{\text{Mn}}$ values.

Using this recalculated K_I factor, and the measured ^{57}Fe quadrupole splittings, it is now possible to predict η and the unmeasured $\nu(\pm 3/2 \leftrightarrow \pm 1/2)$ ^{55}Mn nqr transition frequency^{54,55} in some manganese analogues of the iron compounds. These are summarised in Table 5.3.

The predicted e^2qQ and η values would not be expected to be more accurate than ca. ± 2 MHz and ± 0.2 respectively. (The results for the triphenylphosphine derivative (η^2 (calculated) < 0) are indicative of these errors.) However, the results do indicate that the variations in both the ^{57}Fe Mössbauer quadrupole splittings and in the ^{55}Mn $\nu(\pm 5/2 \leftrightarrow \pm 3/2)$ values are probably largely due to variation in η . For example, the acetonitrile derivative has a larger ^{57}Fe quadrupole splitting than its carbon monoxide analogue (and a smaller ^{55}Mn nqr $\nu(\pm 5/2 \leftrightarrow \pm 3/2)$), yet their calculated e^2qQ values are identical within expected error.

It can be concluded, then, that even after the signs of the e^2qQ parameters have been assigned in such complexes, a substantial part of the variations in Mössbauer quadrupole splittings are due to changes in η . This places discussions concerning variations of quadrupole splittings with bonding properties of the ligands L in these systems on an even more tenuous footing.

Finally, it would be very useful to know the quadrupole splittings for the series of isostructural and isoelectronic species $\text{Mn}(\text{CO})_5^-$, $\text{Fe}(\text{CO})_5$, and $\text{Co}(\text{CO})_5^+$. The e^2qQ value for $\text{Fe}(\text{CO})_5$

table 5.3

Predicted Quadrupole Parameters* for Isoelectronic $\text{cpM}(\text{CO})_2\text{L}$ ($\text{M} = \text{Mn}, \text{Fe}$) Derivatives

L	^{57}Fe data		^{55}Mn data			η
	$e^2qQ(1 + \eta^2/3)^{1/2}$ observed	e^2qQ predicted	$(\pm 5/2 \leftrightarrow \pm 3/2)$ observed	$(\pm 3/2 \leftrightarrow \pm 1/2)$ predicted	e^2qQ predicted	
CO	44.2	(+)44.2	10.29	9.65†	+64.29†	0.0†
py	43.3	(+)42.0	17.62	11.0	+60.9	0.45
MeCN	45.4	(+)44.2	18.71	11.2	+64.3	0.40
Ph ₃ P	42.1	-(+)42.1	18.82	††	††	††

*MHz

†Observed values, reference 54

†† $\eta^2 < 0$, and values cannot be calculated.

is known from ^{57}Fe Mössbauer spectroscopy to be $+5.14 \text{ mm s}^{-1}$ ($\equiv +59.8 \text{ MHz}$)¹⁵. Thus, from the K_1 value for Mn/Fe calculated in this study, e^2qQ for $\text{Mn}(\text{CO})_5^-$ is predicted to be 86.7 MHz. A similar comparison can be made for Fe/Co. The K_1 factor for this pair of elements is 3.13 from the study of Bancroft², or 2.99 from a comparison of the measured values of cp_2Fe (53.6 MHz)¹⁵ and cp_2Co^+ (166 MHz)^{1,65}; yielding e^2qQ values of 187 MHz and 179 MHz respectively for $\text{Co}(\text{CO})_5^+$.

The uncertainty in these estimated values is, of course, fairly large, mainly due to the assumption of identical bonding in the series of isoelectronic species. For example, it is known that CO in Mn(I) compounds is a worse σ donor, but better π acceptor than in the isoelectronic Fe(II) compounds⁶⁶. However, because quadrupole splittings are proportional to $\sigma - \pi$ ^{15,60}, the two trends tend to cancel. Harris¹ has estimated that the cumulative error in derived parameters, due to the assumption of identical bonding in cp_2Fe and cp_2Co^+ , will be ~15%; and it is likely that the uncertainty for the $\text{M}(\text{CO})_5$ parameters will be similar. $\text{Co}(\text{CO})_5^+$ has not yet been isolated as a stable chemical species, but the compound $\text{NaMn}(\text{CO})_5$ is well known, and it is likely that e^2qQ for $\text{Mn}(\text{CO})_5^-$, from ^{55}Mn nqr studies, will be reported in the future.

E. References

1. C. B. Harris; *J. Chem. Phys.* (1968) 49, 1648.
2. G. M. Bancroft; *Chem. Phys. Lett.* (1971) 10, 449.
3. G. M. Bancroft, H. C. Clark, R. G. Kidd, A. T. Rake and H. G. Spinney; *Inorg. Chem.* (1973) 12, 728.
4. G. M. Bancroft, K. D. Butler and E. T. Libbey; *J.C.S. Dalton* (1972), 2643.
5. J. G. Stevens and S. L. Ruby; *Phys. Lett.* (1970) 32A, 91;
G. G. Long, J. G. Stevens, R. J. Tulbane and L. H. Bowen;
J. Am. Chem. Soc. (1970) 92, 4230.
6. L. H. Bowen, J. G. Stevens and G. G. Long; *J. Chem. Phys.* (1969)
50, 2010.
7. T. Birchall, B. Della Valle, E. Martineau and J. B. Milne;
J. Chem. Soc. (A) (1971), 1855.
8. J. M. Friedt, G. K. Shenoy and M. Burgard; *J. Chem. Phys.* (1973)
59, 4468.
9. R. V. Parish and R. H. Platt; *J. Chem. Soc. (A)* (1969), 2145;
Inorg. Chim. Acta (1970) 4, 65.
10. J. Ensling, P. Gutlich, K. M. Hasselbach and B. W. Fitzsimmons;
J. Chem. Soc. (A) (1971), 1940.
11. R. V. Parish and C. E. Johnson; *J. Chem. Soc. (A)* (1971), 1906.
12. D. Cunningham, M. J. Fraser and J. Donaldson; *J. Chem. Soc. (A)*
(1971), 2049; (1972), 1647.
13. J. Philip, M. A. Mullen and C. Curran; *Inorg. Chem.* (1968) 7, 1895.
14. P. A. Yeats, J. R. Sams and F. Aubke; *Inorg. Chem.* (1970) 9, 740.
15. G. M. Bancroft and R. H. Platt; *Adv. Inorg. Radiochem.* (1972) 15, 59.
16. D. Cunningham, M. J. Fraser and J. D. Donaldson; *J.C.S. Dalton*
(1972) 1647.
17. S. M. Ohlberg; *J. Am. Chem. Soc.* (1959) 81, 811; R. F. Bryan;
J. Am. Chem. Soc. (1963) 86, 733.
18. K. Olie, C. C. Smitskamp and H. Gerding; *Inorg. Nucl. Chem.*
Lett. (1968) 4, 129; R. F. Schneider and J. V. Di Lorenzo;
J. Chem. Phys. (1967) 47, 2343.
19. J. G. Stevens and L. H. Bowen; *Mössbauer Effect Methodology*
(1970) 5, 38.

20. G. Engel; Z. Krist. (1935) A90, 341.
21. G. Markstein and H. Nowotny; Z. Krist. (1939) A100, 265.
22. J. A. Creighton and J. H. S. Green; J. Chem. Soc. (A) (1968), 808.
23. C. I. Branden and I. Lindqvist; Acta. Chem. Scand. (1963) 17, 759.
24. M. Webster and H. E. Blayden; J. Chem. Soc. (A) (1969), 2443.
25. H. Binas; Z. Anorg. Allg. Chem. (1967) 352, 271.
26. A. F. Wells; Z. Krist. (1938) 99, 367.
27. T. N. Polynova and M. A. Porai-Koshits; Zhur. Strukt. Khim. (1960) 1, 159; (1966) 7, 642, 742.
28. P. J. Vergamini, H. Vahrenkamp and L. F. Dahl; J. Am. Chem. Soc. (1971) 93, 6327
29. T. Srivastava; J. Organomet. Chem. (1967) 10, 375.
30. M. G. Clark, A. G. Maddock and R. H. Platt; J. Chem. Soc. (A) (1972), 281.
31. A. J. F. Boyle, D. St. P. Bunbury and C. Edwards; Proc. Phys. Soc. (1962) 79, 416.
32. M. Cordey-Hayes; J. Inorg. Nucl. Chem. (1964) 26, 915.
33. N. N. Greenwood and T. C. Gibb; "Mössbauer Spectroscopy", Chapman and Hall, London (1971) p. 379.
34. S. L. Ruby, G. M. Kalvius, G. B. Beard and R. E. Snyder; Phys. Rev. (1967) 159, 239.
35. R. G. Barnes and W. V. Smith; Phys. Rev. (1954) 93, 95.
36. "Mössbauer Effect Data Index", ed. J. G. Stevens and V. E. Stevens, Plenum Press, N. Y. (1972).
37. A. Micklitz and P. H. Barrett; Phys. Rev. (1972) 85, 1704.
38. T. N. Polynova and M. A. Porai-Koshits; Zhur. Strukt. Khim. (1966) 7, 146.
39. F. R. Paulsen and S. E. Rosmussen; Acta Chem. Scand. (1970) 24, 150.
40. J. K. Stalick, D. W. Meek, B. Y. K. Ho and J. J. Zuckerman; Chem. Comm. (1972), 630.
41. M. J. Mays and P. L. Sears; J. C. S. Dalton (1974), in the press.

42. H. C. Clark, R. J. O'Brien and J. Trotter; *J. Chem. Soc.* (1964), 2332.
43. A. G. Davies; personal communication to R. H. Platt.
44. W. R. Cullen, D. J. Patmore, J. R. Sams and J. C. Scott; *Inorg. Chem.* (1974) 13, 649.
45. J. R. Sams; private communication.
46. F. W. B. Einstein and R. D. G. Jones; *Inorg. Chem.* (1973) 12, 1690.
47. J. E. O'Connor and E. R. Corey; *Inorg. Chem.* (1967) 6, 968.
48. O. A. Gansow, D. A. Sheknyader and B. Y. Kimura; *J. Am. Chem. Soc.* (1972) 94, 3406.
49. P. C. Lauterbur and R. B. King; *J. Am. Chem. Soc.* (1965) 87, 3266.
50. R. H. Herber, R. B. King and G. K. Wertheim; *Inorg. Chem.* (1964) 3, 101.
51. K. Burger, L. Korecz, P. Mag, V. Belluco and L. Busetto; *Inorg. Chim. Acta* (1971) 5, 362.
52. R. B. King; *Inorg. Chim. Acta* (1968) 2, 454.
53. A. N. Nesmeyanov, Yu A. Chapovskii, L. I. Denisovitch, B. L. Lokshien and I. Y. Polovyanyuk; *Dokl. Akad. Nauk SSR* (1967) 174, 1342.
54. W. P. Anderson, T. B. Brill, A. R. Schoenberg and C. W. Stanger; *J. Organomet. Chem.* (1972) 44, 161.
55. T. B. Brill and G. G. Long; *Inorg. Chem.* (1971) 10, 74.
56. A. N. Nesmeyanov, G. K. Semin, E. V. Bryuchova, T. A. Babyshkina, K. N. Anisimov, N. E. Kolobova and Yu V. Makarov; *Tetrahed. Lett.* (1968) 37, 3987.
57. M. D. Fayer and C. B. Harris; *Inorg. Chem.* (1969) 8, 2792.
58. G. M. Bancroft, M. J. Mays and B. E. Prater; *J. Chem. Soc. (A)* (1970), 956.
59. G. M. Bancroft and E. T. Libbey; *J. C. S. Dalton* (1973), 2103.
60. G. M. Bancroft, R. E. B. Garrod, A. G. Maddock, M. J. Mays and B. E. Prater; *J. Amer. Chem. Soc.* (1972) 94, 647.
61. G. M. Bancroft, K. D. Butler, L. E. Manzer, A. Shaver and J. E. H. Ward; *Canad. J. Chem.* (1974) 52, 782.
62. B. Hofflinger and J. Voltlander; *Z. Naturforsch* (1963) A18, 1065.

63. E. Handrick, A. Stendel and H. Walther; Phys. Lett. (1969) A29, 486.
64. B. A. Goodman, R. Greatrex and N. N. Greenwood; J. Chem. Soc. (A) (1971), 1868.
65. J. Voitlander, H. Klocke, R. Longino and H. Thieme; Naturwissenschaften (1962) 49, 491.
66. M. B. Hall and R. F. Fenske; Inorg. Chem. (1972) 11, 1619.

CHAPTER 6

The Effect of *trans* Ligands on 129-Iodine Mössbauer Parameters in Square-Planar Platinum(II) Complexes

A. Introduction - The "*trans*-Influence"

The *trans*-influence is a thermodynamic phenomenon, which has been defined by Pidcock et al¹ as the extent to which a ligand weakens the bond *trans* to itself in the equilibrium state of the complex. The mechanism most widely invoked to explain this phenomenon is that postulated by Syrkin², involving rehybridization of the metal orbitals. In square-planar complexes, such as those of platinum(II), a metal ion is considered to use $5d_{x^2-y^2}$, $6s$, $6p_x$, $6p_y$ hybrid orbitals. If a ligand, L, forms a strong covalent bond with the metal, M, the hybrid orbital used by the metal in the M-L bond will tend to have a high proportion of metal 5d and 6s character, and less 6p character, since the orbital energies are $5d \sim 6s < 6p$. Since L, and the *trans* ligand, T, must share the same s-d hybrid orbitals, then additional d and s participation in the M-L bond will result in decreased availability of these orbitals for bonding by T, resulting in a weaker M-T bond. The ligands *cis* to L use an independent s-d hybrid orbital,

and are affected to a lesser extent. Syrkin predicted a slight strengthening of the bond to *cis* atoms. Except for strongly π bonding ligands, such as C_2H_4 and CO, it has now been shown^{1,3,4} that π effects are much less important than was originally thought, and the relative *trans*-influences of ligands can generally be rationalised purely in terms of metal-ligand σ bonding. The various experimental manifestations of the *trans*-influence in complexes of a variety of transition metals have been recently reviewed.⁴

The most detailed theoretical study of the *trans*-influence published so far is that of Zundahl and Drago⁵, who carried out molecular orbital calculations for the series *trans*- $Cl_2Pt(NH_3)X$. They concluded that the Pt—N bond *trans* to X is weakened progressively in the order $X = CH_3 > H > PH_3 > H_2S > Cl > NH_3 > H_2O$; and that the weakening of the bond *trans* to X is due primarily to a lessening of the Pt(6s)—N and Pt($5d_{x^2-y^2}$)-N interactions, and not to the decreased availability of $6(p_{x,y})$, in agreement with Syrkin's theory.

The *trans*-influence has been most widely examined in platinum(II) complexes, and relative *trans*-influence series have been established for a wide variety of ligands from infrared, nmr and nqr spectroscopic and X-ray crystallographic parameters⁴. In this study, the effect of *trans* ligands has been studied by recording the 129-iodine Mössbauer parameters for three neutral complexes, *trans*- $[^{129}IQ_2PtX]$ ($X = Me, CF_3, I$; $Q = Me_2PhP$), and six cationic complexes, *trans*- $[^{129}IQ_2PtL]^+$ ($L = P(OMe)_3, P(OMe)_2Ph$,

PPh_3 , AsPh_3 , EtNC , $p\text{-MeO.C}_6\text{H}_4\text{.NC}$; $\text{Q} = \text{Me}_2\text{PhP}$). ^{129}I Mössbauer spectra will yield less ambiguous results than those from some other Mössbauer isotopes, such as ^{119}Sn or ^{121}Sb , which have other ligands bonded to them. The parameters from the spectra of these latter elements will also reflect the bonding characteristics and structural distortions of the other ligands about the Mössbauer atom.

Since the completion of this work, the ^{129}I Mössbauer parameters for some platinum complexes of the type *cis*- and *trans*- $^{129}\text{I}_2\text{PtL}_2$ and *trans*- $^{129}\text{IHPTL}_2$ ($\text{L} = \text{neutral ligand}$) have been reported^{6,7}. A *cis* influence of ligands was obtained from the *trans* compounds, but the change in parameters in the *cis*-compounds is clearly due to both a *cis* and a *trans* influence.

B. Results

(i) Structures

The *trans* configuration for all the iodide complexes was unequivocally established by the presence of the expected⁸ triplet of triplet proton nmr signals for the methyl groups in the Me_2PhP ligands (due to coupling with ^{31}P and ^{195}Pt) (in CDCl_3 solution), except in the case of the complexes with $\text{L} = \text{Ph}_3\text{P}$, Ph_3As . Several pieces of evidence indicate that these compounds were a mixture of *cis* and *trans* isomers. When these compounds were crystallised from dichloromethane solutions, using pentane, they both yielded bright yellow solids which had satisfactory elemental analyses (see table 6.2), but which melted

over ranges of -30° . When the $L = Ph_3P$ complex was re-dissolved in methanol and crystallised with ether/pentane, a pale yellow solid formed which melted over a much smaller range ($126.5-133^{\circ}C$). 1H nmr spectra of the $L = Ph_3P$ compound in CD_2Cl_2 and CD_3OD solutions showed that a mixture of species was present, and the pattern of the spectra could be associated with both a *trans* (triplet of triplets) and a *cis* (triplet of triplets, and triplet of doublets) isomer being present. The intensities of the signals indicated that the *trans* isomer was predominant (*trans:cis* approx. 3:1 in both solvents).

The ^{129}I spectra for $L = Ph_3P$ (see table 6.1) showed a marked decrease in linewidth from the bright yellow (sample I) to the pale yellow (sample II) compounds; though the other parameters were changed surprisingly little. Together with the melting point data and the colour, this line narrowing probably indicates that sample II contained a much higher proportion of the *trans* isomer than sample I; and the derived Mössbauer parameters for sample II are probably very close to those for the pure *trans* isomer.

No sample of the $L = Ph_3As$ compound could be obtained which melted over a small range, and, again, the 1H nmr spectrum (in $CDCl_3$) indicated that both *cis* and *trans* isomers were present, with the *trans* isomer predominant. The ^{129}I Mössbauer spectrum for this compound was somewhat unsatisfactory in several ways. It could be computed only with some difficulty, and the best fit to the spectrum yielded unrealistic intensity ratios for a

couple of the lines. Also, the linewidths were much greater than for any of the other compounds, though the $Q(5/2)/Q(7/2)$ value is in good agreement with the other values. Thus the calculated parameters for this compound (table 6.1) should be treated with some caution.

(ii) Mössbauer Spectra

The 129-iodine Mössbauer spectrum for *trans*-[^{129}I ,PtP(OMe) $_3$]PF $_6$ is shown in figure 6.1; and the method of spectral analysis to yield the hyperfine parameters, together with a sample calculation for the above compound, are described in appendix 1. The χ^2 for the computed fits to the data, the widths of the peaks at half height and all the derived parameters are listed in table 6.1. Generally, relative intensities were within $\pm 20\%$ of the values expected from the Clebsch-Gordan co-efficients for random samples⁹; except for the most intense line (3), which was consistently up to 40% less than expected, perhaps due to a saturation effect. This may account for the poor χ^2 values sometimes reported^{6,7} for ^{129}I spectra, though quite large changes in relative line intensities seem to have a much smaller effect on computed line positions. Other than for line 3, the observed intensity ratios indicated that orientation, saturation and Goldanskii-Karyagin effects are relatively small.

The excellent agreement between the η values for the two energy levels (never different by more than 0.07) and the consistent value $Q(5/2)/Q(7/2)$ from compound to compound indicates that very accurate parameters may be derived using the Williams-

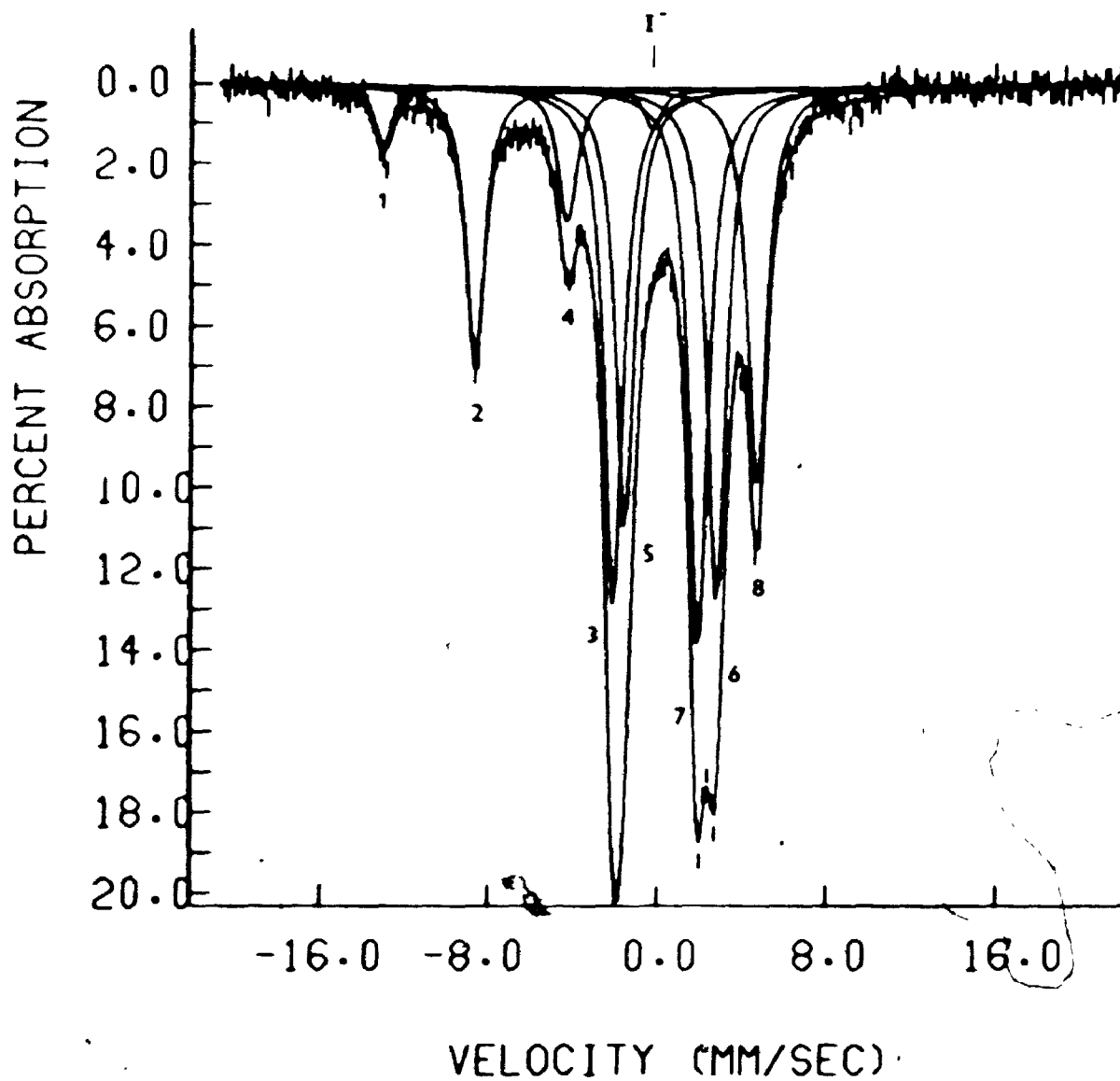


figure 6.1: ^{129}I -iodine Mössbauer spectrum of $\text{trans-}[\text{}^{129}\text{I}]\text{PtP}(\text{OMe})_3\text{PF}_6$ at 4.2K, showing the line numbering convention used, and the best computed 9 peak fit.

Table 6.1

120-Iodine Mossbauer Parameters for trans-1,1,1,1-tetra- and trans-1,1,1,2-tetra- PF_6 (Mossbauer) $\text{Mn}_2\text{P}_2\text{O}_7$

X or L	$e^{100(I/\gamma)}$ mm	$e^{100(I/\gamma)}$ MHz	$e^{100(I/\gamma)}$ MHz	$\frac{Q(I/\gamma)}{Q(I/\gamma)}$	$\frac{Q(I/\gamma)}{Q(I/\gamma)}$	$\frac{Q(I/\gamma)}{Q(I/\gamma)}$	$\frac{Q(I/\gamma)}{Q(I/\gamma)}$	$\frac{Q(I/\gamma)}{Q(I/\gamma)}$	$\frac{Q(I/\gamma)}{Q(I/\gamma)}$	$\frac{Q(I/\gamma)}{Q(I/\gamma)}$	$\frac{Q(I/\gamma)}{Q(I/\gamma)}$	$\frac{Q(I/\gamma)}{Q(I/\gamma)}$	$\frac{Q(I/\gamma)}{Q(I/\gamma)}$	$\frac{Q(I/\gamma)}{Q(I/\gamma)}$	$\frac{Q(I/\gamma)}{Q(I/\gamma)}$
1. CH_3	-23.77	-774.0	-869.0	1.251	0.28	0.21	-0.64	2.33	1.94	1.63	0.34	0.42	0.96	1.94	231
2. CF_3	-27.79	-905.0	-1125	1.243	0.28	0.26	-0.61	2.33	1.93	1.77	0.40	0.47	1.07	1.95	225
3. $\text{P}(\text{O}(\text{H}))_3$	-31.14	-1015	-1257	1.239	0.30	0.26	-0.36	2.00	1.92	1.72	0.44	0.57	1.07	1.96	235
4. $\text{CH}_3\text{CH}_2\text{NC}$	-31.87	-1038	-1282	1.235	0.16	0.16	-0.30	2.00	1.95	1.53	0.65	0.52	0.96	0.97	234
5. $\text{P}(\text{O}(\text{H}))_2\text{Ph}$	-32.30	-1052	-1304	1.239	0.27	0.31	-0.29	2.00	1.91	1.70	0.46	0.59	0.97	1.19	262
6. $\text{P}(\text{O}(\text{H}))_2\text{C}_6\text{H}_4\text{NC}$	-32.62	-1063	-1316	1.239	0.16	0.13	-0.33	2.00	1.95	1.51	0.66	0.53	0.96	0.99	235
7. AsPh_3	-34.47	-1123	-1389	1.237	0.16	0.22	-0.25	2.00	1.94	1.48	0.49	0.58	0.96	1.32	325
8. PPh_3 (I)	-35.29	-1150	-1410	1.227	0.19	0.19	-0.21	2.00	1.94	1.47	0.50	0.60	0.96	1.17	290
8. PPh_3 (II)	-35.45	-1155	-1418	1.228	0.22	0.22	-0.23	2.00	1.93	1.46	0.50	0.61	0.97	0.98	215
9. I	-35.96	-1172	-1447	1.235	0.19	0.17	-0.30	2.00	1.94	1.46	0.51	0.60	0.97	1.04	260

a ± 4 MHz
b ± 0.03
c relative to ZnFe at 4.2 K
d peak width at half height

Bancroft method¹⁰, which is simpler than other methods used previously¹¹⁻¹³, and involves no approximations.

As a further test of the method, the errors which would occur in the derived e^2qQ and η values as a result of errors in the line positions have been estimated statistically (see appendix 2). The results strongly suggest that e^2qQ is accurate to better than ± 4 MHz, and η to better than ± 0.03 . For example, for the three compounds given in table A2.1, 2σ (the 95% confidence level) is never greater than ± 7 MHz for e^2qQ and ± 0.04 for η , or then is never larger than ± 4 MHz for e^2qQ , and ± 0.03 for η . The excellent agreement between the internal and external estimates of the error in η indicate that the accuracy of η values derived by the Williams-Bancroft method¹⁰ is limited by the accuracy of the spectroscopic data, rather than inherent inaccuracies in the treatment.

The average $Q(5/2)/Q(7/2)$ value from the data is 1.239, and the standard deviation in the nine values is 0.007. This is in excellent agreement with the value (1.2385 ± 0.0011) given by Collins¹³, but larger than the value of 1.231 commonly used¹⁰. Alternatively, if it is considered that the error in $Q(5/2)/Q(7/2)$ is due to a 4 MHz error in each of the e^2qQ values, then the resultant error in the Q ratio is calculated to be 0.009. This would seem to indicate that, if anything, the estimated error of ± 4 MHz in the e^2qQ values is overly cautious.

The measured CS values (table 6.1) are small and negative, approaching the values observed for ionic iodides^{9,14}. A relatively

large error of $\pm 0.05 \text{ mm s}^{-1}$ is associated with these values.

C. Discussion

(1) The trans-influence series

The following equations, derived from the Townes-Dailey theory¹⁵ for the analysis of nqr spectra, are those derived in chapter 1 to calculate the U_p , N_{p_x} , N_{p_y} , N_{p_z} , h_p and h_s parameters:

$$U_p = -e^2qQ(127I)/2293 \quad (\text{MHz}) \quad \dots(6.1)$$

$$\eta = -3/2(N_{p_x} - N_{p_y})/U_p \quad \dots(6.2)$$

$$U_p = -N_{p_z} + 1/2(N_{p_x} + N_{p_y}) \quad \dots(6.3)$$

$$h_p = 6 - (N_{p_x} + N_{p_y} + N_{p_z}) \quad \dots(6.4)$$

$$CS(\text{ZnTe}) = -9.2 h_s + 1.5 h_p - 0.54 \text{ (mm s}^{-1}\text{)} \quad \dots(6.5)$$

Clearly there are five equations, but six variables, so that some reasonable approximation(s) must be made in order for them to be solved. The non-zero η values for the compounds show that $N_{p_x} \neq N_{p_y}$. If we assume pure iodine σ -bonding, then we can say $U_p = h_p$ as did Parish^{6,7}. Using this approximation, we find that the computed population of the p_x orbital, in each case, is slightly greater than two, which is not chemically reasonable. Consequently the parameters in table 6.1 were calculated by arbitrarily setting N_{p_x} to 2.00. The derived values of N_{p_y} and N_{p_z} differ from those computed assuming $U_p = h_p$ by < 0.04 .

and the very small values of h_s indicate that the assumption of almost pure iodine p-bonding is reasonable.

From the treatment of Townes and Dailey¹⁵, the iodine e^2qQ essentially reflects (1) any s-character s in the orbital of iodine participating in the ~~sigma Pt~~ σ -I bond, (2) the covalency (σ) (degree of overlap of the appropriate orbitals) of the platinum-iodine interaction, and (3) any π character (π) in the platinum-iodine interaction. Equation 6.1 may be expressed in terms of these parameters¹⁶, so that

$$(e^2qQ)_{\text{mol.}} = (e^2qQ)_{\text{at.}} \{ (1-s)\sigma - \frac{1}{2}\pi \} \quad \dots (6.6)$$

From the h_s values in table 6.1, it can be seen that the s character in the iodine "sp₂" hybrid is almost constant from compound to compound, and is very small. (However, equation 6.5 shows that even very small h_s values will have a disproportionately large effect on the CS, so that the low CS parameters measured for these compounds - almost as low as those for ionic iodides - are due, in this case, to the participation of a small amount of the iodine's orbitals in the platinum-iodine bond). Thus we can approximate $s \sim 0$.

The non-zero η values (table 6.1) are not unexpected in these compounds, since the p_x and p_y orbitals do not "see" a similar environment in the square planar complexes. In addition, η would be expected to be fairly constant from compound to compound as the environment of the p_x and p_y orbitals is approximately constant, though the value of U_p is not. This can be seen from table 6.1, where N_{p_y} varies much less, relatively,

than U_p . (The fixed value of N_{p_x} will not invalidate this conclusion, since N_{p_x} and N_{p_y} are independent variables in equations 6.1 - 6.5). The actual magnitude of η will depend on its sensitivity to interactions of the p_x and p_y orbitals with nearby atoms; but N_{p_y} is only reduced by a small amount from 2.00, compared with N_{p_z} , which is much smaller because of the σ interaction. This indicates that any π interaction of the p_y orbital with unfilled Pt d orbitals is very small, and approximately constant. Consequently, $e^2qQ \approx -\sigma$ (since $(e^2q^2Q)_{at.}$ is negative), and the e^2qQ values measured will reflect the strength of the platinum iodine bond*. Thus from table 6.1, for the series of complexes *trans*-[IQ²PtL] (L is a neutral or anionic ligand), e^2qQ is largest (least negative) and the platinum-iodine bond is weakest; for L = Me; and e^2qQ most negative and σ greatest for L = I. Parish has reported⁷ the e^2qQ values for *trans*-[HIPtP₂] as -792 MHz for P = Ph₃P and -779 MHz for P = Et₃P. It is reasonable to assume that e^2qQ for P = Me₃PhP will lie between these values. From this result, and the e^2qQ values reported in this study, the order of the *trans*-influence for the series *trans*-[I(PMe₂Ph)₂PtL] is established to be

L = Me > H > CF₃ > P(OMe)₃ > EtNC > P(OMe)₂Ph > p-MeO.C₆H₄.NC > Ph₃As > Ph₃P > I.

*Because η is not precisely constant, the relative N_{p_z} values in table 6.1 do not always follow exactly the same order as e^2qQ . It is preferable to use the e^2qQ values rather than N_{p_z} values as an indication of σ , because of the relatively large errors in η compared with those for e^2qQ .

The ^{129}I Mössbauer technique appears to show excellent sensitivity in reflecting the different bonding characteristics of even closely related ligands. For example, there is a substantial difference between the e^2qQ values for the two isocyanide ligands - the alkyl isocyanide proving to be a better σ donor than the aryl isocyanide as would be expected. Similarly, in the series with $L = \text{P}(\text{OMe})_n\text{Ph}_{3-n}$ ($n = 0, 2, 3$), the range of e^2qQ values is relatively large (1015 - 1155 MHz for the $7/2$ level) with the σ donor ability of the phosphine ligand increasing regularly as the number of methoxy groups on the phosphorus atom is increased.

Parish, in his study⁷ of the compounds $\text{cis-}[L_2\text{Pt}^{129}\text{I}_2]$, concluded that the order of *trans*-influence for the ligands L in these compounds is $\text{Ph}_3\text{Sb} < \text{Ph}_3\text{As} < \text{Ph}_3\text{P} < \text{RPh}_2\text{P} < \text{R}_2\text{PhP} < \text{R}_3\text{P}$ ($R = \text{Me}, \text{Et}$). However, in these systems, the magnitude of the iodine e^2qQ is clearly affected by both a *trans*- and a *cis*-influence. In other studies of these two effects, using infrared and nmr spectroscopic, and X-ray crystallographic data, it has generally been concluded⁴ that the magnitude of the *trans*-influence is several times greater than that of the *cis*-influence. However, the ^{129}I Mössbauer study⁶ of the compounds $\text{trans-}[L_2\text{Pt}^{129}\text{I}_2]$ ($L = \text{PEt}, \text{R}_2\text{S}, \beta\text{-picoline}, \text{py}, \text{NH}_3$) suggested that the influence of the *cis* ligands on the ^{129}I e^2qQ parameters is comparable to that of the *trans* ligand. Unfortunately, this problem cannot be resolved using the data from this study, as there is little overlap in the series of ligands studied.

(ii) Correlations

With reference to previous studies of the *trans*-influence in square planar Pt(II) complexes, our results are most directly comparable with those obtained by Fryer and Smith^{16,17}, since they used ³⁵Cl and ³⁷Cl nuclear quadrupole resonance (nqr) parameters to set various ligands into their relative orders of *trans*- and *cis*-influences. Unfortunately, the compounds studied by these workers do not include any series in which only the *trans*-influence is varying from compound to compound; but do contain the series *cis*-Cl₂PtL₂ (L = py, COD, PEt₃), analogous to the iodides studied by Parish⁷, in which both a *cis*- and a *trans*-influence must be considered to be varying. As noted by Parish⁶, the ¹²⁹I Mössbauer technique appears to be more sensitive to the influence of the other ligands in the square planar Pt(II) system, and in addition provides the parameter η and the sign of the efg, which are not available from ³⁵Cl nqr results, and which are very informative when elucidating the bonding in these systems.

As noted by Clark et al⁴, the order of *trans*-influence of various ligands in any given system, established using different experimental techniques, is not always consistent. To a first approximation, the *trans*-influence of a ligand L depends on (1) the effect of L on the character of the hybrid orbital used by the metal in its bond to the *trans* ligand, and (2) the net overlap (both σ and π) of the metal and ligand orbitals. Different experimental techniques have different sensitivities to these two phenomena.

For example, many ligands which form strong covalent bonds with Pt(II) do have a large metal s-participation in their M—L bonds, so that the metal ligand bond *trans* to it is weakened through low s character in the metal hybrid. However, the condition for optimum overlap (and, thus, maximum bond strength) is not always that the metal hybrid orbital should have maximum s character (e.g. for N-donors, halides). Thus, although the Pt—N bond for most nitrogen ligands is quite strong in terms of bond energy¹⁸, the metal-ligand bond *trans* to it is not greatly depleted in s-character.

The nmr spin-spin coupling between a central metal atom and nearby ligand atoms is commonly considered⁴ to be dominated by a Fermi-contact mechanism; and the observed coupling constant, J, is generally interpreted as being mainly determined by the interaction of the nuclear spin with s-electrons in the overlapping metal and ligand orbitals. Consequently we might expect that comparisons of nmr coupling constants with ¹²⁹I Mössbauer e²qQ values - which depend more on the total orbital overlap - to formulate relative orders of *trans* influence may yield inconsistencies for series of ligands with widely different bonding modes.

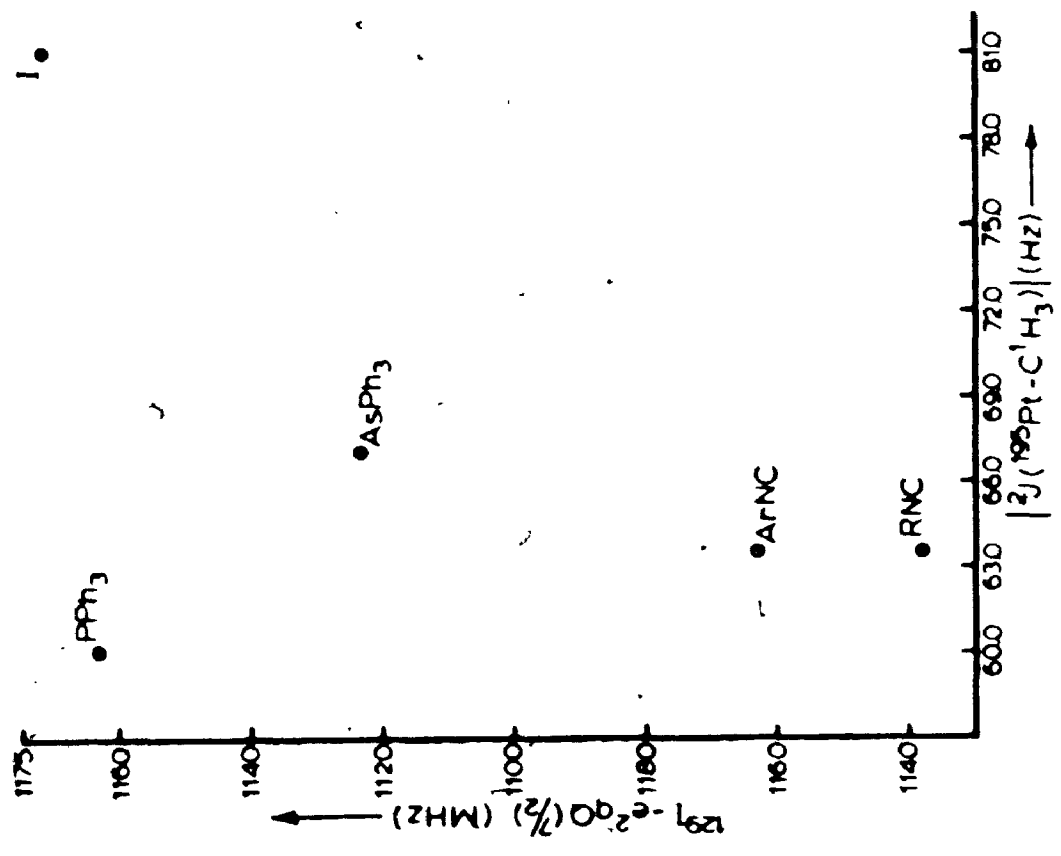
The correlation of some of the ¹²⁹I e²qQ (7/2) values with |²J(Pt-CH₃)| values^{8,19,20} (figure 6.2a) for the complexes *trans*-[(CH₃)₂Q₂PtL] shows that a linear relationship between the two sets of parameters is not observed. From this diagram it could be speculated that the Pt—PPh₃ bond has a particularly high s-character (reflected in the J values), but which does not

figure 6.2

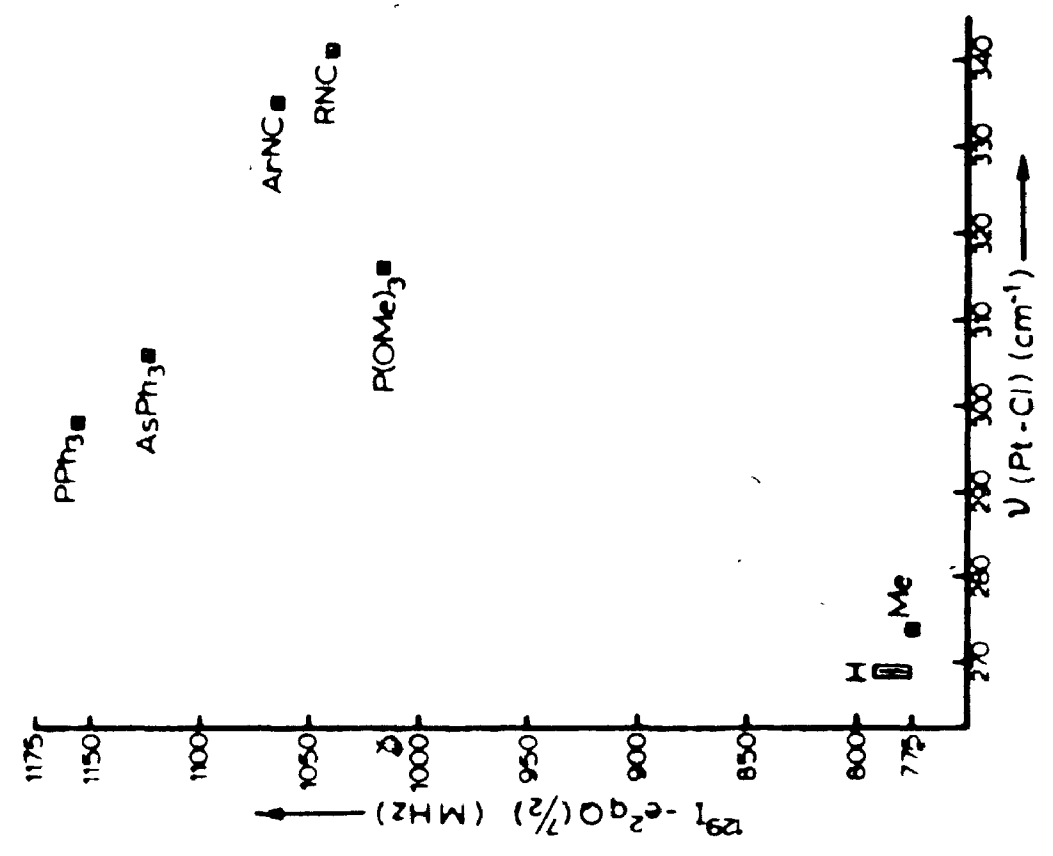
Plots of $^{129}\text{I } e^2qQ(7/2)$ values
for the complexes $\text{trans-}[^{129}\text{I}Q_2\text{PtL}]$
($Q = \text{Me}_2\text{PhP}$), against

(a) $|^2J(^{195}\text{Pt}-\text{C}^1\text{H}_3)|$ for $\text{trans-}[\text{Me}Q_2\text{PtL}]$
and (b) $\nu(\text{Pt}-\text{Cl})$ for $\text{trans-}[\text{Cl}(\text{PEt}_3)_2\text{PtL}]$

Axes are oriented to show a positive correlation
in both cases.



(a)



(b)

imply that the orbital overlap (as measured by e^2qQ (7/2)) is as great as that for some of the other ligands which have a lower s character in the metal-ligand bond.

One useful point to note is that the order of *trans*-influence $\text{Me} > \text{CF}_3 > \text{I}$ is unambiguously established. In a ^{13}C nmr study²¹ of $(\text{COD})\text{PtX}_2$ ($\text{X} = \text{Me}, \text{CF}_3, \text{I}$; COD = 1,5-cyclo-octadiene) the magnitude of the coupling between ^{195}Pt and the COD olefinic carbon atoms was found to be the same for $\text{X} = \text{CF}_3$, and Me. This is unexpected because of the large difference in electronegativity between these ligands (as reflected by the chemical shifts of the alkyl carbon signals). However, this has recently been re-interpreted²² as indicating that the J values must be of opposite sign, and only co-incidentally of the same magnitude. Thus the coupling constants indicate that the order of *trans*-influence is $\text{Me} > \text{CF}_3 > \text{I}$.

It might be expected that ^{129}I e^2qQ values would be more consistent with the order of metal-ligand infrared stretching frequencies found for a constant ligand *trans* to the series of ligands being studied; as these latter parameters are dependent on both of the two phenomena mentioned above. Figure 6.2b shows some of the ^{129}I e^2qQ (7/2) parameters plotted against $\nu(\text{Pt}-\text{Cl})$ observed²³ for the series of complexes *trans*- $[\text{Cl}(\text{PEt}_3)_2\text{PtL}]$. The consistency of these two series is no more satisfactory. Clark et al⁴ noted that $\nu(\text{Pt}-\text{Cl})$ is fairly insensitive to the *trans* ligand over part of the *trans*-influence series. In addition, the difference in bonding mode between $\text{Pt}-\text{I}$ and $\text{Pt}-\text{Cl}$

(especially in terms of Pt 6s character in the metal hybrid) will reflect differently in the bonding of the *trans* ligand. Finally, the "purity" of the $\nu(\text{Pt-Cl})$ mode could well vary significantly from compound to compound as this bond lies in a region of the infrared spectrum which has a number of other absorptions nearby; so that the observed band would reflect more than just the influence of the *trans* ligand on the strength of the platinum-chlorine interaction.

D. Conclusion

The ^{129}I probe is found to be very sensitive to the nature of the *trans* ligand, and hence should be very useful in the future for studying subtle changes in iodine bonding. Because the ^{129}I e^2qQ reflects more of the total bonding situation between platinum and iodine, it may be more useful than some other techniques which rely heavily on a single aspect of the bonding - such as s character in nmr coupling constants.

Excellent χ^2 values, a detailed analysis of the errors in the method, and the internal consistency checks which the method affords, strongly suggest that the William-Bancroft method for multiline Mössbauer and nqr spectral analysis leads to very accurate parameters with no approximations and straightforward calculations.

E. Experimental

Radioactive Na^{129}I was purchased from the U.S. Atomic

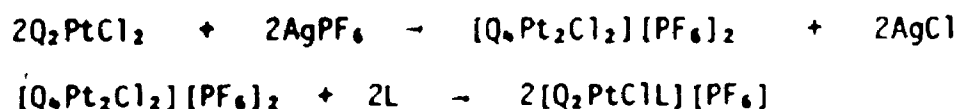
Energy Commission, Oak Ridge National Laboratory, as an aqueous solution with basic sodium metabisulphite. The Na^{129}I was isolated by removal of the water solvent under vacuum, and extraction with several portions of acetone. The acetone was removed under vacuum, and the resulting solid used without further purification.

The compounds *trans*- ClMePtQ_2 , *trans*- $\text{I}(\text{CF}_3)\text{PtQ}_2$, and *cis*- Cl_2PtQ_2 ($\text{Q} = \text{Me}_2\text{PhP}$) were kindly donated by Dr. L. E. Manzer. The desired radioactive iodine complexes *trans*- $^{129}\text{I}_2\text{PtQ}_2$ and *trans*- $^{129}\text{IMEPtQ}_2$ were prepared from the chloride precursors by metathetical reaction with a stoichiometric amount of Na^{129}I ; and *trans*- $^{129}\text{I}(\text{CF}_3)\text{PtQ}_2$ was prepared by treatment with one mole equivalent of AgClO_4 , filtration to remove AgI and addition of Na^{129}I . The identity and purity of the complexes was checked by comparison of melting point, ^1H nmr and infrared data with that in the literature^{8,19,24,25}.

The cationic complexes were all synthesised by the following method, based partly on that previously used for related compounds²⁶.

Typically, 0.75 mmole. (408 mg) of Cl_2PtQ_2 was suspended in 30 ml of methanol, and 0.75 mmole (194 mg) of AgPF_6 dissolved in acetone was added dropwise with stirring. The precipitated AgCl was removed by centrifugation, and 0.75 mmole of the appropriate neutral ligand L was added to the pale yellow supernate, and stirred for an hour. (Cleavage of the chloro-bridged dimer was also attempted using pyridine, but without success, even with heating). The product was isolated by concentrating the

solution under vacuum, and crystallizing by slow addition of pentane or ether.



The iodide complexes were then synthesised from the corresponding chlorides by a metathetical reaction with sodium iodide. The appropriate chloro-complex was dissolved in methanol, and an equimolar amount of sodium iodide, dissolved in acetone, was added dropwise with stirring. After several hours the solvent was removed under vacuum, and the solid extracted with water to remove sodium chloride and any unreacted sodium iodide. The remaining solid was taken up in a minimum of dichloromethane, an equal amount of methanol added, and the product crystallised with pentane and cooling.



Radioactive $Na^{129}I$ is expensive, so that only small amounts of the ^{129}I complexes were made. Satisfactory ^{129}I Mössbauer spectra were obtained when the final products contained 25 - 45 mg. of ^{129}I .

The analytical and physical data for the iodo-complexes are shown in table 6.2. This data refers to products synthesised using naturally occurring $Na^{127}I$. The final complexes, containing ^{129}I , were then made identically, and their identity and purity checked using 1H nmr, infrared spectra and melting points. The physical properties shown in table 6.2 agreed well with previous

table 6.2

Physical Data for the Complexes $\text{trans-[ILPtQ}_2\text{]PF}_6$ and $\text{trans-[XPtQ}_2\text{]}$. (Q = Me₂PhP)

L or X	colour	yield (%)	m.p. (°C)	ELEMENTAL ANALYSES					
				C		H		I	
				found	calc.	found	calc.	found	calc.
EtNC	white	78	120-122	28.7	28.6	3.42	3.41	15.0	15.9
p-MeO.C ₆ H ₄ .NC	white	68	184-185	32.9	32.9	3.20	3.34	13.2	13.5
P(OMe) ₃	white	65	136.5-138	27.0	26.3	3.86	3.60	14.5	14.6
P(OMe) ₂ Ph	white	85	85.5 d	31.8	31.6	3.88	3.64	13.5	13.9
PPh ₃ (sample I)	*	72	*	40.6	40.6	3.87	3.71	12.6	12.6
AsPh ₃	*	54	*	38.5	38.9	3.72	3.55	11.9	12.1
CH ₃	white	87	133-134						
CF ₃	cream	73	126-127						
I	yellow	90	166-167.5						

*see text

literature reports for the compounds where $L = EtNC^{26}$, and $X = I, Me, CF_3$,^{8,19,24,25}. The cationic complexes where $L = p-MeO.C_6H_4.NC, P(OMe)_3, P(OMe)_2Ph, PPh_3$, and $AsPh_3$, appear to be new. Elemental analyses for all the cationic compounds are satisfactory.

F. References

1. A. Pidcock, R. E. Richards and L. M. Venanzi; *J. Chem. Soc. (A)* (1966), 1707; L. M. Venanzi; *Chem. Brit.* (1968), 162.
2. Y. K. Syrkin; *Izv. Akad. Nauk SSSR, Otd. Khim. Nauk* (1948), 69.
3. F. Basolo, J. Chatt, H. B. Gray, R. G. Pearson and B. L. Shaw, *J. Chem. Soc. (London)* (1952), 4300; (1956), 525.
4. T. G. Appleton, H. C. Clark and L. E. Manzer; *Co-ord. Chem. Rev.* (1973) 10, 335.
5. S. S. Zumdahl and R. S. Drago; *J. Am. Chem. Soc.* (1968) 90, 6669.
6. B. W. Dale, R. J. Dickinson and R. V. Parish; *Chem. Comm.* (1974) 35.
7. B. W. Dale, R. J. Dickinson and R. V. Parish; *Chem. Phys. Lett.* (1974) 24, 286.
8. T. G. Appleton, M. H. Chisholm, H. C. Clark and L. E. Manzer; (1972) 11, 1786.
9. N. N. Greenwood and T. C. Gibb; "Mössbauer Spectroscopy", Chapman and Hall (1971), London, U.K.
10. P. G. L. Williams and G. M. Bancroft; *Mol. Phys.* (1970) 19, 717; *Mössbauer Effect Methodology* (1971) 7, 39.
11. J. R. Gabriel and S. L. Ruby; *Nucl. and Instr. Methods*, (1965) 36, 23.
12. B. S. Ehrlich and M. Kaplan; *J. Chem. Phys.*, (1969) 50, 2041.
13. R. Robinette, J. G. Cosgrove and R. L. Collins; *Nucl. Instr. Methods*, (1972) 105, 509.
R. Robinette and R. L. Collins; *J. Chem. Phys.*, (1972) 57, 4319.
14. G. M. Bancroft; "Mössbauer Spectroscopy: An Introduction for Inorganic Chemists and Geochemists", McGraw-Hill (1973) U.K.
15. C. H. Townes and D. P. Dailey; *J. Chem. Phys.*, (1949) 17, 782.
16. C. W. Fryer and J. A. S. Smith; *J. Organometal. Chem.*, (1969) 18, P35, *J. Chem. Soc. (A)*, (1970), 1029.
17. C. W. Fryer; *Chem. Comm.* (1970), 902.
18. W. A. Partenheimer; *Inorg. Chem.*, (1972) 11, 743.
19. J. D. Ruddick and B. L. Shaw; *J. Chem. Soc. (A)* (1969), 2801.

20. H. C. Clark and J. D. Ruddick; *Inorg. Chem.*, (1970) 9, 1226.
21. M. H. Chisholm, H. C. Clark, L. E. Manzer and J. B. Stothers;
J. Amer. Chem. Soc., (1972) 94, 5087.
22. M. H. Chisholm, H. C. Clark, L. E. Manzer, J. B. Stothers and
J. E. H. Ward; *J. Amer. Chem. Soc.*, submitted for publication.
23. M. J. Church and M. J. Mays; *J. Chem. Soc. (a)* (1968), 3074.
24. H. C. Clark and J. D. Ruddick; *Inorg. Chem.*, (1970) 9, 2556.
25. J. M. Jenkins and B. L. Shaw; *J. Chem. Soc. (A)* (1966), 770.
26. H. C. Clark and L. E. Manzer; *Inorg. Chem.*, (1972) 11, 503.

APPENDIX 1

Analytical Determination of the Hyperfine Mössbauer Parameters from 129-Iodine Spectra

A. The EFG-Nuclear Quadrupole Interaction

The method outline here follows the general method of Williams and Bancroft¹ for the determination of hyperfine parameters for multiline Mössbauer spectra.

The Hamiltonian describing the quadrupole and/or magnetic interaction of the particular nuclear state under consideration with the electric field gradient may be written down, and the Hamiltonian matrix over the basis set of spin components constructed. This leads to a secular determinant which may be expanded to give a polynomial in E, the energy, whose n roots (where $n = 2I + 1$) are the eigenvalues of the energy of the nucleus in the environment described by the Hamiltonian. This polynomial may be expressed as follows¹:

$$E^n + a_{n-1}E^{n-1} + a_{n-2}E^{n-2} \dots + a_1E^1 \dots + a_1E + a_0 = 0 \dots (A1.1)$$

where the coefficients a_i are analytical functions of some or all of the hyperfine parameters.

Now if the roots of this polynomial (ie. the energy levels of the nuclear state) are E_i for $i = 1$ to n , then

$$(E - E_n)(E - E_{n-1}) \dots (E - E_1) \dots (E - E_1) = 0$$

or $E^n - E^{n-1}(\sum E_i) + E^{n-2}(\sum_j E_i E_j) \dots + (-1)^n E_1 E_2 \dots E_n = 0 \dots (A1.2)$

is identical to A1.1. Therefore, equating coefficients, we obtain:

$$\begin{aligned} a_{n-1} &= -\sum_i E_i \\ a_{n-2} &= \sum_{i>j} E_i E_j \\ \dots a_0 &= (-1)^n E_1 E_2 \dots E_n \end{aligned} \quad \dots (A1.3)$$

Equations A1.3 comprise a set of n equations relating functions of the hyperfine parameters (the coefficients a_i) to products of the energy levels of the nucleus. The energy levels of the nuclear state may be obtained from the energy level diagram, which may, in turn, be derived directly from the observed spectrum. In many cases, these equations (A1.3) may be solved directly to yield the hyperfine parameters e^2qQ , n , $Q_{ex.}/Q_{gr.}$ and δ .

The Hamiltonian representing the interaction of a nucleus having spin I and quadrupole moment Q , with an efg specified, as usual, by eq and n , may be written:

$$\mathcal{H} = \frac{e^2qQ}{4I(2I-1)} [3I_z^2 - I(I+1) + \frac{n}{2}(I_+^2 + I_-^2)] \quad \dots (A1.4)$$

where I is the total nuclear spin operator, $I_{\pm} = I_x \pm iI_y$, and I_x , I_y and I_z are the nuclear spin component operators.

From this, a matrix \mathcal{H} may be constructed over the $(2I+1)$ -fold base set $|m\rangle$ in which $\mathcal{H}_{ij} = \langle m_i | \mathcal{H} | m_j \rangle$. The reduction of \mathcal{H} to diagonal form gives the $2I+1$ eigenvalues of the energy of the nucleus in the field system specified by eq and n .

Equivalently, a secular determinant

$$|\mathcal{H} - EI|_{ij} = \mathcal{H}_{ij} - E\delta_{ij} \quad \dots (A1.5)$$

, where I is the unit matrix, may be constructed, and on expansion this yields a secular polynomial in E whose $2I + 1$ roots are the eigenvalues of the energy of the nucleus in the field system eq. n.

Writing the Hamiltonian as

$$\mathcal{H} = \mu(3I_z^2 - I(I+1)) + \frac{\mu\eta}{2}(I_+^2 + I_-^2), \quad \dots (A1.6)$$

$$\text{where } \mu = \frac{e^2 q Q}{4I(2I-1)} \quad \dots (A1.7)$$

, the secular polynomials obtained by expansion of the determinants for the excited ($I = 5/2$) and ground ($I = 7/2$) states of 129-iodine are:

$$\text{excited (5/2)} \quad [E^3 - 28\mu_{5/2}^2(3 + \eta^2)E - 160\mu_{5/2}^3(1 - \eta^2)] = 0 \quad \dots (A1.8a)$$

$$\text{ground (7/2)} \quad [E^5 - 126\mu_{7/2}^2(3 + \eta^2)E^2 - 1728\mu_{7/2}^3(1 - \eta^2)E + 945\mu_{7/2}^4(3 + \eta^2)^2] = 0 \quad \dots (A1.8b)$$

Comparing equations A1.8a and b with equations A1.3, it is obvious that,

$$\text{for } I = 5/2 \quad -28\mu_{5/2}^2(3 + \eta^2) = \sum_{i>j} E_i E_j \quad \dots (A1.9a)$$

$$160\mu_{5/2}^3(1 - \eta^2) = E_1 E_2 E_3 \quad \dots (A1.9b)$$

$$\text{and, } I = 7/2 \quad -126\mu_{7/2}^2(3 + \eta^2) = \sum_{i>j} E_i E_j \quad \dots (A1.10a)$$

$$1728\mu_{7/2}^3(1 - \eta^2) = \sum_{i>j>k} E_i E_j E_k \quad \dots (A1.10b)$$

$$945\mu_{7/2}^4(3 + \eta^2) = E_1 E_2 E_3 E_4 \quad \dots (A1.10c)$$

The energy levels, E_n , for use with these equations are determined from the Mössbauer spectrum.

B. The Determination of Energy Levels

In order to use the equations just derived, the energy level diagram must be constructed and all the E_i values calculated. This is easily done if most of the lines are well resolved so that the line positions can be accurately obtained.

In a field-free absorber, the single Mössbauer line would lie at a velocity

$$\delta = \gamma_{E_a} - \gamma_{E_s} = ({}^e E_a - {}^g E_a) - ({}^e E_s - {}^g E_s) \quad \dots (A1.11)$$

where δ is the centre shift of the absorber with respect to the particular source used. A general line would lie at velocity z_k where

$$z_k = ({}^e E_a + {}^e E_j) - ({}^g E_a + {}^g E_i) - ({}^e E_s - {}^g E_s)$$

for $i = 1 \rightarrow 4$ and $j = 1 \rightarrow 3$.

$$\therefore z_k = {}^e E_j - {}^g E_i + \delta \quad \dots (A1.12)$$

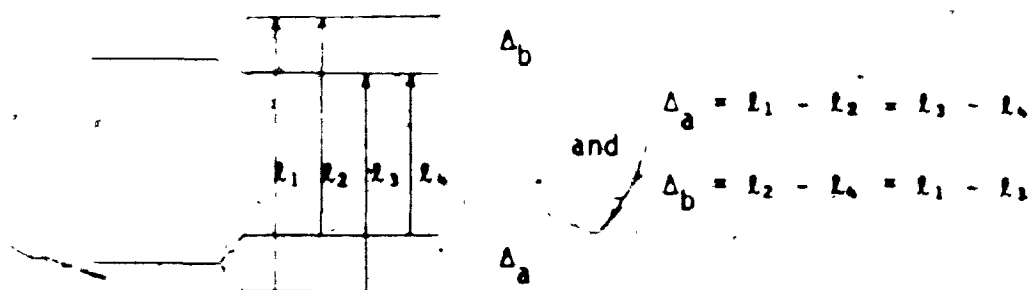
$$\text{where } \sum {}^e E_j = \sum {}^g E_i = 0 \quad \dots (A1.13)$$

Excited	Ground
state	state

For $n = 0$, the energy levels of the ground and excited states may be labelled by the appropriate spin quantum number m_I . The selection rule $\Delta m_I = 0, \pm 1$ limits the number of permitted

transitions between the energy levels of the ground and excited state. The ratio of the intensities, as deduced from the Clebsch-Gordan coefficients² helps to assign the lines, and the energy level diagram can be constructed. For small values of η , in which the number of lines capable of resolution is still the same as for $\eta = 0$, (ie. mixing of states $m_J \pm 2$ into each state m_J by the second term in the Hamiltonian is small), and thus m_J can still serve as an approximate quantum number, the Clebsch-Gordan coefficients may still be used as a guide to assignment. (For large values of η , in which the eigenstates of the ground and excited states may not be labelled by a simple spin quantum number m_J , the spectrum becomes more complex as more transition probabilities become non-zero). For all spectra in this study, η is small.

The lines in a spectrum are most easily assigned by subtracting each line position from each other line position, thus constructing a table of differences. This table is searched until a pair of similar differences is found; which indicates the following situation:



For 129-iodine spectra, four such pairs of differences are to be expected (defining Δ_{1-4}). Using these assignments

Δ_3 may be found, and all spectral lines assigned to particular transitions. The line and transition numbering convention is shown in figures 6.1 and A1.1.

Using these assignments, together with equation A1.13, the following equations are generated.

$$E_{5/2}(\pm 1/2) = (2\Delta_1 + \Delta_2)/3 \quad \dots (A1.14a)$$

$$E_{5/2}(\pm 3/2) = (-\Delta_1 + \Delta_2)/3 \quad \dots (A1.14b)$$

$$E_{5/2}(\pm 5/2) = (-\Delta_1 - 2\Delta_2)/3 \quad \dots (A1.14c)$$

$$E_{7/2}(\pm 1/2) = (3\Delta_1 + 2\Delta_2 + \Delta_3)/4 \quad \dots (A1.15a)$$

$$E_{7/2}(\pm 3/2) = (-\Delta_1 + 2\Delta_2 + \Delta_3)/4 \quad \dots (A1.15b)$$

$$E_{7/2}(\pm 5/2) = (-\Delta_1 - 2\Delta_2 + \Delta_3)/4 \quad \dots (A1.15c)$$

$$E_{7/2}(\pm 7/2) = (-\Delta_1 - 2\Delta_2 - 3\Delta_3)/4 \quad \dots (A1.15d)$$

C. Solution of the Polynomials

Equations A1.9a and b are combined for $I = 5/2$, and equations A1.10a and b for $I = 7/2$, to give the following equation entirely in μ .

$$4\mu_I^3 - C_1\mu_I - C_2 = 0 \quad \dots (A1.16)$$

$$\text{where } C_1 = \frac{\sum_{i>j} E_i E_j}{28} \quad \text{and } C_2 = \frac{E_1 E_2 E_3}{160} \quad \text{for } I = 5/2$$

$$\text{and } C_1 = \frac{\sum_{i>j} E_i E_j}{126} \quad \text{and } C_2 = \frac{\sum_{i>j>k} E_i E_j E_k}{1728} \quad \text{for } I = 7/2$$

(It may be noted that there is, clearly, a redundant equation (A1.10c) for $I = 7/2$).

Each of these cubic equations has three real roots for μ_I , which will be proportional to the components of the electric field gradient³ (V_{XX} , V_{YY} , V_{ZZ}), assigned in the conventional manner so that $|\mu_{XX}| < |\mu_{YY}| < |\mu_{ZZ}|$ (where $\mu_{ii} = -eV_{ii}Q/4I(2I-1)$). Thus V_{ZZ} and e^2qQ can be calculated for $I = 5/2$ and $I = 7/2$ from equation A1.7, and $n(5/2)$ and $n(7/2)$ found by substitution back into equations A1.9 and A1.10. The e^2qQ values are then converted to the usual ^{127}I MHz scale, using the calibration factor² $e^2qQ(^{127}\text{I}) \text{ MHz} \equiv 32.58 e^2qQ(^{129}\text{I}) \text{ mm s}^{-1}$.

A FORTRAN IV computer program was written by this author to process the 129-iodine Mössbauer data using the above analysis. A listing of the program is included at the end of this appendix.

D. Sample Calculation - Mössbauer Parameters for $\text{trans-}[^{129}\text{IQ}_2\text{PtP(OMe)}_3]\text{PF}_6$

The 129-iodine Mössbauer spectrum for $\text{trans-}[^{129}\text{IQ}_2\text{PtP(OMe)}_3]\text{PF}_6$ was shown (figure 6.1) in chapter 6, and Mössbauer hyperfine parameters for it were calculated as shown below.

It can be seen from the spectrum in figure 6.1 that lines 3 and 5 are poorly resolved. Since line 1 has the lowest intensity, it was often badly defined. Consequently the errors in line positions will be greatest for these three, so that calculations were performed using only the better defined line positions where a choice was possible. For example, Δ_1 (see

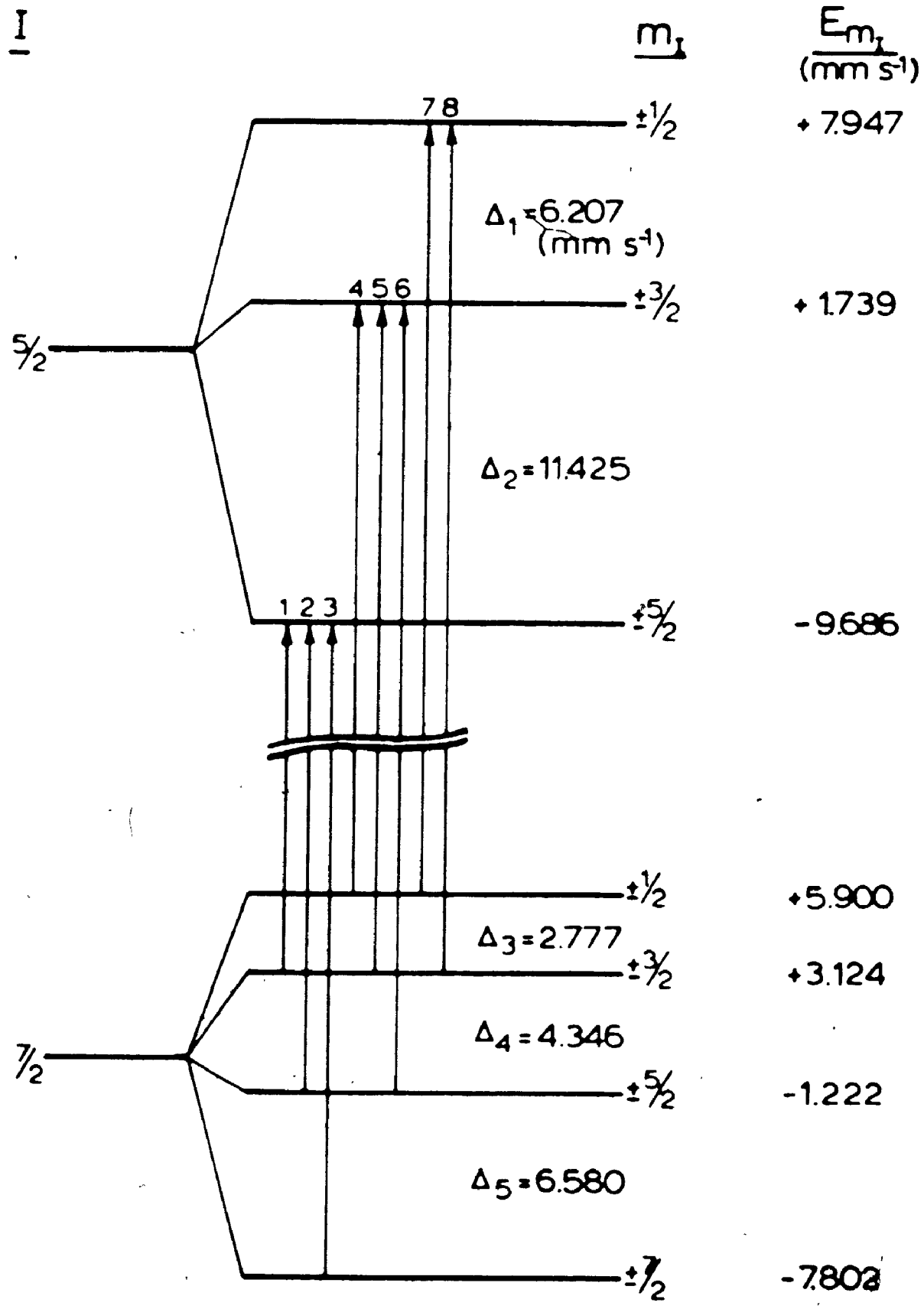


figure A1.1: Nuclear energy level diagram for the ^{129}I atom in $\text{trans-}[\text{Pt}(\text{OAc})_2]\text{PF}_6$; with the transitions numbered as for figure 6.1, together with calculated energy levels and splittings.

figure A1.1) is given by both $\ell_7 - \ell_4$ and by $\ell_8 - \ell_5$; but only the former difference was used to measure Δ_1 .

For the CS, equation A1.12, when expressed in terms of Δ_i values for each of the eight lines of the spectrum, gives only three independent equations defining δ . In this study, the CS quoted in each case is the average of these three values of δ .

The following line positions were computed for the spectrum of *trans*-[^{129}I Q $_2$ PtP(OMe) $_3$]PF $_6$.

<u>Line</u>	<u>Line Position (mm s$^{-1}$)</u> (rel. to ZnTe at 4.2K)
1	-13.204
2	- 8.838
3	- 2.258
4	- 4.466
5	- 1.737
6	+ 2.588
7	+ 1.741
8	+ 4.518

The Δ_i values calculated from these, and the energy levels then computed via equations A1.14 and A1.15 are shown in figure A1.1. Thus the following polynomials were set up using equation A1.16.

$$4\mu_{3/2}^3 - 2.857\mu_{5/2} + 0.8368 = 0$$

$$4\mu_{7/2}^3 - 0.4244\mu_{7/2} + 0.4646 = 0$$

These were solved using a standard computer subroutine for solution of polynomials which utilised a Newton-Raphson iterative technique, supplied by U.W.O. computing centre.

The solutions were

$$\begin{array}{ll} \mu_{XX} (5/2) = 0.3561 & \mu_{XX} (7/2) = 0.1304 \\ \mu_{YY} (5/2) = 0.6088 & \mu_{YY} (7/2) = 0.2403 \\ \mu_{ZZ} (5/2) = -0.9649 & \mu_{ZZ} (7/2) = -0.3707 \end{array}$$

Therefore, from equation A1.7,

$$e^2qQ(5/2) = -38.60 \text{ mm s}^{-1} \text{ and } e^2qQ(7/2) = -31.14 \text{ mm s}^{-1}$$

Resubstitution of these values into equations A1.9 or A1.10 gave

$$n(5/2) = 0.26 \quad n(7/2) = 0.30$$

Alternatively, n values could be calculated from

$n = (\mu_{YY} - \mu_{XX})/\mu_{ZZ}$. Finally, the mean calculated δ from equation A1.12 gave

$$\delta = -0.34 \text{ mm s}^{-1}$$

(relative to $^{66}\text{Zn}^{129}\text{Te}$ at 4.2 K)

E. References

1. P. G. L. Williams and G. M. Bancroft; *Mol. Phys.*, (1970) 19, 717; *Mössbauer Effect Methodology*, (1971) 7, 39.
2. N. N. Greenwood and T. C. Gibb; "Mössbauer Spectroscopy", Chapman and Hall (1971) London, U. K.
3. M. G. Clark; *J. Chem. Phys.*, (1971) 54, 697.

```

C PROGRAM TO CALCULATE ROSSBAUER PARAMETERS
C - CENTRE SHIFT, NUCLEAR ENERGY LEVELS,
C QUADRUPOLE SPLITTINGS, FTA, Q(5/2 / 7/2) -
C FOR 129-IODINE ROSSBAUER SPECTRA.
C
C AUTHOR - K.D.POTTER, UNIVERSITY OF WESTERN ONTARIO (1974)
C
C INPUT PARAMETERS ARE - LINE POSITIONS(CHANNELS),
C SCAN ZERO(CHANNELS), CALIBRATION(CHANNELS/MM/SEC)
C
C INPUT FORMAT IS
C CARDS 1 - TITLE (15A4)
C 2 - CAL (F), S7 (F)
C 3 - CL(1)-CL(11) (F)
C MORE THAN ONE SET OF SPECTRAL DATA
C MAY BE LISTED CONSECUTIVELY
C FINAL CARD IS * AS END OF DATA MARK.

```

```

-----
C
C REAL CL(8), XL(8), DEL(5,3), TITLE_(12), XCOF(4), COF(4)
C COMMON /BLK 1/ ROOTP(3), ROOTI(3)
C COMMON /BLK 2/ EF(3), SE(4), CB(8)
C
C 200 CONTINUE
C
C READ TITLE AND PEAK POSITIONS IN CHANNELS
C
C READ(5,299) (TITLE(I), I=1,12)
799 FORMAT(12A4)
IF(TITLE(1).EQ.'*') GO TO 1000
WRITE(6,890)TITLE
890 FORMAT(111,12A4)
WRITE(6,897)
897 FORMAT(11E,37(11-))
READ(5,898) CAL,S7,(CL(I), I=1,8)
898 FORMAT(2F,1F)
WRITE(6,899)CAL,S7
899 FORMAT(///,' CALIBRATION = ',F6.3,' CHANNELS/MM/SEC',/
1 ' SCAN ZERO - CHANNEL ',F7.2,///)
DO 100 I=1,8
XL(I)=(CL(I)-S7)/CAL
100 CONTINUE
WRITE(6,900)(CL(I),XL(I), I=1,8)
900 FORMAT(' LINE POSITIONS ',///, ' CHANNELS ',4X, ' MM/SEC '
1 ' /,1(11),F8.4,2X,F8.4,/,///)

```

```

C          CALCULATE ENERGY LEVEL SPLITTINGS
C
DEL (1,1)=ML (7)-ML (4)
DEL (1,2)=ML (8)-ML (5)
DEL (2,1)=ML (6)-ML (2)
DEL (2,2)=ML (5)-ML (1)
DEL (3,1)=ML (8)-ML (7)
DEL (3,2)=ML (5)-ML (4)
DEL (4,1)=ML (2)-ML (1)
DEL (4,2)=ML (6)-ML (5)
DEL (5,1)=ML (3)-ML (2)
DEL (5,2)=V.
WRITE (6,9K1) (I, (DEL (I,J), J=1,2), I=1,5)
9K1 FORMAT (' DELTA VALUES (ME/SEC) ', //, 5(I3,2F15.5, /))
C
DO 1K1 I=1,4
1K1 DEL (I,3)=(DEL (I,1)+DEL (I,2))/2.
DEL (5,3)=DEL (5,1)
C
C          CALCULATE NUCLEAR ENERGY LEVELS
C
GE (1)=(3.*DEL (3,3)+2.*DEL (4,3)+DEL (5,3))/4.
GE (2)=(-DEL (3,3)+2.*DEL (4,3)+DEL (5,3))/4.
GE (3)=(-DEL (3,3)-2.*DEL (4,3)+DEL (5,3))/4.
GE (4)=(-DEL (3,3)-2.*DEL (4,3)-3.*DEL (5,3))/4.
EE (1)=(2.*DEL (1,3)+DEL (2,3))/3.
EE (2)=(-DEL (1,3)+DEL (2,3))/3.
EE (3)=(-DEL (1,3)-2.*DEL (2,3))/3.
WRITE (6,9K2) EE, GE
9K2 FORMAT (////, ' NUCLEAR ENERGY LEVELS ', //
1      , 3(F15.5, /), /, 4(F15.5, /))
C
C          CALCULATE C1,C2,C3,C4
C
EIJ5=EE (1)*EE (2)+EE (1)*EE (3)+EE (2)*EE (3)
EIJ5=EE (1)*EE (2)*EE (3)
WRITE (6,9K5) EIJ5, EIJK5
9K5 FORMAT (//, ' EIJ5= ', F12.5, '12X, ' EIJK5= ', F12.5)
EIJ7=GE (1)*GE (2)+GE (1)*GE (3)+GE (1)*GE (4)
1      +GE (2)*GE (3)+GE (2)*GE (4)+GE (3)*GE (4)
EIJ7=GE (1)*GE (2)*GE (3)+GE (1)*GE (2)*GE (4)
1      +GE (1)*GE (3)*GE (4)+GE (2)*GE (3)*GE (4)
WRITE (6,9K6) EIJ7, EIJK7
9K6 FORMAT (' EIJ7= ', F12.5, '12X, ' EIJK7= ', F12.5, /)
COEF 2=-EIJ5/16.
COEF 1=EIJ5/28.
COEF 2=V.
COEF 3=4.
WRITE (6,9K4) COEF 3, COEF 2, COEF 1, COEF 0
9K4 FORMAT (////, ' COEFFICIENTS OF POLYNOMIAL FOR 5/2 STATE
1      , /, 4(F12.5, /))
C

```


SUBROUTINE VTEST(VXX,VYY,VZZ)

C
C
C
C
C

TESTS SOLUTIONS TO THE POLYNOMIALS
(A) TO CHECK THAT ALL ARE REAL
(B) TO IDENTIFY THE SOLUTIONS WITH VXX,VYY,AND VZZ

```

REAL R(3)
COMMON /BLK1/ RR(3),RI(3)
DO 1V I=1,3
  IF((ABS(RI(I))-F.VK1).GT.F.V2) WRITE(6,996)
996 FORMAT(///,' NOT ALL ROOTS OF THE
1 POLYNOMIAL ARE REAL',///)
  R(I)=ABS(RR(I))
10 CONTINUE
DO 2V J=1,3
  IJ=J+1
DO 2V J=IJ,3
  IF(R(I).LT.R(J)) GO TO 2V
  TEMP=R(I)
  R(I)=R(J)
  R(J)=TEMP
  TEMP=RR(I)
  RR(I)=RR(J)
  RR(J)=TEMP
20 CONTINUE

C
VXX=RR(1)
VYY=RR(2)
VZZ=RR(3)

C
RETURN
END

```

C
C
C
C
C
C
C
C
C

SUBROUTINE USETA(EIJ5,EIJK5,EI17,EIJK7,RH05,RH07)

CALCULATES U.S.,ETA, AND U(5/2 / -7/2)

```

RH05=RH05*RH05
RH07=RH07*RH07
RH5RH7=RH05*22.8454
RH7RH2=RH07*22.1454
RH5127=RH5RH7*1.4261
RH7127=RH7RH2*1.4261
WRITE(6,913)RH05,RH5RH7,RH5127,RH07,RH7RH2,RH7127
913 FORMAT(///,' F**2.0,0 (5/2) = F 10.4 MU/SEC'///)
1 5X, ' F 10.2, RH7 (REL TO I-129)'///
2 5X, ' F 10.2, RH7 (REL TO I-127)'///
3 ' F**2.0,0 (7/2) = F 10.6 MU/SEC'///
4 5X, ' F 10.2, RH7 (REL TO I-129)'///
5 5X, ' F 10.2, RH2 (REL TO I-127)'///
ETA5=SIGN(-EIJ5/(2E.0*RH05*RH05),-)
ETA7=SIGN(-EIJ7/(2E.0*RH07*RH07),-)
ETA=-(ETA5+ETA7)/2.

```



```

WRITE (6,911)ETA7,ETA8V
911 FORMAT('ETA(5/2) = ',F7.4,'(X) ',ETA(7/2) = ',F7.4,'(X) ',
1      'ETA(AV) = ',F7.4,'(//)')

```

C
C
C

DERIVED SFG PARAMETERS

```

UP=-QS7127/2293.
WRITE (6,916) UP
916 FORMAT('/',UP = ',F7.4)
RATIO=QS5/QS7
WRITE (6,915)RATIO
915 FORMAT('/',COMPOUND MOMENT RATIO (5/2)/(7/2) = ',
1      'F10.5,//)

```

C

RETURN
END

C
C

C

SUBROUTINE TCS(SI)

C

C

C

TO CALCULATE CENTRE SHIFTS

```

REAL SI(8)
COMMON /PLX2/ EF(3),CF(4),CS(8)
CS(1)=SI(1)+CF(2)-EF(3)
CS(2)=SI(2)+CF(3)-EF(3)
CS(3)=SI(3)+CF(4)-EF(3)
CS(4)=SI(4)+CF(1)-EF(2)
CS(5)=SI(5)+CF(2)-EF(2)
CS(6)=SI(6)+CF(3)-EF(2)
CS(7)=SI(7)+CF(1)-EF(1)
CS(8)=SI(8)+CF(2)-EF(1)
CSAV=CS(1)+CS(2)+CS(3)+CS(4)+CS(5)+CS(6)+CS(7)+CS(8)
CSAV=CSAV/8.
WRITE (6,988) (CS(I),I=1,8)
988 FORMAT('///// CENTRE SHIFT LINE ',//,(F14.4,4X,T2))
WRITE (6,981)CSAV
981 FORMAT('///. AVERAGE CS = ',F8.4)

```

C

RETURN
END

C

C

APPENDIX 2

Estimation of the Errors in the Derived ^{129}I Mössbauer Parameters

Considering the 5/2 (excited) ^{129}I nuclear state; then, in the solution of e^2qQ and η from the spectral line positions, using the Williams-Bancroft method¹, the following equations pertain (see appendix 1).

$$\Delta_1 = \epsilon_7 - \epsilon_4 \qquad \Delta_2 = \epsilon_6 - \epsilon_2 \qquad \dots (A2.1,2)$$

$$E_1 = (2\Delta_1 + \Delta_2)/3 \qquad \dots (A2.3)$$

$$E_2 = (-\Delta_1 + \Delta_2)/3 \qquad \dots (A2.4)$$

$$E_3 = (-\Delta_1 - 2\Delta_2)/3 \qquad \dots (A2.5)$$

$$C_1 = -\frac{1-3}{12} \sum_j E_1 E_j / 28 \qquad C_2 = E_1 E_2 E_3 / 160 \qquad \dots (A2.6,7)$$

$$4\mu^3 - C_1\mu - C_2 = 0 \qquad \dots (A2.8)$$

where ϵ_n is the position (cm^{-1}) of line n

Δ_1, Δ_2 are the excited nuclear energy level splittings

E_n is the energy of the n th nuclear level

C_1, C_2 are the co-efficients in the cubic polynomial

μ_n is the n th solution to the polynomial

In order to estimate the errors in the solutions, μ_n , to the cubic polynomial, resulting from errors in the computed line positions, a method commonly used in Econometrics² may be utilised. For a set

of standard normal variables, Δ_i , the chi-square distribution is given by²:

$$D^T V^{-1} D < \chi_c^2 \quad \dots (A2.9)$$

where $D = \begin{bmatrix} \Delta_1 - \bar{\Delta}_1 \\ \Delta_2 - \bar{\Delta}_2 \end{bmatrix}$ and $V = \begin{bmatrix} \sigma_{\Delta_1}^2 & \sigma_{\Delta_1 \Delta_2}^2 \\ \sigma_{\Delta_1 \Delta_2}^2 & \sigma_{\Delta_2}^2 \end{bmatrix}$ for two

degrees of freedom, and

$$\sigma_{\Delta_n}^2 \equiv \text{variance in } \Delta_n$$

$$\sigma_{\Delta_n \Delta_m}^2 \equiv \text{co-variance of } \Delta_n \text{ and } \Delta_m$$

$$\bar{\Delta}_n \equiv \text{calculated mean value of } \Delta_n$$

$$\chi_c^2 \equiv \text{chi-squared value corresponding to confidence level } c.$$

From experimental results from the ^{129}I Mössbauer spectra, except for the poorly resolved lines 3 and 5, $\sigma_{\Delta_n \Delta_m}^2 \ll \sigma_{\Delta_n}^2, \sigma_{\Delta_m}^2$; so that

Δ_1 and Δ_2 are essentially independent, and $\sigma_{\Delta_1 \Delta_2}^2 = 0$. Thus,

$$D^T V^{-1} D = \begin{bmatrix} \Delta_1 - \bar{\Delta}_1 & \Delta_2 - \bar{\Delta}_2 \end{bmatrix} \begin{bmatrix} \sigma_{\Delta_1}^{-2} & 0 \\ 0 & \sigma_{\Delta_2}^{-2} \end{bmatrix} \begin{bmatrix} \Delta_1 - \bar{\Delta}_1 \\ \Delta_2 - \bar{\Delta}_2 \end{bmatrix}$$

$$= (\Delta_1 - \bar{\Delta}_1)^2 / \sigma_{\Delta_1}^2 + (\Delta_2 - \bar{\Delta}_2)^2 / \sigma_{\Delta_2}^2$$

$$< \chi_c^2$$

$$\text{The equation } \frac{(\Delta_1 - \bar{\Delta}_1)^2}{\chi_C^2 \cdot \sigma_{\Delta_1}^2} + \frac{(\Delta_2 - \bar{\Delta}_2)^2}{\chi_C^2 \cdot \sigma_{\Delta_2}^2} = 1$$

is the equation to an ellipse on the Δ_1, Δ_2 axes, with centre $(\bar{\Delta}_1, \bar{\Delta}_2)$, and half axes equal to $(\chi_C^2 \cdot \sigma_{\Delta_1}^2)^{1/2}$ and $(\chi_C^2 \cdot \sigma_{\Delta_2}^2)^{1/2}$. In this case, the ellipse encloses an area in which are included all the values of Δ_1 and Δ_2 which are within the confidence limit c (as represented by the χ_C^2 value). The appropriate χ_C^2 values are shown in the table below³.

confidence level (c)	50% ($\approx \frac{2}{3}\sigma$)	75%	95% ($\approx 2\sigma$)
χ_C^2	1.387	2.77	5.99

for two degrees of freedom. (A similar ellipsoid, in three dimensions, could be derived for the $\frac{7}{2}$ (ground) state - where there are three Δ_n values - but the derivation becomes more complex).

Thus, if points (Δ_1, Δ_2) on the ellipse are used to generate C_1 and C_2 values - using equations A.3 - A.7 - and the cubic polynomial A.8 solved for μ_n ($n = 1-3$), then the resulting range of μ_n values reflects the errors in μ_n to the appropriate confidence level, c , resulting from the corresponding errors in Δ_1 and Δ_2 . The errors in e^2qQ and η can then be calculated from

$$e^2qQ \left(\frac{7}{2}\right) = 4I(2I - 1)\mu_{ZZ}$$

$$\approx 40 \times 32.58 \mu_{ZZ} \text{ (MHz)}$$

and $\eta = (\mu_{YY} - \mu_{XX})/\mu_{ZZ}$ (assigned from the μ_n by $|\mu_{XX}| < |\mu_{YY}| < |\mu_{ZZ}|$)

as outlined earlier.

For this treatment to be valid, in this case, the solutions to the cubic equation must all be real; so that the inequality $-4C_1 + 27C_2^2 < 0$ must hold.

In practice, eight points were sampled from the ellipse for each spectrum. The resulting derived parameter ranges, together with the appropriate confidence levels, are shown for three compounds in table A2.1 as examples.

Using these values, we can assign reasonable error limits to our experimentally measured e^2qQ and η values. Taking the 95% confidence level (2σ) as a guide, errors (σ) of ± 4 MHz can be assigned to the e^2qQ values. For η there is an internal and an external check on the error estimation. The 95% confidence limit ranges for η from table A2.1 indicate that ± 0.03 is a reasonable estimate of the accuracy for η . This agrees excellently with the difference in η values measured from the $\frac{5}{2}$ and $\frac{7}{2}$ levels for each of the compounds in this study, as shown earlier (table 6.1).

References

1. P. G. L. Williams and G. M. Bancroft; Mol. Phys. (1970) 19, 717; Mössbauer Effect Methodology (1971) 7, 39.
2. R. J. Wonnacott and T. H. Wonnacott; "Econometrics" (1970) Wiley, New York.
3. P. R. Bevington; "Data Reduction and Error Analysis for the Physical Sciences", (1969) McGraw-Hill, New York; table C-4, p. 314-5.

table A2.1

Derived Errors in η and e^2qQ , with Confidence Limits, for
some trans- $^{129}\text{I}Q_2\text{PtL}$ Complexes

L =		EtNC	CF ₃	P(OMe) ₃
mean		1282	1125	1257
$e^2qQ(5/2)$ (MHz)	95%	1277-1287	1118-1132	1254-1261
	75%	1279-1285	1121-1130	1255-1260
	50%	1280-1284	1122-1129	1256-1259
η	mean	0.138	0.261	0.262
	95%	0.097-0.169	0.221-0.296	0.247-0.276
	75%	0.112-0.160	0.234-0.285	0.251-0.272
	50%	0.120-0.154	0.242-0.278	0.255-0.269